

HEATSTORE

Screening of the national potential for UTES

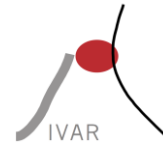
Prepared by: Luca Guglielmetti, University of Geneva
Alexandros Daniilidis, University of Geneva
Benoit Valley, University Neuchatel
Charles Maragna, BRGM
Camille Maurel, BRGM
Dorien Dinkelman, TNO
Joris Koornneef, TNO
Peter Oerlemans, IF Technology
Benno Drijver, IF Technology
Anders Juhl Kallesøe, GEUS
Mette Hilleke Mortensen, GEUS
Claus Ditlefsen, GEUS
Thomas Vangkilde-Pedersen, GEUS
Stefan Klein, IEG Fraunhofer

Checked by: Thomas Vangkilde-Pedersen, GEUS (WP1 leader)

Approved by: Holger Cremer, TNO (HEATSTORE coordinator)

Please cite this report as: Guglielmetti L., et al. 2021: Screening of national potential for UTES, GEOHERMICA – ERA NET Cofund Geothermal. 87 pp.

This report represents HEATSTORE project deliverable number D1.3



HEATSTORE (170153-4401) is one of nine projects under the GEOTHERMICA – ERA NET Cofund aiming at accelerating the uptake of geothermal energy by 1) advancing and integrating different types of underground thermal energy storage (UTES) in the energy system, 2) providing a means to maximise geothermal heat production and optimise the business case of geothermal heat production doublets, 3) addressing technical, economic, environmental, regulatory and policy aspects that are necessary to support efficient and cost-effective deployment of UTES technologies in Europe.

This project has been subsidized through the ERANET cofund GEOTHERMICA (Project n. 731117) from the European Commission, RVO (the Netherlands), DETEC (Switzerland), FZJ-PtJ (Germany), ADEME (France), EU DP (Denmark), Rannis (Iceland), VEA (Belgium), FRCT (Portugal), and MINECO (Spain).



Table of Content

About HEATSTORE	5
1 Introduction	6
2 Screening of National Potential in the Netherlands	7
2.1 Context: Opportunities for HT-ATES in NL	7
2.2 Subsurface criteria for HT-ATES in the Netherlands	8
2.2.1 Subsurface Criteria for HT-ATES	9
2.2.2 Data	10
2.3 HT-ATES potential map from SGE-study	10
2.3.1 Introduction	10
2.3.2 Methods	11
2.3.3 Results and discussion	12
2.4 HT-ATES potential maps from Dutch National Subsurface Database	13
2.4.1 HT-ATES potential maps (subsurface criteria)	13
2.4.2 HT-ATES potential maps (flow rate).....	14
2.5 Comparison of the two potential maps based on flow rate	15
2.5.1 Maassluis Formation	15
2.5.2 Oosterhout Formation.....	16
2.5.3 Differences between the maps	16
2.5.4 Notes regarding all Dutch HT-ATES potential maps	17
2.6 Conclusions and recommendations on HT-ATES potential in NL	18
2.7 References	18
3 Screening of National Potential in Switzerland	20
3.1 Context	20
3.2 Methods	20
3.3 Available data	24
3.3.1 District heating network	24
3.4 Waste heat	26
3.5 Subsurface data	28
3.5.1 Geologic data.....	28
3.5.2 Temperature data	30
3.5.3 Petrophysical data	30
3.5.4 Borehole and Seismic data.....	31
3.6 Results	31
3.6.1 Proximity analysis of surface components	31
3.6.2 Fault Favourability	33
3.6.3 Transmissivity threshold	34
3.6.4 Proximity analysis of exploration boreholes and seismic data	35
3.6.5 Storage capacity assessment.....	36
3.6.6 Favourability assessment	38
3.7 References	39
4 Screening of National Potential in Germany	40
4.1 General overview of existing calculated potential (LANUV, 2018):	41
4.2 State of the Art Mine Water Projects in NRW (Germany)	41
4.3 Overview thermal utilization possibilities of existing shafts	45
4.4 Possible Locations for MTES in the Ruhr-area (NRW)	45

4.5	Status Quo	48
4.6	References	48
5	Screening of national potential in Denmark	49
5.1	Context	49
5.2	First edition web tool for national UTES screening	49
5.3	Initial screening of shallow formations in first edition tool	50
5.3.1	Access to shallow subsurface information	50
5.3.2	Main types of suitable aquifers	50
5.3.3	Areas with limited groundwater flow	51
5.4	Local investigations of deeper formations	51
5.4.1	Access to deep geothermal information	51
5.4.2	Evaluation of heat storage in deeper sandstone reservoirs in the Aalborg area	51
5.4.3	Evaluation of heat storage in deeper chalk formations in the Copenhagen area	52
5.4.4	Feasibility study of high-temperature ATES in the Stenlille structure	53
5.5	HEATSTORE survey of interests amongst District Heating utilities	53
5.6	Characterization of geology in specific areas	55
5.6.1	Miocene deposits in the central part of Jutland	56
5.6.2	Esbjerg area, Western Denmark	57
5.6.3	Odense area, Island of Funen	59
5.6.4	Guldborgsund, Southeast Denmark	60
5.6.5	Aarhus (synergy with the MUSE, GeoERA, project)	62
5.7	Expansion of web screening tool – new data and added value	65
5.7.1	Purpose and functionality	65
5.7.2	Data overview	65
5.7.3	Perspectives for further activities.....	66
5.8	References	66
6	Screening of Potential in France: Focus on Ile-de-France	67
6.1	Context	67
6.2	Available data	68
6.2.1	7.2.1 District heating network	68
6.2.2	7.2.2 Waste heat.....	70
6.2.3	7.2.3 Underground data.....	73
6.3	Elements of methodology	77
6.4	Recovery efficiency in the mid-Jurassic Dogger limestone aquifer	78
6.5	Recovery efficiency in the Albian and in the Neocomien sand aquifers	84
6.6	Conclusions	86
6.7	References	87

About HEATSTORE

High Temperature Underground Thermal Energy Storage

The heating and cooling sector is vitally important for the transition to a low-carbon and sustainable energy system. Heating and cooling is responsible for half of all consumed final energy in Europe. The vast majority – 85% - of the demand is fulfilled by fossil fuels, most notably natural gas. Low carbon heat sources (e.g. geothermal, biomass, solar and waste-heat) need to be deployed and heat storage plays a pivotal role in this development. Storage provides the flexibility to manage the variations in supply and demand of heat at different scales, but especially the seasonal dips and peaks in heat demand. Underground Thermal Energy Storage (UTES) technologies need to be further developed and need to become an integral component in the future energy system infrastructure to meet variations in both the availability and demand of energy.

The main objectives of the HEATSTORE project are to lower the cost, reduce risks, improve the performance of high temperature (~25°C to ~90°C) underground thermal energy storage (HT-UTES) technologies and to optimize heat network demand side management (DSM). This is primarily achieved by 6 new demonstration pilots and 8 case studies of existing systems with distinct configurations of heat sources, heat storage and heat utilization. This will advance the commercial viability of HT-UTES technologies and, through an optimized balance between supply, transport, storage and demand, enable that geothermal energy production can reach its maximum deployment potential in the European energy transition.

Furthermore, HEATSTORE also learns from existing UTES facilities and geothermal pilot sites from which the design, operating and monitoring information will be made available to the project by consortium partners.

HEATSTORE is one of nine projects under the GEO THERMICA – ERA NET Cofund and has the objective of accelerating the uptake of geothermal energy by 1) advancing and integrating different types of underground thermal energy storage (UTES) in the energy system, 2) providing a means to maximize geothermal heat production and optimize the business case of geothermal heat production doublets, 3) addressing technical, economic, environmental, regulatory and policy aspects that are necessary to support efficient and cost-effective deployment of UTES technologies in Europe. The three-year project will stimulate a fast-track market uptake in Europe, promoting development from demonstration phase to commercial deployment within 2 to 5 years, and provide an outlook for utilization potential towards 2030 and 2050.

The 23 contributing partners from 9 countries in HEATSTORE have complementary expertise and roles. The consortium is composed of a mix of scientific research institutes and private companies. The industrial participation is considered a very strong and relevant advantage which is instrumental for success. The combination of leading European research institutes together with small, medium and large industrial enterprises, will ensure that the tested technologies can be brought to market and valorised by the relevant stakeholders.

1 Introduction

The work carried out in this task comprise a screening of the national potential for UTES in the Netherlands, Switzerland, Germany, Denmark and France. Geological, hydrogeological, geochemical, etc. (sedimentary basins, mining basins, host rock formations) have been analysed to identify and characterize locations with more favorable conditions for different types of UTES systems.

In the Netherlands, the three different types of subsurface potential maps illustrate a high subsurface potential at a regional scale for HT-ATES in the Netherlands, especially in the western part of the country, where, conveniently, heat demand likewise is high (metropolitan area, greenhouses, high geothermal potential).

In Switzerland a spatial multi-criteria play-fairway framework was implemented focussing on the potential of implementation of HT-ATES systems in two main geologic units: the Cenozoic sediments (target of the Bern project) and the fractured Upper Mesozoic carbonates (target of the Geneva project). Subsurface data down to 2000m in depth as well as surface constraints have been combined to produce a set of favourability maps representing different potential scenarios.

In Germany focus was directed to the Ruhr-area thanks to its significant amounts of former collieries and the biggest population density in Germany. This offers a big potential to include MTES to modern low-ex-heat grids.

In France the ATES potential is evaluated according to available public data, by combining subsurface data (e.g. depth of the targeted geological formation, thickness, petrophysical parameters, temperature distribution at different depth, geochemistry of waters), surface data (e.g. location of district heating and cooling networks, land occupation) and energy data (e.g. heat demand, heat demand distribution in time, excess heat sources, excess heat supply in time, geographical distribution). The results show that HT-ATES could be implemented in the Dogger carbonate reservoirs, therefore can play a key role in increasing the share of waste heat onto DHH

In Denmark targeted geological characterization was carried out in five selected sites based on the results of a survey of interest and subsequently dialog with several interested utilities. An important criterion in this work has been to cover different geological settings in the Danish subsurface and thereby cover cases of regional relevance for a wide group of stakeholders.

2 Screening of National Potential in the Netherlands

2.1 Context: Opportunities for HT-ATES in NL

In the Netherlands, thousands of low temperatures (5 - 25 °C) ATES systems are in use for heating and cooling of buildings and greenhouses. The widespread application of this sustainable technique is possible thanks to the highly favourable subsurface characteristics in most parts of the country: within the uppermost ~200 m below the surface, there is an alteration of unconsolidated sand and clay layers with large thickness and high permeabilities, allowing for high flow rates in ATES wells. Clear legislation exists for the permission of these low temperature systems, facilitating the increased implementation of this technique.

The interest in storage of heat at higher temperatures (>25 °C) has increased over the last decade, based on the successful experiences with low temperature ATES and recognizing its potential contributions to global climate goals by providing the required flexibility for heat supply in district heating networks. In the Netherlands, the surface potential for the High Temperature Aquifer Thermal Energy Storage (HT-ATES) is estimated to be large (Dinkelman et al., 2020). Production of sustainable heat from different sources, like geothermal and solar heat, is growing rapidly (Figure 2-1) and both could benefit from HT-ATES as it enables an increase in their net annual heat production. They can supply low marginal cost heat to store in a HT-ATES. Also, there is a large amount of waste heat available from industries (Figure 2-1), waste incineration plants, CHP plants, and data centres that is currently being disposed of but can potentially be stored in aquifers. In the Netherlands, a relatively densely populated country, district heating networks are being developed and/or expanded on a large scale, connecting local heat producers and consumers/greenhouses (Figure 2-2). HT-ATES has a large potential to increase the flexibility of the heating grid, as it can buffer heat from any heat sources on the grid, and supply it back to the grid when net demand occurs. By making optimal use of sustainable and waste heat the sustainability of heat supply can improve drastically.

The Dutch Water Law (Waterwet) covers the legal framework for the permission of ATES systems up to 500 mbgl (meters below ground level). HT-ATES systems are legally categorized as ATES systems with a special status, allowing these systems to be permitted by the same legal procedures, although the permitting process is typically somewhat more complex because of the high temperatures and associated temperature related effects. In geological formations deeper than 500 mbgl, different legislation applies (i.e. the 'Mining Act'), which brings about more complex procedures. Also, deeper than 500 mbgl, drilling costs are significantly higher due to more complex and expensive drilling techniques and more stringent safety requirements. Given these legal and technical considerations, HT-ATES development in the Netherlands currently focuses on the depth range up to 500 mbgl. Therefore, we here present the HT-ATES subsurface potential in the Netherlands for this depth range.

In the following chapters, an overview is presented of the subsurface parameters that play a key role in the determination of HT-ATES potential first. Subsequently, three different types of subsurface potential maps are presented for HT-ATES in the Netherlands, each with different inputs and/or workflows considering that standardized methodologies are not (yet) available. Finally, the results of these maps are compared and the overall subsurface potential for HT-ATES application in the Netherlands is discussed.

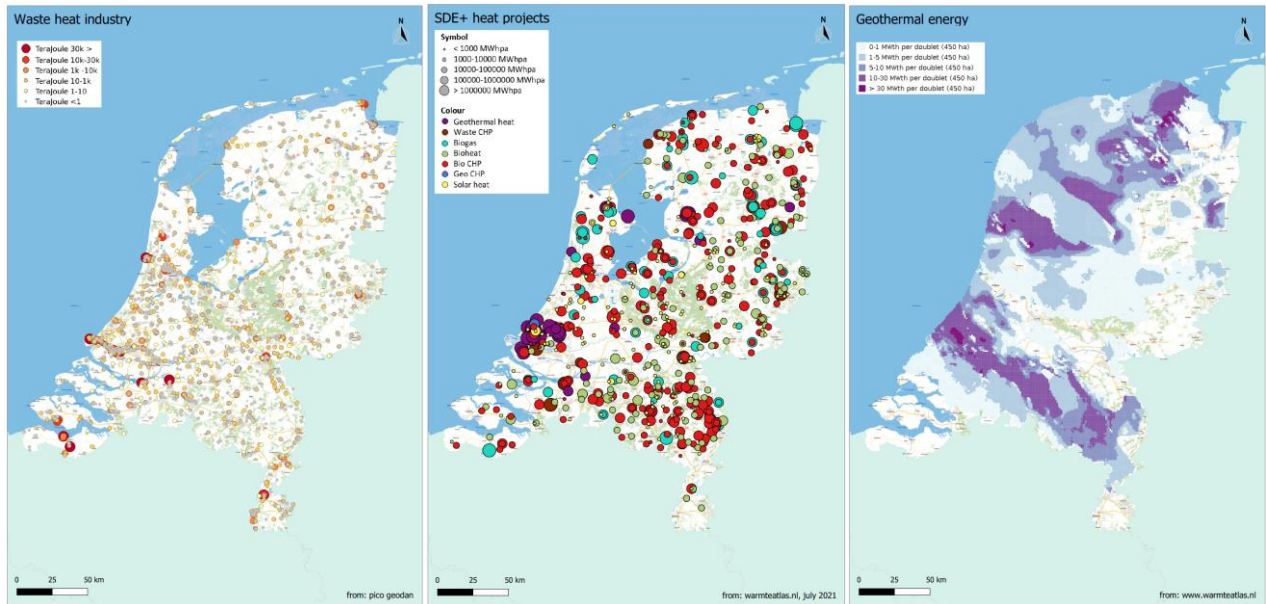


Figure 2-1 - Upper left: Locations of waste heat from industry. Upper right: SDE+ (subsidy) sustainable heat projects (to be) developed in the Netherlands. Lower left: Potential of geothermal energy in the Netherlands. From: www.warmteatlas.nl.

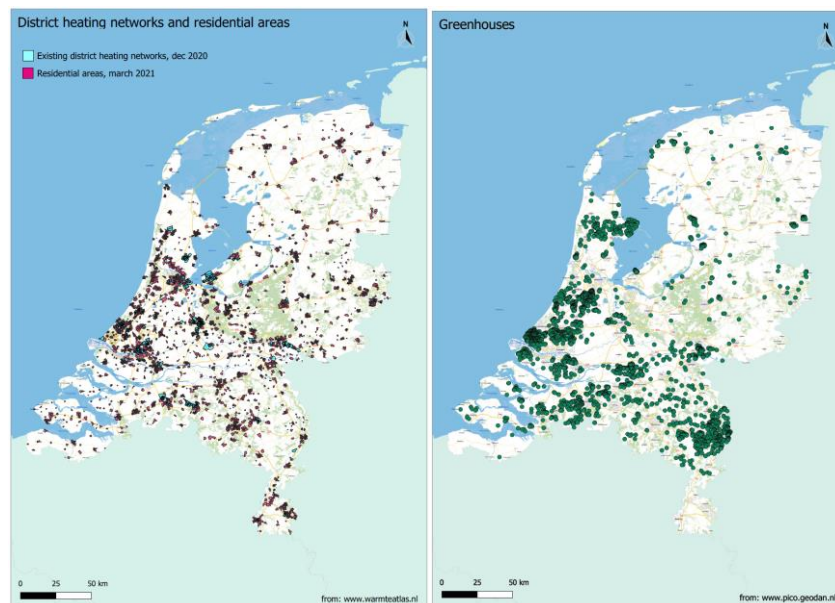


Figure 2-2. Left: district heating networks (blue) and densely populated residential areas (pink) with heat demand (potential). Right: location of greenhouses in the Netherlands. From: www.warmteatlas.nl, www.pico-geodan.nl

2.2 Subsurface criteria for HT-ATES in the Netherlands

The subsurface of the Netherlands up to a depth of ~500 mbgl generally consists of an alternation of unconsolidated sand and clay layers (Figure 2-3). Over 2500 low-temperature ATES systems (injection temperatures < 25°C) exist in the Netherlands (Fleuchaus et al., 2018), typically within the depth range 0 – 250 mbgl. Other subsurface and groundwater applications are most numerous in this depth range as well. Subsurface temperatures at 0-500 m depth vary between ~10-25°C (ThermoGIS.nl). For HT-ATES the aim is to store temperatures between 60-90°C.

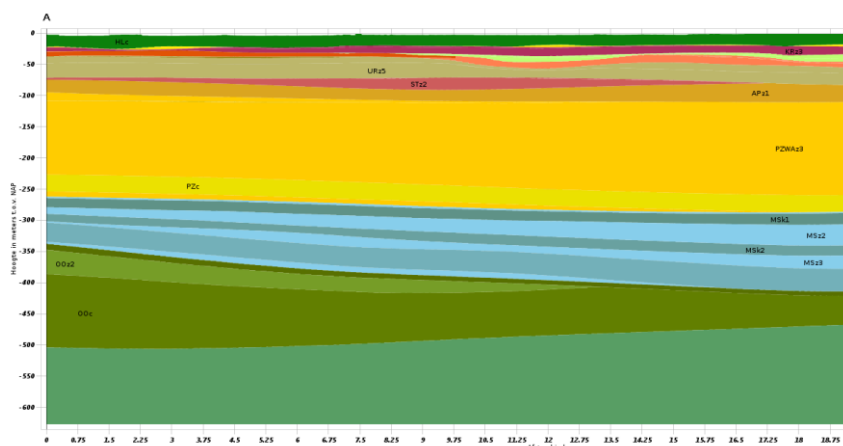


Figure 2-3 - Example of a cross-section of the Dutch subsurface in the province of Noord-Holland. Each colour represents a hydrogeological formation. Darker colours within a formation show units with low permeability (clay, complex layers), lighter colours have higher permeability (sand) (REGIS II v2.2, www.dinoloket.nl).

2.2.1 Subsurface Criteria for HT-ATES

Table 2-1 summarizes the relevant subsurface criteria for safe and efficient HT-ATES systems based on the range in subsurface properties values that are generally found in the shallow Dutch subsurface (max 500 mbgl). These criteria have been defined in a dedicated workshop with researchers and a variety of stakeholders in the Dutch WINDOW project¹. For the HEATSTORE project, this list has been used in the generation of the potential maps. The criteria are discussed in more detail in the next sections.

2.2.1.1 Storage aquifer

In the Netherlands, an aquifer is considered suitable for HT-ATES when it has a certain thickness and permeability. For the following criteria, it is assumed that HT-ATES wells are technically comparable to lower temperature (<25°C) ATES wells in unconsolidated layers, meaning that a similar drilling technique and well development process is applied. Given these starting points, a minimum hydraulic conductivity of 3-5 m/d (at 15°C) is recommended (so the minimum permeability is approximately 4-7 Darcy). The minimum aquifer thickness is about 15 m. Furthermore, lithology of the storage aquifer is an important factor, medium- to fine-grained sand is generally favoured. In case an aquifer consists of very fine sand or silt it is considered less suitable for HT-ATES due to the higher risk of production of sand and/or fines and the low permeability. Very coarse sand has high permeabilities hence allows large volumes to be stored with high flow rates, but coarse-grained aquifers are considerably more sensitive to low recovery efficiencies because of a high impact of buoyancy flow. Depending on the parameters that influence buoyancy flow (aquifer dimensions, storage volume, storage temperature, native groundwater temperature etc.), maximum hydraulic conductivities are 20 – 50 m/d (at appx. 15°C). Because of the high hydraulic conductivity values that are found in many of the shallow aquifers that are used for low temperature ATES systems, these highly permeable shallow aquifers are considered to be less suitable for HT-ATES.

2.2.1.2 Confining layer above storage aquifer

The presence of a confining layer on top of (and preferably also below) the storage aquifer is a requirement to limit 1) the impact of buoyancy flow on the recovery efficiency and 2) the temperature and associated geochemical effects in the shallower layers. The confining layer acts as a physical boundary preventing hot water from flowing to shallower aquifers. The advective losses of hot water are restricted to the horizontal dimension when confining layers are present both at the top and the bottom of a storage aquifer, resulting in a higher recovery efficiency.

2.2.1.3 Depth of aquifer

Shallow aquifers (< 50 m below ground level) are seen as less suitable for HT-ATES due to the potential negative thermal effects on the surface and shallow subsurface, where many stakeholders are located, e.g. groundwater levels are managed and (protected) nature is present. Additionally, the heat losses to the surface are relatively large for shallow HT-ATES systems.

¹ WINDOW - Warmtevoorziening In Nederland Duurzamer met Ondergrondse Warmteopslag | RVO.nl | Rijksdienst

2.2.1.4 Groundwater flow in the storage aquifer

The ambient groundwater flow velocity should be limited, to prevent the hot stored water from being drifted away. Because of the limited relief in the Netherlands, groundwater flow velocities are relatively low (<25 m/y) in most places.

2.2.1.5 Faults

When faults are present in the area, the location should be handled with care. The injected hot water might affect shallower aquifers by leakage through the faults. HT-ATES can be operated with relatively low pressures in the unconsolidated sands, because of the relatively high permeabilities. This reduces the risks of seismic activities in fault areas.

2.2.1.6 Water quality: fresh-salt water interface

The last subsurface parameter taken into account is the chloride concentration, as this to some extent reflects the quality of the groundwater (fresh/brackish/saline). High-quality fresh groundwater is a valuable natural resource in the Netherlands (~50% of Dutch drinking water is produced from groundwater). In case the target aquifer holds freshwater or a fresh-salt water interface, the possible impact on the groundwater composition requires extra attention. Freshwater should not be mixed with brackish or saline water. The use of aquifers holding saline water (>1 g Cl/l) is less critical and is favoured for storage purposes.

Table 2-1 - Subsurface (unconsolidated) criteria taken into account for the Dutch WINDOW project.

	One or more barriers	Possible barriers	Favourable
Lithology (<i>not</i> included in potential maps)	Silt-clay	Limey-sand, glauconite	Sand
Depth		<50, >500 mbgs*	50-500 mbgs*
Thickness sand layer	< 10m	10-15 m	> 15 m
Horizontal hydraulic conductivity – kh value	< 5 m/d		> 5 m/d
Presence of confining cap layer (clay)		Risk absence cap layer, min thickness ~ 5 m	No risk
Faults		< 1 km	> 1 km
Groundwater flow velocity		> 25 m/y	< 25 m/y
Chloride concentration		Freshwater & saline/freshwater interface (< 1 g/l)	Saline water (> 1 g/l)
Protected groundwater areas		Within protected area	Outside protected area

2.2.2 Data

Data for analysis of the Dutch subsurface were collected from:

- REGIS II v2.2, a publicly available hydrogeological model of the Dutch subsurface, with information on the formations in the Upper North Sea Group and hydrogeological units within each formation. The model ranges up to ~500/1000 m depth. The database holds information on the lithology of the units, depth, thickness, hydraulic conductivity, borehole information, well log data (www.dinoloket.nl).
- ThermoGIS, for deeper aquifers – starting at ~0-500m up to Carboniferous aquifers > 5 km depth (www.thermogis.nl).
- Deep well data (oil, gas, deep geothermal wells at www.nlog.nl)
- Chloride concentration (Deltares, www.grondwatertools.nl)
- Groundwater flow (Deltares, www.grondwatertools.nl)
- Faults from the H3O project (Deckers et al., 2014)
- Available direct field data, like borehole logs and well tests

2.3 HT-ATES potential map from SGE-study

2.3.1 Introduction

In 2012, IF Technology has constructed subsurface potential maps for Shallow Geothermal Energy (SGE) in the Netherlands, in which the flow rates applicable for SGE were derived for various geological formations up to 1.000 mbgl (Hellebrand et al., 2012). Within HEATSTORE Task 1.3, these existing SGE potential maps

were used as a basis to construct HT-ATES potential maps. The methodology used and the resulting potential maps are described below.

2.3.2 Methods

In the study performed by IF Technology in 2012, the potential for SGE production was mapped for the Maassluis Formation (MS), Oosterhout Formation (OO), Breda Formation (BR) and Brussels Sand Member (BSM). HT-ATES potential maps were constructed only for MS and OO, because these formations were expected to have the highest HT-ATES potential (both technically and legally), because of their relatively shallow depth (<500 mbgl) and their relatively high hydraulic conductivity compared to the deeper layers of BR and BSM.

For the MS and OO, the following available information of the SGE study (2012) was used to construct a HT-ATES potential map:

- Potential flow rate maps
- raster-files of the Net sand thickness, for each formation
- raster-files of the Temperature at formation depth, for each formation

The potential flow rate maps of the SGE-study show four categories of SGE potential (see Figure 2-4 for an example). An expression of SGE potential flow rate in terms of Net sand thickness was derived to obtain a SGE flow rate raster-file (in m³/h). Onto this SGE potential raster, two corrections were applied to obtain the HT-ATES potential flow rate (m³/h), as described below.

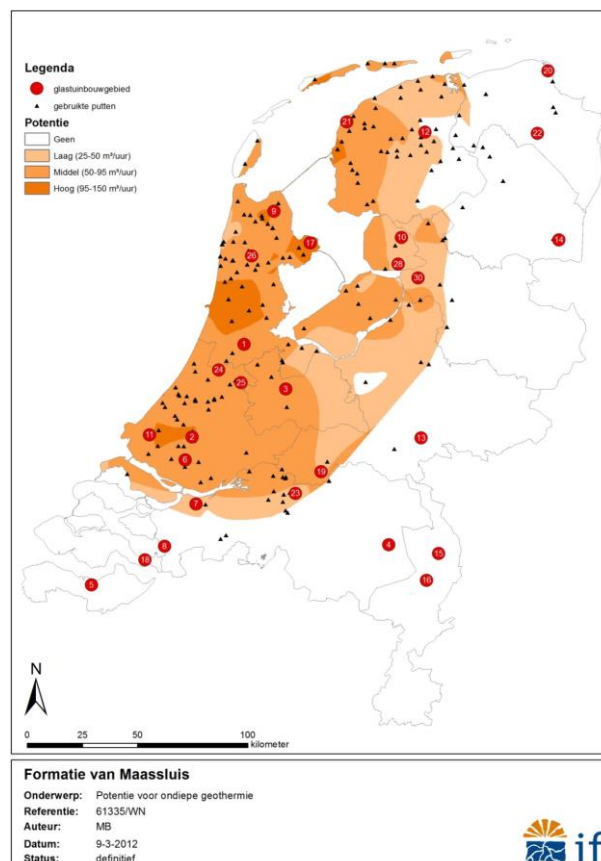


Figure 2-4. The SGE potential flow rate map of the Maassluis Formation. This was used as base to construct HT-ATES potential map. The black triangles indicate the wells that were used for the construction of this SGE potential map.

2.3.2.1 Correction factor 1: Temperature

In unconsolidated formations, sand production and prevention of well clogging by particles are generally the limiting factors for the flow rate. In aquifers with a relatively low hydraulic conductivity (which are used for HT-ATES), the well design standards for extraction wells are usually decisive. The well design standards for

extraction wells are meant to prevent (significant) sand production in the well. The guidelines define the maximum production flow rates for (HT-)ATES wells, based on the hydraulic conductivity (m/d) and thickness of the aquifer, using the following equation based on the NVOE guidelines (2006):

$$Q_w = 4\pi r \times kH$$

Where,

Q_w = Maximum well capacity [m³/h]
 r = Radius of the borehole at well screen depth [m]
 k = Hydraulic conductivity of the aquifer [m/d]
 H = Length of the well screen [m]

At higher temperatures, the hydraulic conductivity of a formation is higher because the water has a lower dynamic viscosity, meaning the maximum flow rates are higher too. Therefore, the maximum flow rate of a doublet (one cold and one warm well) is determined by the minimum temperature of the groundwater that is produced from the HT-ATES system, i.e. at the cold well. For the design of a HT-ATES system, it is also important to check the well design standards for injection wells and the guidelines for maximum injection pressure.

In HT-ATES, the hot well typically has injection temperatures of 60 – 90 °C, and the cold well around 30 °C. This means that after some heat storage-recovery cycles, the temperature around the cold well will be around 30 °C. Therefore, for the HT-ATES potential flow rate map construction, it is assumed that the minimum production temperature at the cold well is 30 °C. The SGE flow rates are based on the hydraulic conductivity of the aquifer, which is valid for the natural temperature of the groundwater, which for the MS and OO formations is typically lower than 30 °C. Since the hydraulic conductivity is higher at 30 °C, a correction has to be applied to the SGE potential flow rate maps, in order to obtain the HT-ATES potential. This factor is defined by the ratio of the viscosity at native groundwater temperature (as derived from the SGE temperature map) and the minimum temperature of 30 °C at the cold HT-ATES well. The dependency of dynamic viscosity (μ in unit centiPoise, cP) with temperature according to Huyakorn and Pinder (1977) is approached by the following formula (with T in °C):

$$\mu(T) = 2,394 * 10^{-2} * 10^{\frac{248,37}{T+133,15}}$$

For the cold HT-ATES well (30 °C), the dynamic viscosity is 0.797 cP. For the MS and OO formations, a cP-value map for native temperatures was calculated with the formula above, using the available temperature raster-files of the formations. Then, the temperature correction factor raster was constructed by dividing the cP-value map for native temperatures by the cP-value at 30 °C (i.e. 0.797):

$$TempCorrectionFactor_{raster} = \frac{cP_{raster}}{0.797}$$

$$TempCorrectionFactor_{raster} = \frac{2,394 * 10^{-2} * 10^{\frac{248,37}{T+133,15}}}{0.797}$$

With T the temperature raster for the formation. These correction factor maps were constructed for the Maassluis and Oosterhout Formations, based on their natural temperature maps.

2.3.2.2 Correction factor 2: Well screen length

For (HT-)ATES wells, only part of the total sand thickness of the aquifer is used for placing well screens. Here, it is assumed that well screens will be installed in 75% of the total sand thickness of a formation. Therefore, an additional correction factor of 0.75 was applied to obtain the HT-ATES potential flow rates.

Finally, for each formation, the HT-ATES potential flow rate (m³/h) was calculated by multiplying the SGE potential flow rate map with the temperature correction factor map and 0.75:

$$FlowRate_{HTATES,raster} = FlowRate_{SGE,raster} * TempCorrectionFactor_{raster} * 0.75$$

2.3.3 Results and discussion

Using the calculated flow rates the potential for HT-ATES was mapped in three classes: low potential (calculated flow rate 0-50 m³/h), medium potential (calculated flow rate 50-100 m³/h) and high potential (calculated flow rate 100-150 m³/h). It has to be stressed, that the calculated flow rates are based on

parameters that have a relatively large uncertainty. Moreover, there are indications that the extraction flow rate following from the well design standards can be exceeded in certain cases (Drijver et al., 2020), which is a subject of further research. Therefore, the calculated flow rates are only used as an indication of the relative potential and the calculated flow rates were not included in the legend of the maps. The HT-ATES potential flow rate maps for the Maassluis and Oosterhout Formations are shown in the map on the right hand side of Figure 2-5 and Figure 2-6 respectively.

HT-ATES potential in the Maassluis Formation is limited to the western half of the Netherlands, with the highest potential flow rates in the provinces of North-Holland and South-Holland. This means that subsurface potential is highest in the region where demand is likely to be high too since the metropolitan area 'Randstad' is located in these provinces, as well as the major large-scale greenhouse areas near Rotterdam, Amsterdam and Hoorn. Additionally, there is a significant amount of waste heat available in this region.

The HT-ATES potential map of the Oosterhout Formation shows that the majority of the Netherlands shows at least some potential for HT-ATES application in the Oosterhout Formation, except for the southeasternmost province of Limburg. It shows medium potential for the areas west and east of the IJssel river, between Arnhem and Deventer, and high potential around Apeldoorn. The province of Groningen shows medium potential, as well as the north-south oriented strip through Meppel.

Although this map offers a first order estimate of the HT-ATES potential specifically in the Maassluis and Oosterhout Formations, the following is noted with regard to its representativity:

- The potential maps constructed for the MS and OO are expressed in potential based on calculated flow rates. Although this is an important indicator for the overall subsurface potential of a HT-ATES system, the other subsurface criteria (shown in section 2.2) should be addressed too when HT-ATES feasibility is studied.
- The spatial distribution of datapoints used in the original SGE-map contributes to varying uncertainties of the maps in space. It is noted that the highest data point densities apply to the provinces of North-Holland, South-holland and Friesland (see black triangles in Figure 2-4 for the locations of used well data).
- The subsurface information from which the SGE flow rates were calculated, is derived from deep oil and gas wells (Figure 2-4). As these wells have target depths of over 2,000 mbgl, it may be that the information on the shallower region (<500 mbgl, which is the target depth for HT-ATES in NL) was less accurately logged and interpreted.

2.4 HT-ATES potential maps from Dutch National Subsurface Database

TNO manages several large national databases which hold information on the (hydro)geological properties of the subsurface in the Netherlands (see also www.dinoloket.nl). One of these models TNO developed is the hydrogeological model REGIS II v2.2, based on the Digital Geological Model (DGM v2.2). REGIS II v2.2 distinguishes geological formations, each containing one or more hydrogeological units with more or less uniform hydrogeological characteristics (Figure 2-3). Each hydrogeological unit has been assigned properties like depths, thicknesses and hydraulic conductivity with a horizontal resolution of 100x100m.

The data from the REGIS II v2.2 model was used as input for two types of potential maps, constructed by TNO:

- HT-ATES potential based on the subsurface HT-ATES criteria of section 2.2 (Table 2-1), expressed in qualitative categories (probability of possible barriers).
- HT-ATES potential based on hydrogeological data and calculated flow rates.

The workflows and the resulting maps are discussed below.

2.4.1 HT-ATES potential maps (subsurface criteria)

In 2020, HT-ATES potential maps have been created in the Dutch national HT-ATES research programme WINDOW, categorizing the favourability for HT-ATES application based on the set of subsurface criteria shown in Table 2-1. At the onset of the project a selection of 25 locations that would be of interest for the realization of a HT-ATES system was made. This selection was primarily based on the availability of a (near-future) source of heat and/or the presence of a (near-future) heat network. Additionally, there was a need for the evaluation of the nationwide potential. It was decided to address this question by imposing the same subsurface criteria as used in the location-specific quick scans on a regional/nationwide scale by the high-resolution geographical information from the REGIS II v2.2 model.

The criteria have been determined in a workshop with the Dutch partners of the WINDOW project: KWR, IF Technology, Deltares and TNO. Some of the criteria have been slightly adapted for the potential maps in order to be able to quantify and use the values. The full report is available (in English) from Dinkelman et al. (2020). Geological input data, e.g. depth, kh-value etc., per sand layer of a geological formation (up to ~ 500 m depth) were derived from REGIS II v.2.2. Groundwater flow velocity data and chloride concentration grids were provided by Deltares. Information on the restriction areas for groundwater protection was deduced from the RIVM environmental and public health maps (www.geodata.rivm.nl).

For each hydrogeological unit classified in REGIS II v2.2 as sand layer, the allocated criteria values of all parameters are screened. The overall interpretation of a location is performed by including all evaluated criteria. If the value for one of the parameters indicates 'one or more barriers' (colour orange), the overall interpretation of that particular grid cell is set to 'one or more barriers'. If one of the parameters indicates 'possible barrier', the overall assignment of the grid cell is "possible barriers" (yellow). In case all criteria are met for a particular grid cell, the grid cell is interpreted as 'favourable' (green).

To calculate the potential per formation, which can comprise several sand layers, the different sand layers are screened in such a way that if one sand layer has potential, that area is marked as 'favourable' (green). After that, 'possible barriers' (yellow), and at last when all sand layers are defined as 'one or more barriers' in one grid cell, it is marked as 'one or more barriers' (orange). For the national potential maps, the same approach is used. A remark on this approach is that the criterion for the thickness of the individual layers is >15 m per layer. However, the sum of several stacked sand layers of <15m can cause the stacked sand layers to be of sufficient thickness and together they can serve as a good aquifer for HT-ATES.

The resulting potential maps give a national overview of areas where HT-ATES development has a high probability of becoming successful, where extra attention should be paid to one or more criteria or where one or more possible barriers apply for the implementation of a HT-ATES project, all based on subsurface conditions.

For the resulting maps, the 'WarmingUP' link above can be used (Dinkelman et al., 2020).

2.4.2 HT-ATES potential maps (flow rate)

As an addition to the qualitative potential maps based on subsurface criteria, also potential maps derived from calculated flow rate were created based on the REGIS II v.2.2 geological model for the Maassluis and Oosterhout Formations, allowing for a comparison with the potential maps of IF Technology. This exercise is merely performed as a means to compare the two maps with different data origins, rather than to obtain a preferential map for HT-ATES potential. Possible differences are an indication of the uncertainty that applies to the subsurface conditions.

The results are visualized in maps, which are to be compared to the maps developed by IF Technology, in which a different set of input data is used. Both potential maps will also be compared to the qualitative criteria maps for HT-ATES (Dinkelman et al., 2020).

For each formation, maps (grids) with the following information were available:

- Depth of base (REGIS II v2.2)
- Total sand thickness, total clay thickness (REGIS II v2.2)
- Hydraulic conductivity (REGIS II v2.2)
- Temperature at mid aquifer depth (depth and thickness maps, REGIS II v2.2 and the shallow subsurface temperature model from Dinkelman et al. (2020))

Note that the map for the Maassluis Formation is based on a much larger number of data points than the map for the Oosterhout Formation. The larger depth of the Oosterhout Formation results in much smaller number of boreholes that are deep enough to provide the required information. The potential for HT-ATES application was reconstructed, expressed as maximum flow rate possible in the aquifer (in m³/h). The following workflow was applied:

1. Gathering input data from REGIS II v2.2
2. Calculation of maximum flowrate (Q_{max} in m³/d) for each individual sand layer according to NVOE guidelines (NVOE, 2006), including correction for well screen: well screen can be placed in only 75% of the sand thickness (equation given in paragraph 2.3.2.1).
3. Correction of the maximum flow rate for temperature, using the same relation between viscosity and temperature as in section 2.3 by Huyakorn and Pinder (1977).
4. Sum individual sand layers within a formation to obtain flow rate maps for the total formation.
5. Translation of the map with calculated flow rates to HT-ATES potential.

The resulting maps are shown on the left-hand side of Figure 2-5 and Figure 2-6 for the Maassluis and Oosterhout formations respectively.

Regarding the potential maps of TNO, the following is noted:

- Input data used by TNO are the REGIS II v2.2 maps for thickness, depth and hydraulic conductivity. The maps for formations at depths > 200 m are based on a limited amount of data points (wells/boreholes) which are interpolated to create national maps. This may cause the values, especially for hydraulic conductivity, on a national scale to be different from the values found in a local study. This has to be kept in mind while reading/using the maps.
- The potential for HT-ATES in a certain formation is based on the potential flow rate of a doublet during heat storage, which may be realized when the minimum production temperature of the cold well is 30°C.
- The potential represents the potential flow rate for HT-ATES, assuming that a well screen can be installed in 75% of the net sand thickness of a formation. Clay layers above and below potential storage layers are not contributing to the potential flow rate.
- Thermal recovery efficiency, which is dependent on the temperature, volume and dimension of the heat storage, is not specifically included in the definition of the HT-ATES potential. However, the criteria were chosen in such a way that recovery efficiency is taken into account to some extent.

2.5 Comparison of the two potential maps based on flow rate

2.5.1 Maassluis Formation

The two constructed HT-ATES potential maps are shown in Figure 2-5. The Maassluis Formation is only present in the western half of the Netherlands, accounting for the lack of potential in the (south)eastern parts of the Netherlands. Overall, both maps show a similar national trend for the HT-ATES potential, with higher potential in the western part of the Netherlands. However, there are also significant differences. The REGIS II v2.2 maps have more positive estimations in the province of Zuid-Holland and near Apeldoorn. The REGIS II v2.2 map also shows a lower potential in the province of Noord-Holland compared to the SGE-study map.

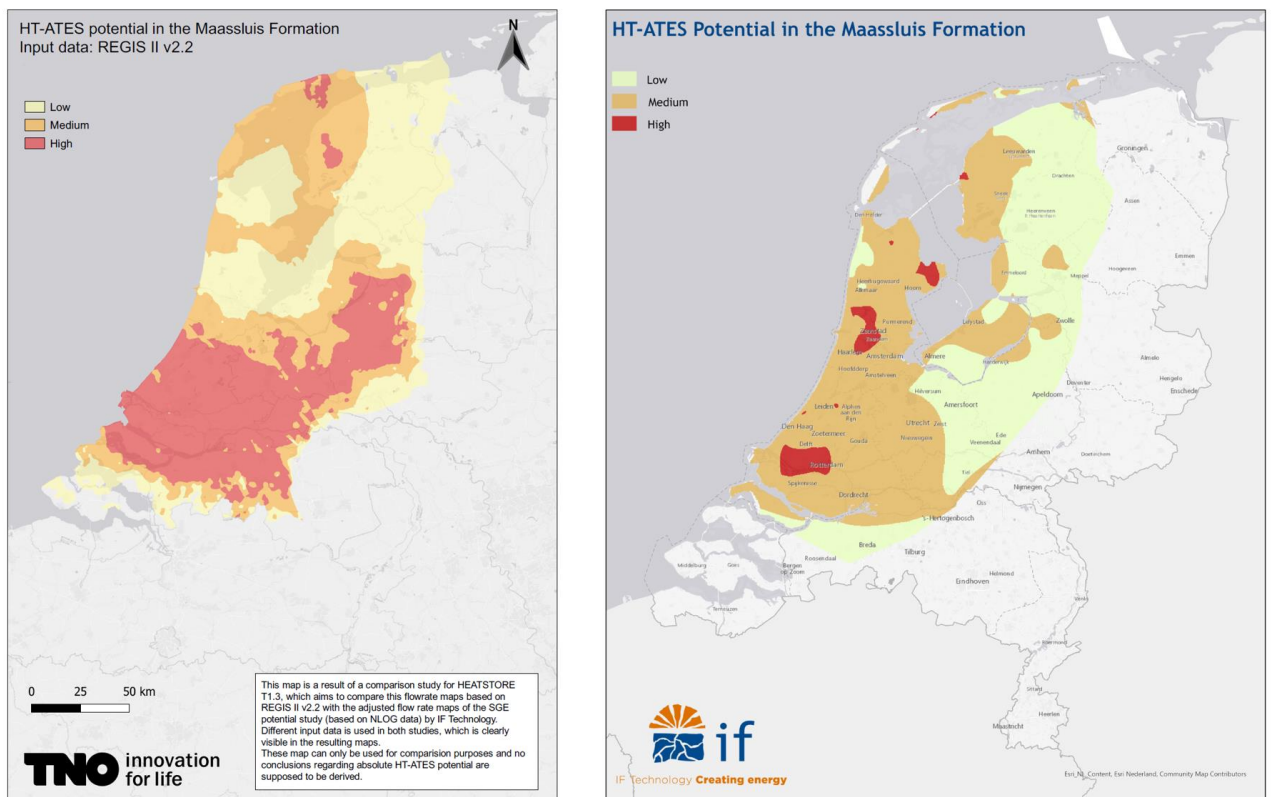


Figure 2-5. HT-ATES potential maps for the Maassluis Formation as derived from REGIS II v2.2 (left) and the SGE-study with input data from NLOG (right).

2.5.2 Oosterhout Formation

Except for the southeast, the Oosterhout Formation is present all over the Netherlands (Figure 2-6), hence at least some potential for HT-ATES may be expected at most locations. Following the REGIS II v2.2 map, the potential is very high in a large region in the southwest, whereas the SGE-study map does only feature high potential in the central-south area. Both maps show medium to very high potential in and around Apeldoorn. The SGE-study map indicates a low potential in the central north part of the Netherlands (Friesland), but according to the REGIS II v2.2 map, the Oosterhout formation is not present there. Note that the number of data points in REGIS II v2.2 is much lower for the Oosterhout Formation than for the Maassluis Formation.

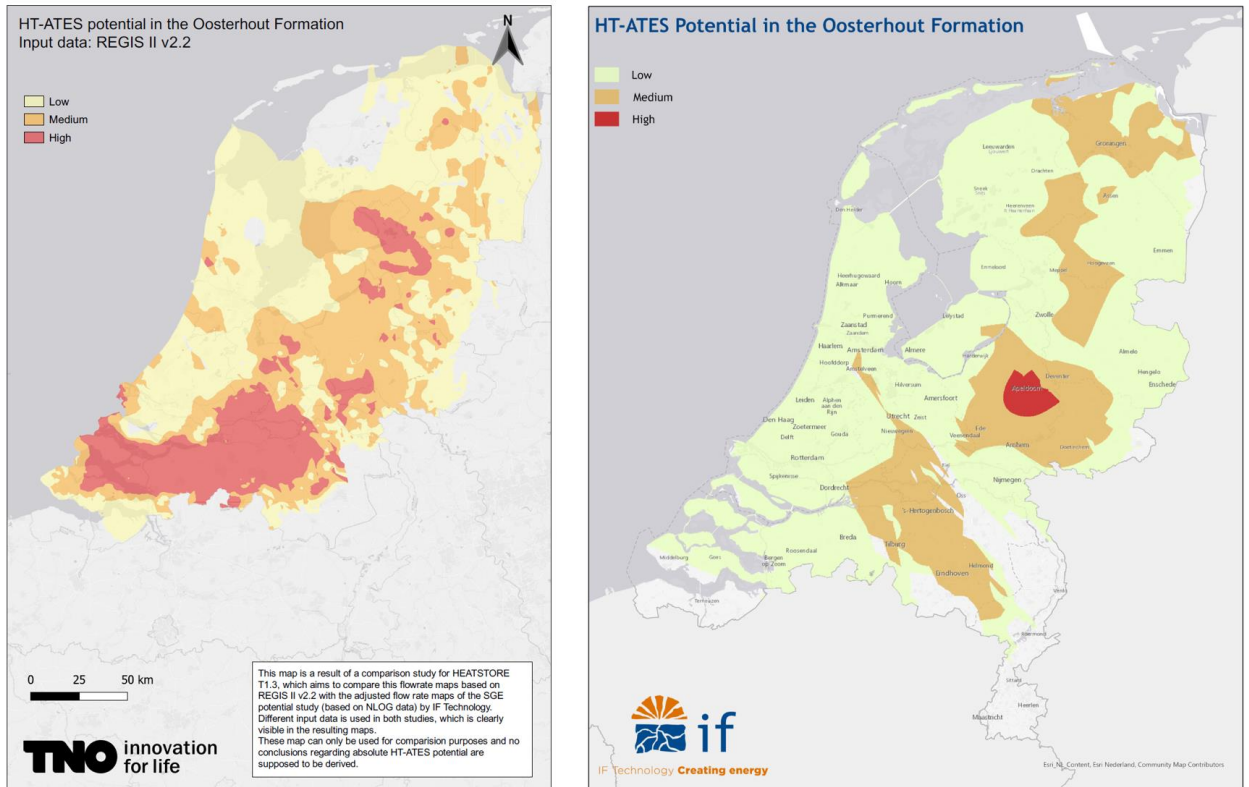


Figure 2-6. HT-ATES potential maps as derived from REGIS II v2.2 (left) and the SGE-study with input data from NLOG (right).

2.5.3 Differences between the maps

The subsurface data behind the potential maps of TNO and IF Technology is different, as well as the workflow used to obtain the potential. The most important differences are:

Input data

- The origin of the (hydro)geological information used to derive the flow rates differs for the two potential maps (Table 2-2): data from the REGIS II v2.2 hydrogeological model are used for the one, the NLOG data for the other. The main differences in these subsurface (hydro)geological information data sources are:
 - o REGIS II v2.2 comprises relatively shallow wells (on average <200 mbgl), whereas NLOG holds the information from deeper oil and gas wells (typically > 2000 mbgl). The shallow parts (0-1000 mbgl) of the oil and gas wells are generally less extensively and accurately logged because the target area was at larger depth.
 - o The number of datapoints is considerably higher for REGIS II v2.2 compared to NLOG, but most datapoints in REGIS II v2.2 do not go deeper than ~200 mbgl.
 - o This means that REGIS II v2.2 is better capable of distinguishing lateral varieties on a smaller scale, but is only accurate in the depth range up to ~200 mbgl. The potential maps based on NLOG (to some extent) complement the REGIS II v2.2 model at greater depths, although the accuracy is less.
- The temperature-correction map used for the REGIS II v2.2-derived potential maps is based on a recently developed temperature map of the Dutch subsurface, whereas the temperature map from the

SGE-study is older. However, the differences are probably limited, meaning that this factor cannot account for large differences between the potential maps.

Workflow

- Both flow rates are calculated based on the NVOE guideline for maximum production rates for low temperature ATES systems, to limit sand production. However, the construction from the various raster files from the REGIS II v2.2 model is a more direct way to derive the potential than adapting the raster-files of the SGE study.
- The interpolation method used in the potential maps is different for the two maps, which may account to some extent for differences in the results.

Table 2-2 - Overview of input data from REGIS II v2.2 and NLOG (used in SGE study)

	REGIS II v2.2 model data	NLOG data used in SGE potential study
Amount of wells included	26376 wells, of which ~90% is in the range of 0-200 mbgl. At a depth of 50 mbgl, the well density is about 1 well per 7 km ²	> 2000 wells from NLOG
Type of wells	Relatively shallow wells: geological, geotechnical, soil investigation wells, drinking water wells, ATES wells.	Mainly deep oil and gas wells
Depth range of wells	Most wells (90%) are located up to 0-200 mbgl	All wells > 500 mbgl
Grid resolution	100 x 100 m cells	not relevant
Lateral spread	Dependent on formation. On average (independent of depth) most wells in the north (Groningen, Friesland, Drenthe) and Limburg and Zeeland areas.	Generally, most data points in the North and South-Holland provinces.
Interpolation method	Kriging interpolation methods (indicator kriging, ordinary block-kriging)	Kriging interpolation methods

2.5.3.1 Link with other work packages: T6.1

In HEATSTORE work package 6.1, a GIS platform on the technical future potential for underground thermal energy storage (UTES) in the countries under study is developed. The potential maps from WP 1.3 will be collected in a GIS 'story map'. For the Netherlands, the potential criteria maps (section 2.4.1) will be shown, as they provide a qualitative and extensive overview of the HT-ATES potential. It has been decided not to publish the flow rate maps online due to the many uncertainties regarding input data and calculations.

2.5.4 Notes regarding all Dutch HT-ATES potential maps

General notes, applicable to all Dutch HT-ATES potential maps presented here:

- The maps focus on the HT-ATES potential in the geological formations of Maassluis and Oosterhout. Younger sandy sediments overlying the Maassluis formation, like the Peize/Waalre, Sterksel, Kreftenheye formations are used by many low temperature ATES systems. These more shallow formations were not included in this study, because they have a high hydraulic conductivity, leading to relatively large heat losses (and associated thermal effects) by buoyancy flow and regional groundwater flow. Furthermore, the possible effects are more critical in these shallow formations because of the presence of other groundwater users and other interests at the surface.
- The potential maps of Maassluis and Oosterhout Formations provide a first order estimation of the HT-ATES potential. Although it offers insights into regional differences of HT-ATES subsurface potential, a more detailed study is needed to investigate the HT-ATES potential at a specific site. The calculated potential flow rates that were used to create the maps provide some insights in the flow rates, but these are not guaranteed. The limited number of data points in combination with the variable quality of the data does not allow for a reliable local evaluation of the HT-ATES potential. Interpolation between datapoints allows the coverage of large areas, but it can result in a false sense of accuracy when based on too little data. The goal of this part of T1.3 was to offer potential maps with various

- formats and construction workflows, to show how various HT-ATES criteria can be applied in different maps.
- The potential maps based on flow rates constructed in this task are based on the NVOE-guidelines for maximum flow rates, to prevent sand production in wells. These are widely followed in the design of Dutch low temperature ATES systems with positive experiences. The fact that very few ATES systems are affected by sand production hints that higher flow rates may be applied safely, especially in deeper, generally better consolidated, aquifers. This was successfully tested in the Dutch HT-ATES demonstration project in Middenmeer, where well tests showed that no significant sand production occurred, even when the applied flow rate was 3.8 times the NVOE-guideline (Drijver, Oerlemans and Bos, 2020). This suggests that significantly higher flow rates may be feasible, which could have large implications for the potential for HT-ATES. Further research into this topic is recommended.
 - The shallow subsurface up to 500 mbgl in the Netherlands consists mainly of unconsolidated sand and clay layers. The hydrogeological properties of these sediments provide a unique set of hydrogeological characteristics that facilitate low temperature and high temperature ATES: sand layers are sufficiently thick and permeable to facilitate high flow rates. Partly because of these favourable conditions, thousands of low temperature ATES systems are successfully applied in NL. The fact that thousands of low temperature ATES systems are successfully applied in the Netherlands indicates that high level knowledge is available, which helps to develop high temperature ATES successfully as well. However, whether HT-ATES is legally permissible is also determined by other factors, like nearby stakeholders and the applicable policies on provincial/municipal levels.

2.6 Conclusions and recommendations on HT-ATES potential in NL

The three different types of subsurface potential maps presented in this chapter illustrate a high subsurface potential at a regional scale for HT-ATES in the Netherlands, especially in the western part of the country, where, conveniently, heat demand is high too (metropolitan area, greenhouses, high geothermal potential). The first type of potential maps are qualitative in nature and were constructed based on eight relevant subsurface criteria for the development of HT-ATES. They give a good impression of the (legal and technical) possibilities for HT-ATES in various geological formations up to ~500 mbgl. The other two types of potential maps are addressed in a semi-quantitative way and are based on calculated flow rates for the Maassluis and Oosterhout Formations, using existing ATES guidelines for the prevention of sand production and well clogging. These maps were constructed based on two different sets of subsurface data (shallow REGIS II v2.2 model input, and input from a SGE study based on NLOG data from deep oil and gas wells). The resulting maps show similarities: generally, the Netherlands has good potential for HT-ATES especially in the western part, which is in line with the qualitative potential maps (based on criteria). Differences between the two “flow rate based” potential maps are primarily explained by the difference in the input data and their datapoint distribution. The potential maps presented here can be used as a first general screening of HT-ATES subsurface potential in the Netherlands. However, for each future HT-ATES project, a site-specific assessment is required to further quantify the subsurface potential for this technique. Note that the potential of a number of shallow formations has not been addressed here, despite the fact that many low temperature ATES systems are successfully operated in these layers. The main reasons are the relatively high permeability, which leads to large heat losses (and therefore low recovery efficiencies) when high temperature heat is stored, and the more intensive use of these shallow formations by existing users (low temperature ATES, drinking water production, etc.) so that possible environmental effects are more critical. Overall, this study demonstrated that much more (hydro)geological data is required to obtain reliable input for the calculation of HT-ATES potential.

A first step would be to perform a quality control on the (shallow parts of the) NLOG data and combine the useful data with the input in the REGIS II v2.2 model to enlarge the data density. Additional data acquisition is highly recommended to further improve the geological model as input for the HT-ATES potential calculations. This is in agreement with the recommendations from D1.1 and D1.2 that point out the importance of performing a test drilling and associated research.

2.7 References

- Deckers, J., Vernes, R., Dabekaussen, W., Dulk, M. Den, Doornenbal, H., Duser, M., ... Witmans, N. (2014). Geologisch en hydrogeologisch 3D model van het Cenozoïcum van de Roerdalslenk in Zuidoost-Nederland en Vlaanderen (H3O – Roerdalslenk).
- Dinkelmann, D., van Bergen, F., & Veldkamp, J. G. (2020). Geologisch model, temperatuurmodel voor de ondiepe ondergrond en potentieelkaarten voor HTO in Nederland. Retrieved from <https://www.warmingup.info/documenten/window-fase-1---b2---potentieel-en-toepassingscondities.pdf>

- Drijver, B., Oerlemans, P., & Bos, W. (2020). Full-scale ht-ates tests demonstrate that current guidelines considerably overestimate sand production risks in deeper unconsolidated aquifers. 1st Geoscience and Engineering in Energy Transition Conference, GET 2020, (November 2020). <https://doi.org/10.3997/2214-4609.202021060>
- Fleuchaus, P., Godschalk, B., Stober, I., & Blum, P. (2018). Worldwide application of aquifer thermal energy storage – A review. *Renewable and Sustainable Energy Reviews*, 94(June), 861–876. <https://doi.org/10.1016/j.rser.2018.06.057>
- Hellebrand, K., Post, R. J., & in 't Groen, B. (2012). *Kansen voor Ondiepe Geothermie voor de glastuinbouw*. Arnhem.
- Huyakorn, P. S., & Pinder, G. F. (1978). A new finite element technique for the solution of two-phase flow through porous media. *Advances in Water Resources*, 1(5), 285–298. [https://doi.org/10.1016/0309-1708\(78\)90042-8](https://doi.org/10.1016/0309-1708(78)90042-8)

3 Screening of National Potential in Switzerland

3.1 Context

In 2007, the Federal Council based its energy strategy on four pillars: energy efficiency, renewable energy, replacement/construction of new large-scale electricity production facilities (including nuclear power plants), and foreign energy policy.

In the wake of the Fukushima reactor disaster in 2011, the Federal Council and Parliament decided that Switzerland is to withdraw from the use of nuclear energy. This decision, together with various other profound changes in the international energy sector, meant that Switzerland's overall energy system would have to be restructured. For this purpose, the Federal Council prepared a new energy policy called "Energy Strategy 2050".

On 4 September 2013, the Federal Council submitted a bill to Parliament concerning the total revision of the Federal Energy Act. Parliament adopted the revised Act on 30 September 2016 and the Swiss electorate approved it by a clear majority in a referendum that was held on 21 May 2017. The new Federal Energy Act entered into force on 1 January 2018.

Switzerland has therefore, reoriented its energy policy with the intent to gradually phase-out nuclear energy and to gradually transform Switzerland's energy system, without jeopardising neither the high level of security of supply nor the low-cost of its energy supply. In the future, energy efficiency will have to be significantly improved, the proportion of renewable energy sources will have to be increased and energy-related CO₂ emissions will have to be reduced. The energy strategy is closely linked to climate policy, as almost three-quarters of greenhouse gas emissions in Switzerland are caused by the use of fossil fuels. Switzerland has committed itself to halving its greenhouse gas emissions by then compared to 1990 levels. In addition, based on the latest scientific findings of the Intergovernmental Panel on Climate Change (IPCC), the Federal Council decided on 28 August 2019 that by 2050 Switzerland should no longer release more greenhouse gases into the atmosphere than can be absorbed by natural and artificial reservoirs (zero net emissions).

UTES systems can provide a solution to contribute reaching the 2050 strategy, however Switzerland, despite having one of largest market for ground-source heat pumps, only few examples of HT-UTES have been tested or implemented in the past (Kallesøe et al, 2019). Additionally, a screening of the potential has never been carried out since now. In the framework of HEATSTORE, the Swiss potential of HT-ATES is evaluated according to the public data available, by combining subsurface data (e.g. depth of the targets, thickness of the targets, petrophysical parameters, temperature distribution at different depth) and energy data (e.g. heat demand and excess heat configurations and distributions, thermal network distribution) in order to identify the most promising areas for potential future implementations. At this stage economical, regulatory and socio-environmental constraints will not be taken into account.

3.2 Methods

This study focusses on the development of a framework for the assessment of the favourability for HT-ATES development in the Swiss Molasse Plateau (SMP) centred on multi-criteria spatial analysis based on the combination the geologic plays controlling the geologic features suitable of interest for HT-ATES implementations and the energy system components of excess heat and heat demand as well as proximity to thermal networks and waste incineration plants. The choice of focussing on the SWM was driven by the availability of subsurface data as the 3D geologic model available from Swisstopo only covers this region.

Two main reservoirs have been identified in the Cenozoic Molasse (e.g. target of the Bern pilot site) and the Upper Mesozoic carbonates (e.g. target of the Geneva pilot site). Additionally, a minimal underground temperature threshold is set to 25°C which is the temperature commonly considered as separating low temperature ATES from HT-ATES systems. These two units show different lithological, petrophysical and hydraulic conditions, locally enhanced by lithological heterogeneities in the Cenozoic Molasse and by enhanced fracture conditions thanks to the presence of fault corridors in the Mesozoic. A maximal depth of 2000m was set as boundary as it was arbitrarily considered as a reasonable depth for the techno-economic favourable implementation of HT-ATES systems (Figure 3-1).

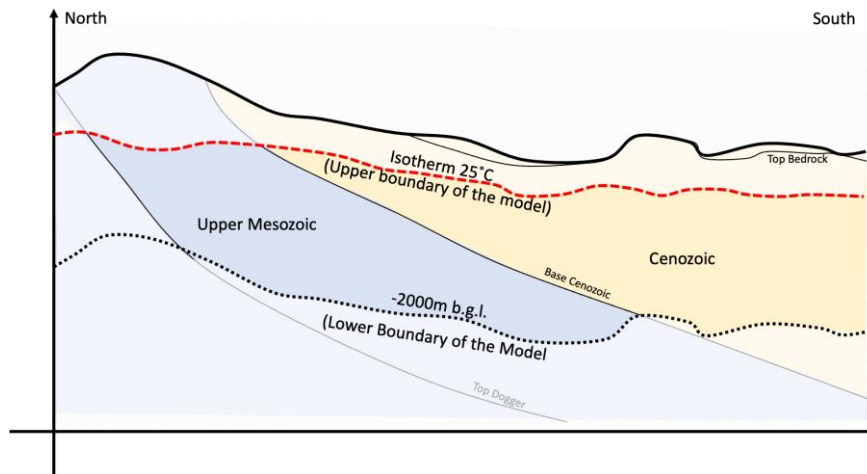


Figure 3-1 – Sketch of the subsurface of interest along a hypothetical N-S oriented cross-section across the SMP.

Selecting favourable sites for HT-ATES systems is a geospatial multi-criteria decision problem. In this study we applied a five-step method to locate favourable areas in SMP. The framework implemented in the favourability assessment is shown in Figure 3-2.

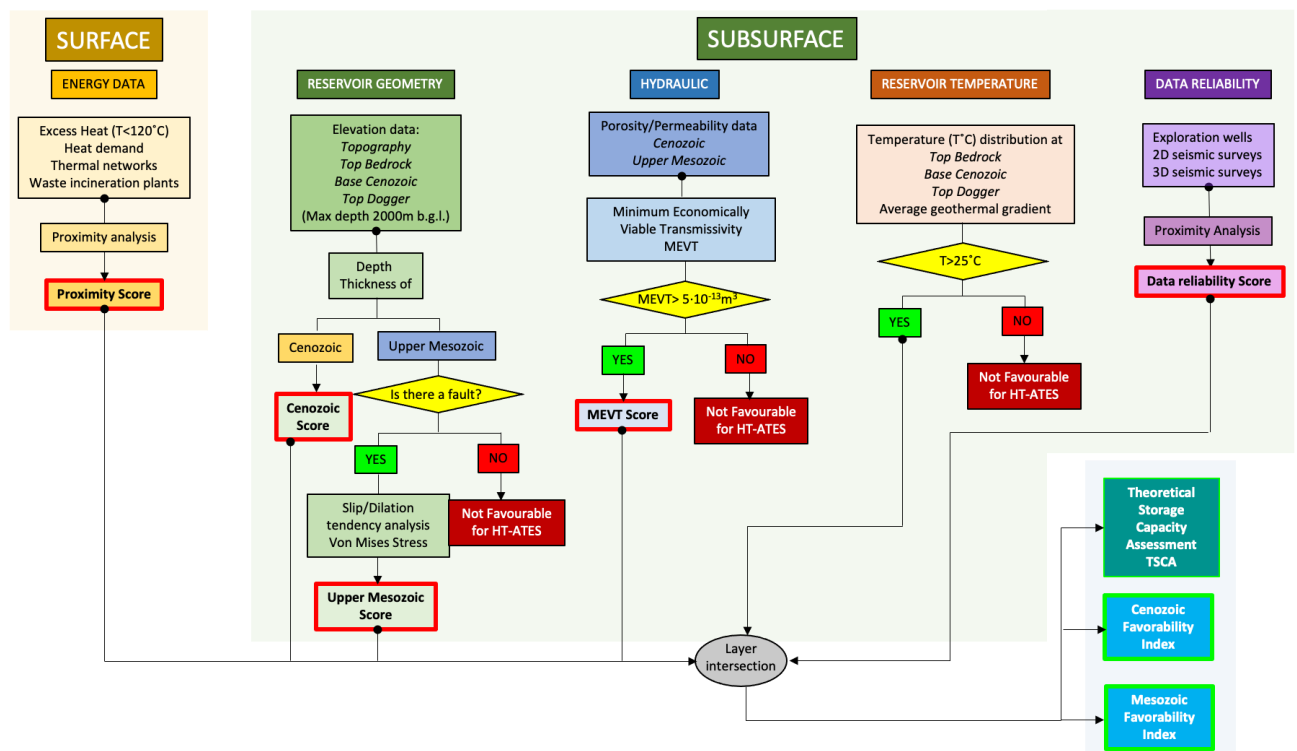


Figure 3-2 Overarching framework for the assessment of favourability in the SMP.

The framework can be broken down as follows:

1. First, a geothermal play analysis approach was applied to identify and weight the subsurface elements controlling the circulation of fluids in the area. This step focussed on the analysis of the depth and thickness of the two main reservoirs as well as the subsurface temperature distribution, the presence of faults and the quantification of their slip/dilation tendencies, considered as key factors to differentiate between fault structures prone to be permeable with respect to faults prone to be tight in the Upper Mesozoic carbonates. The heterogeneous fault data include various fault types (e.g. strike-slip, thrust, etc.) and differ largely in terms of geometry. Some faults are very large (as for example some of the

large thrust faults), while some other faults have been modelled as multiple small fault patches. The eastern part of the Swiss molasse basin present less faults than the western part. This could be due to an interpretation and/or knowledge bias since different work groups have been interpreting structures in various section of the basin according to different type and quality of the data available (i.e. different generations of 2D seismic lines). Another criteria that was implemented is the Minimum Economically Viable Transmissivity defined as the transmissivity below which HT-ATES is sure to be economically unattractive (Birdsell et al., 2021) which was set to $5 \cdot 10^{-13} \text{ m}^3$. All values of transmissivity below such threshold were considered as not-favourable for HT-ATES.

- Secondly a data reliability assessment was carried out based on the proximity from the main source of subsurface data (i.e. exploration wells and 2D-3D seismic surveys). The distance between the same type of data sources was generated using Euclidian distance with the values of the resultant layer having a resolution of $100 \text{ m} \times 100 \text{ m}$, which was selected based on the heat demand grid cell size. Because the nature of each dataset, the grids of each dataset must be standardized. We selected the maximum and minimum method as the most suitable for the study goals. The standardized pixel value x'_{ij} of the grid x_{ij} was thus defined between the minimal value s_{\min} "0" and the maximal value s_{\max} "1", being "1" the closer to the data and 0 the farthest, according to the equation:

$$x'_{ij} = (x_{ij} - x_{ij}^{\min}) \cdot (s_{\max} - s_{\min}) / (x_{ij}^{\max} - x_{ij}^{\min}) + s_{\min}$$

Weighting was given to each dataset according to Table 1, in order to take into account, the proximity and the quality of the information that each dataset can provide to assess the favourability.

Table 3-1. Criteria for subsurface data reliability.

Data Type	Proximity	Score
Exploration wells	0-200	10
	200-1000	Linear interpolation 1-10
	>1000	0
2D seismic	0-200	7
	200-15000	Linear interpolation 1-7
	>15000	0
3D seismic	-	9

- The third step was to compute the storage capacity according to the 3D geometries and temperature distribution from the GeoMol model and petrophysics properties from literature (Guglielmetti and Moscariello, 2021 and references therein). The reservoirs are considered homogeneous since at this scale there are no detailed data provided for more specific, site-specific analysis. Therefore, the results presented serve as an indication of the potential and not as absolute values.

Table 3-2. Petrophysical data used in this study for storage capacity assessment.

Stratigraphic units	Min	Mean	Max	Faulted
Cenozoic permeability (mD/m²)	0.1 / 9.869×10 ⁻¹⁷	13.1 / 1.293×10 ⁻¹⁴	50.75 / 5.009×10 ⁻¹⁴	-
Cenozoic density (kg/m³)	2100	2300	2650	-
Mesozoic permeability (mD/m²)	0.01 / 9.869×10 ⁻¹⁸	3.5 / 3.454×10 ⁻¹⁵	350 / 3.454×10 ⁻¹³	300 / 2.961×10 ⁻¹³
Mesozoic density (kg/m³)	2500	2600	2700	2600

Fluid properties of density, viscosity and heat capacity are computed based on IAPWS97 (Huber et al., 2009), as implemented in the python package IAPWS (Romera, 2020).

The analytical model computes the amount of power that can be stored in an HT-ATES system. The analytical formulation is based on a modified formulation of the maximum flow rate that can be used without hydraulically fracturing the reservoir as previously presented by Birdsell et al., (2021). The storage capacity is computed as follows:

$$P_s = \frac{2\pi kh}{\mu \ln(L/D)} ((a p_r - p_f) g d) p_f C_{p_f} \Delta T$$

in which P_s is the storage capacity (W), k is the permeability (m²), h is the reservoir thickness (m), p_f is the fluid density (kg/m³), p_r is the rock density (kg/m³), a is the parameter indicating the ratio of the minimum principal stress to the lithostatic stress (-), g is the gravitational acceleration (m/s²), d is the middle reservoir depth (m), C_{p_f} is the fluid specific isobaric heat capacity (kJ/m³), ΔT is the temperature difference between the injected fluid temperature and the middle reservoir depth temperature (K), μ is the fluid viscosity (Pa/s), L is the well spacing (m) and D is the well diameter (m). The input parameters that are space dependent (i.e. permeability, reservoir thickness, fluid density, rock density, middle reservoir depth, fluid specific heat capacity, fluid viscosity and ΔT) are computed on a grid of 100 x 100 m for the whole of Switzerland according to data availability. A well spacing equal to the diagonal of the 100 x 100 m grid (141.4m) is used throughout in accordance with previous HEATSTORE studies (Birdsell et al., 2021; Daniilidis et al., 2021; Mindel et al., 2021). Constant inputs are summarized in Table 3-3.

Table 3-3. Analytical model inputs.

Parameter	Value
min principal stress/lithostatic stress (-)	1
gravitational acceleration (m/s ²)	9.81
well spacing (m)	141.4
well diameter (m)	0.261

- The fourth step, was a) to extract the excess heat data (Zuberi et al., 2018) with heat temperature < 120°C and homogenise the excess heat and heat demand data (www.map.geo.admin.ch) in order to have the same units (MWh·year⁻¹·hectare⁻¹) and b) carry out proximity analysis with respect to the thermal networks and waste incineration plants. The temperature threshold of 120°C was identified as Based on the literature (Zuberi et al., 2018), industrial processes in Swiss industries are classified into low (≤120°C), medium (120–380°C) and high temperature (≥380 °C). Also, thermal networks can operate at those temperature and higher storage temperatures might have negative impacts on subsurface elements (i.e. because excessive temperature difference between natural reservoir temperature and injected fluid and associated impacts on mineral dissolution/precipitation and scaling/corrosion at the borehole/plant levels) at the investigated depth range. The proximities scores are defined assuming a cost for the distribution pipes 1400 CHF/m (pipe diameter 100mm) even if higher prices up to 1900 CHF/m can also be considered for pipes with nominal diameter of 200mm (Suisse Energie, 2018). For instance installing a pipe at a distance between 1 and 2.5km can add significant costs (up to 3.5M CHF) to the entire HT-ATES project which can strongly hinder its overall feasibility.

Table 3-4. Input criteria for proximity from thermal networks and waste incineration plants.

Data Type	Proximity	Score
Thermal Networks	0-1000	Linear interpolation 1-10
	1000-2500	
	2500-5000	
	5000-10000	
Waste Incineration Plants	0-1000	Linear interpolation 1-10
	1000-2500	
	2500-5000	
	5000-10000	

5. The final step was then to integrate the different favorability into a combine favorability index, calculated, multiplying the proximity score by the weight:

$$I(x_{ij}) = x'_{ij} \cdot w$$

The final favorability index that combines all the individual favorability indexes is given by the weighted average scheme:

$$I_{comb} = \frac{\sum_{i=1}^n I(x_{ij})}{\sum_{i=1}^n w}$$

3.3 Available data

3.3.1 District heating network

In Switzerland we can retrieve the following indicators (map.geo.admin.ch):

- **Thermal networks:** The demand for heat and cooling is a key element in the strategic planning of thermal networks. Building a thermal network is only viable if sufficient sales turnover can be generated from heat and/or cooling. In strategic planning, heat demand is used to identify large connected areas that may be appropriate for a thermal network. Areas with a heat density of at least 700 MWh/a per hectare are considered suitable.

Thermal networks – including district heating, local heating or district cooling networks – are systems that provide a number of separate buildings with thermal energy. They supply heat to customers through pipelines that carry water or steam. As well as district heating networks there are also district cooling networks – which is why the more general term 'thermal networks' is now used. The energy supplied by thermal networks does not necessarily come from renewable sources, but these systems are often characterized by their low CO₂ emissions, for example when based on heat recovered from waste incineration. District heating is an excellent way of making use of waste heat or renewable energies and is therefore becoming increasingly important. District heating is defined as a system that provides customers with heat that is generated in a central plant and supplied through pipes in the form of hot water or steam; the performance of individual systems varies widely, from less than 100 kW to over 1 GW. The supply of heat to one group of recipients only is not regarded as district heating. The geodata on thermal networks document the district heating networks currently operating in Switzerland and are based entirely on information provided by the network operators. The data are unofficial, are not legally binding, and are provided simply as information for the public.

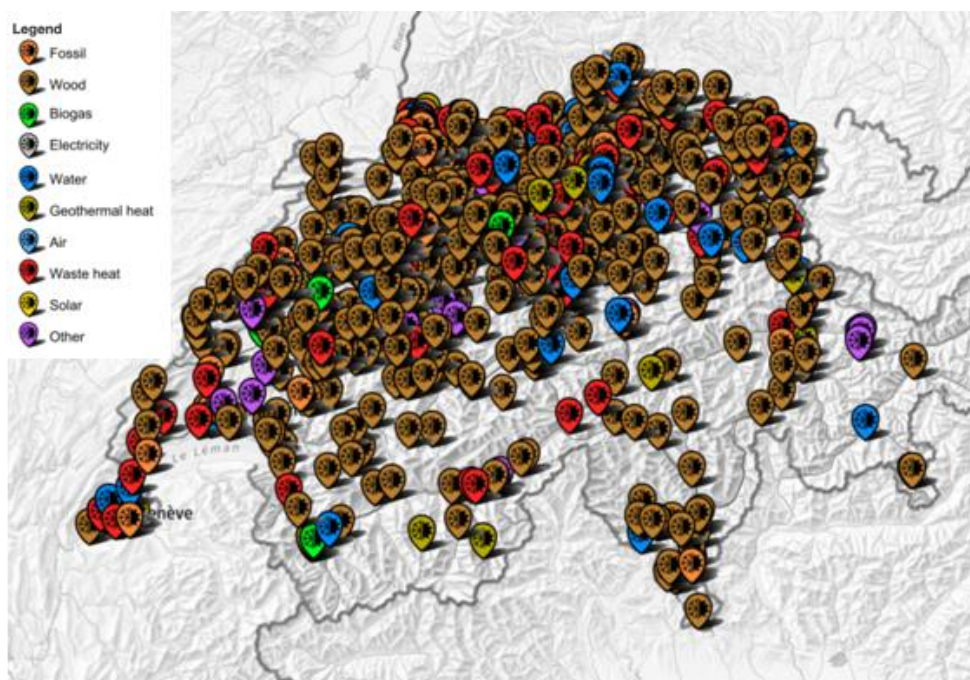


Figure 3-3. Thermal grids of Switzerland (source: map.geo.admin.ch).

- **Heat demand from residential, commercial buildings, and industry:** Of most interest for thermal networks is the heat demand from residential and commercial buildings, since most of such buildings can be served at low temperatures ranging from around 12°C to maximum 90°C.

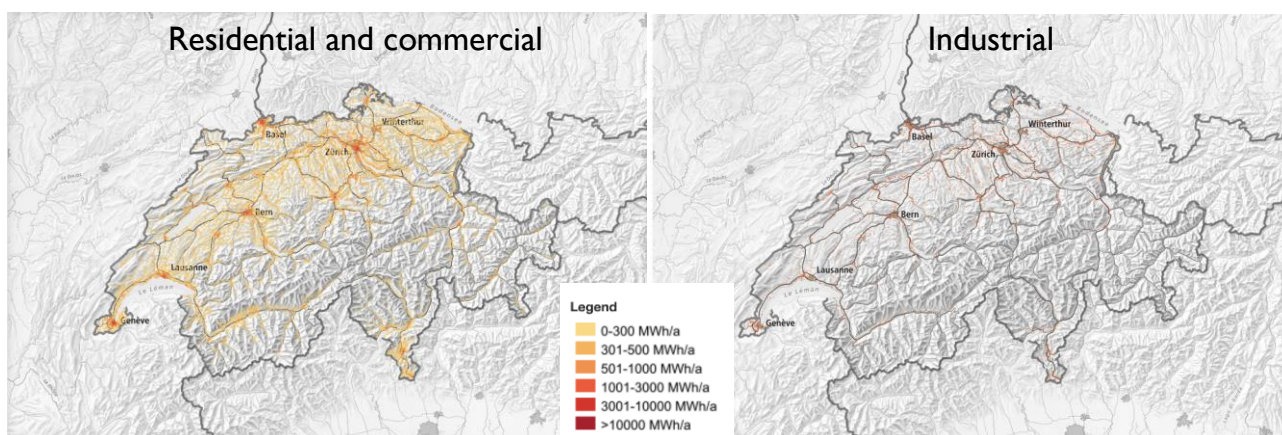


Figure 3-4. Heat demand map of Switzerland (source: map.geo.admin.ch).

- **Heating and cooling sources:** Heat and cooling sources are local, renewable and CO₂-free energy sources which may be of interest for heat production in thermal networks. Nowadays, only renewable or CO₂-free energy sources are considered for heat generation in thermal networks, though peak demand may still be met by fossil fuels. Such sources include waste heat, ambient heat and biomass. While biomass (e.g. woodchips) can be transported almost without restriction, waste heat and groundwater are restricted to a particular location. In areas with high heat demand, such geographically restricted heat sources can be considered for use if the local conditions are suitable. In this study we took into municipal incinerators as these are known sources of excess heat at relatively high temperature. On the contrary, waste heat from tunnels and special incinerators provide no heat potential. Specifically, regarding waste incineration plants, in 2017, Switzerland had 30 municipal waste incineration plants each with a capacity of between 30,000 and 230,000 tonnes per year. About four million tonnes of combustible waste from Switzerland and abroad is incinerated to generate

thermal energy in municipal incinerators. The heat generated during combustion is used to produce electricity, operate district heating networks or as process heat in industrial plants. In 2017, the 30 municipal incinerators produced a record amount of energy totalling 4,036 gigawatt hours (GWh) of heat and 2,338 GWh of electricity. They thus contribute around 2.5 percent of Switzerland's total energy requirements and just under 4 percent of the country's overall electricity production. The geodata document the current volume of recycled waste and the amount of energy generated and supplied. All information is based on the data provided by the plant operators. The information is for the general public and does not constitute official information or legally binding statements.



Figure 3-5. Waste incineration plants in Switzerland (source: map.geo.admin.ch).

3.4 Waste heat

Typically, 70% of the total final energy demand in the industry sector is used for process heat. A substantial share of this energy could be provided by excess heat recovery. Excess heat recovery can be used to produce process steam, other types of process heat, district heat, and electricity. However, as pointed out by Zuberi et al. (2018), challenges associated with harnessing excess heat are

- its occurrence in different forms,
- non-continuous availability,
- insufficient temperature levels,
- the need for heat transfer,
- the distance between excess heat source and sink

The study carried out by Zuberi et al. (2018) evaluates the techno-economic excess heat recovery potential in the Swiss industry through exergy and energy analysis and provides an overview of the spatial distribution of the potential by temperature level. The total amount of potentially recoverable excess heat is estimated at 14 PJ per year, i.e. 12% of the total final energy and 24% of the total process heat demand of Swiss industry in 2016. However, the economic potential amounts to only 5% and 10% if a payback period of 3 and 4 years is assumed, respectively. This study highlights how long payback times of heat recovery measures, and a high percentage of low-quality and small heat streams are the most important barriers to energy efficiency improvement in Swiss industry.

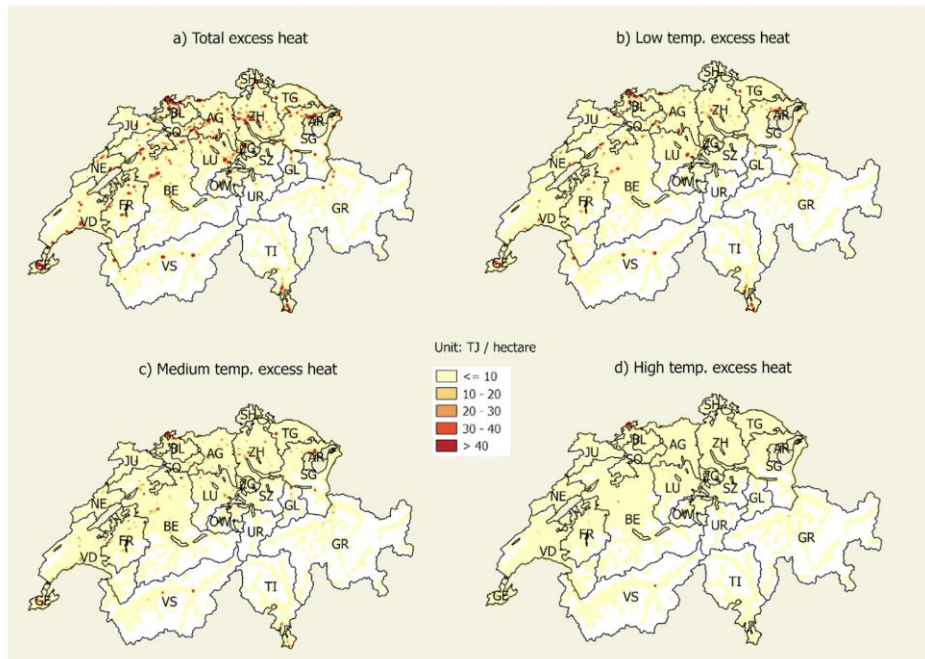


Figure 3-6 – Heatmaps of excess heat sources of Swiss industry (from Zuberi et al. 2018).

Chambers et al. (2019), applied a spatial clustering method to link potential supplies and demands, and monthly supply and demand curves are used to calculate the potential for Industrial Excess Heat (IEH) supply subject to spatiotemporal constraints. A further analysis deals with the technical potential for seasonal storage to shift surplus IEH energy from summer to winter. A total resource of 12TWh/y of IEH was found, but spatial and temporal constraints limited its utilisation to between 7.7TWh/y and 10.5TWh/y depending on the scenario considered. 17.4% of total heat demand could be supplied by IEH using low temperature DHN and seasonal storage.

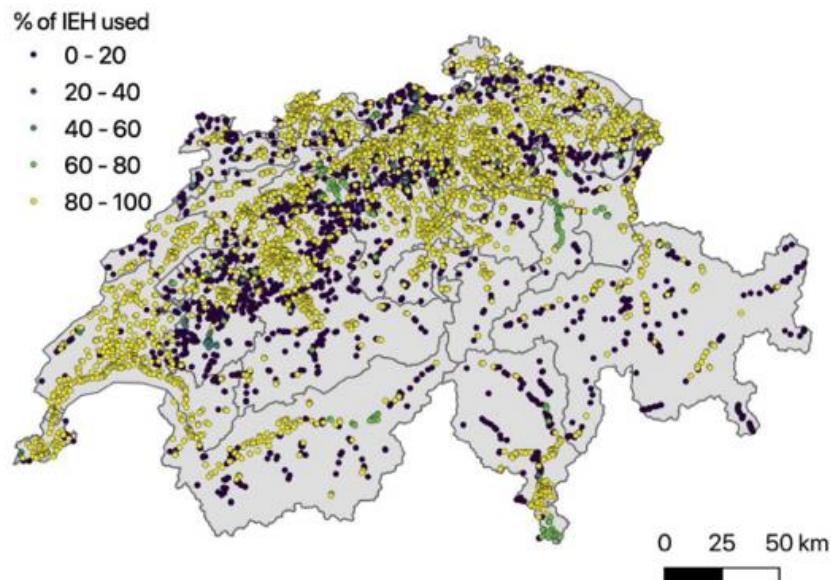


Figure 3-7 – Distribution of the percentage of local IEH that can be directly used by local LTDH systems (from Chambers et al. 2019).

The study carried out by Chambers et al. (2019) shows how IEH could supply up to 17.4% of heat demand in Switzerland when using Low Temperature District Heating (LTDH) technology with seasonal storage and combined with energy savings. However, the spatial analysis of monthly heat balance found that it was not possible to fully use the entirety of the available IEH supply even when using seasonal storage. A large diversity

was found across Switzerland in terms of available IEH, temperature levels, and local utilization potential. The potential for heat from IEH was found to be much smaller than suggested in previous studies for Europe, mainly because Switzerland has minimal thermal electric power generation and relatively little heavy industry such as metals processing. Seasonal storage was considered as an option for recovering additional IEH by storing excess in the summer months. It was found that seasonal storage offers a significant theoretical potential when coupled with LTDH technology, enabling an additional 1.72 TWh/y of IEH to be utilised. In general, seasonal storage could be a convenient method to pool different heat sources and simplify matching of supply and demand by acting as a buffer.

3.5 Subsurface data

Geological, thermal, petrophysical and hydrogeological data can be retrieved by a set of public sources to assess depth, volume, temperature and water quality in different potential reservoir formations.

3.5.1 Geologic data

Geologic data as surfaces limiting the main geologic units and main fault corridors are available, under request to Swisstopo, from the GEOMOL 3D geologic model of the Swiss Molassic Plateau.

This model includes the Molassic sedimentary sequence and the Mesozoic carbonate units which are the targets for the Bern and Geneva regions respectively, allowing the results from the two sites to be used for the potential assessment at the national scale.

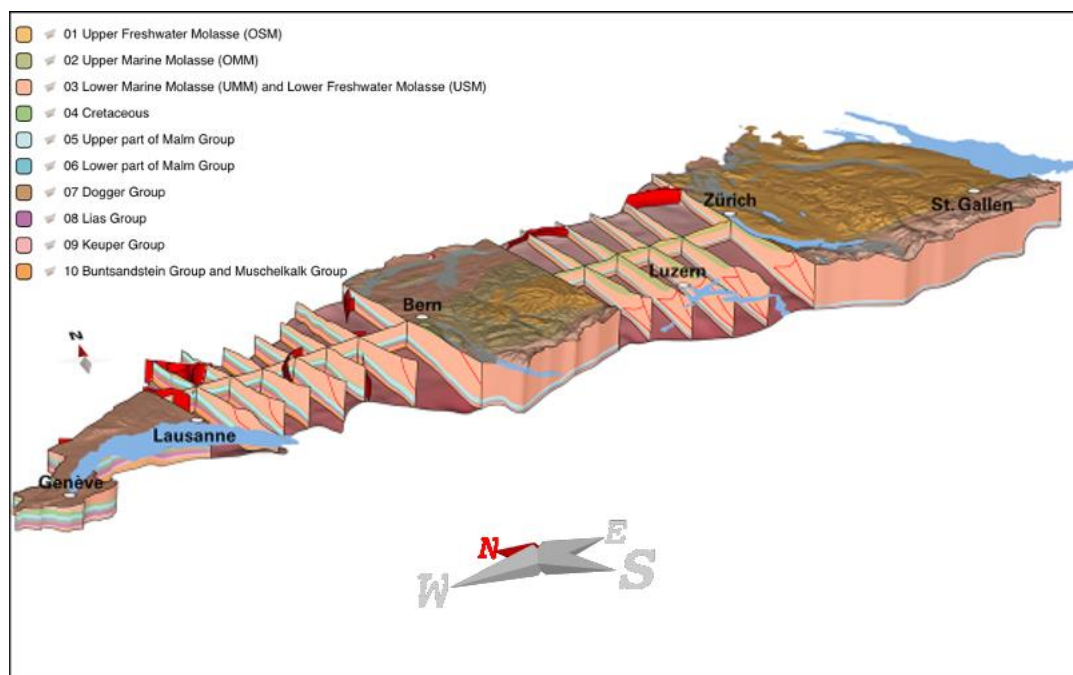


Figure 3-8. 3D geologic model of the Swiss Molasse Plateau (from swisstopo: <https://viewer.geomol.ch/webgui/gui2.php?viewHash=a912caa0eff47583a1e478a4f2b29bd5>).

Figure 3-9 shows the GeoMol dataset available for our analyses and includes more than 550 fault surfaces (version GeoMol18, Allenbach et al. 2017).

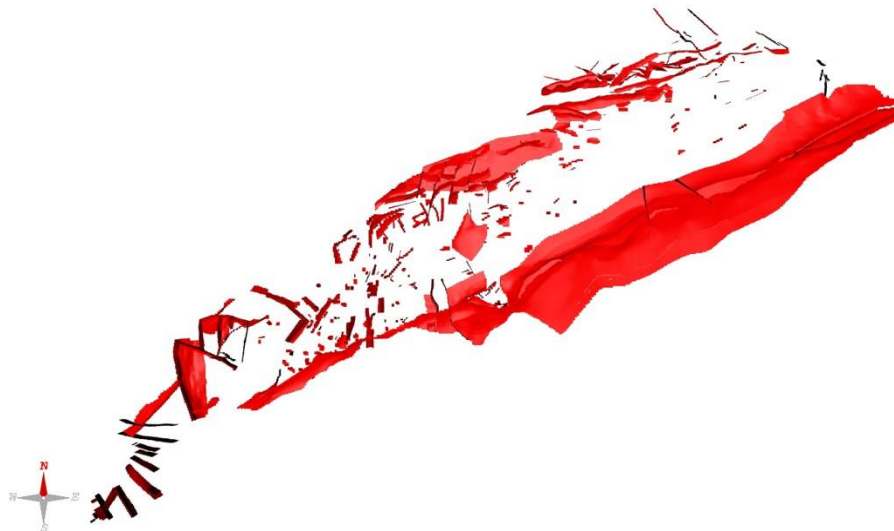


Figure 3-9. View from GeoMol18 modelled faults (figure produced from <https://beta.swissgeol.ch/>).

The depth of the 25°C isotherm, representing the upper boundary of our model, the Base Cenozoic and the Base Upper Mesozoic (down to max 2000m b.g.l.) as well as the thickness of the Cenozoic and Upper Mesozoic units considered in this study are shown in Figure 3-10.

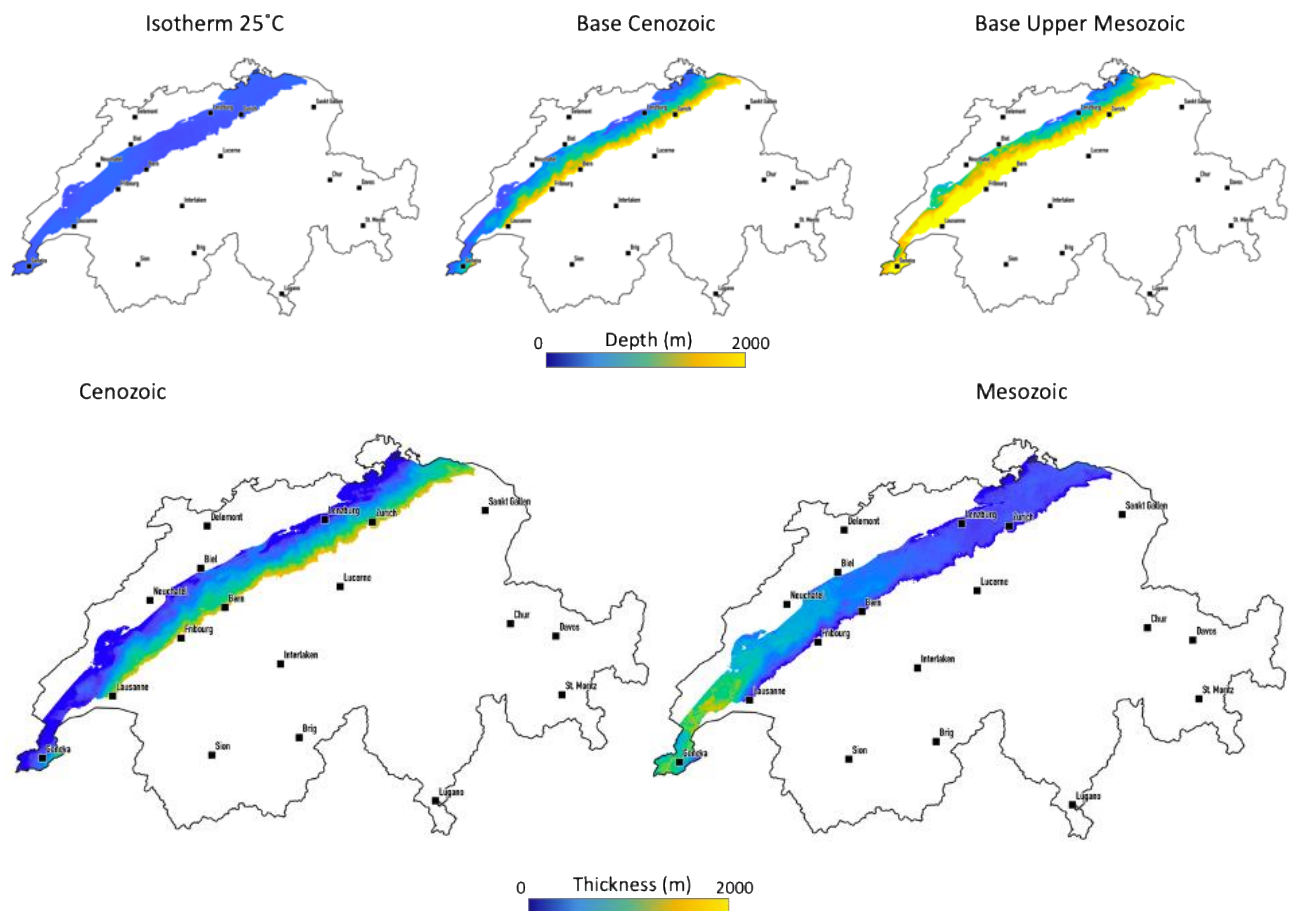


Figure 3-10. Depth and thickness of the geologic horizons of interests (figure produced from data retrieved from <https://beta.swissgeol.ch/>).

3.5.2 Temperature data

Temperature distribution in the subsurface on selected surfaces representing seismic marker horizons, fixed depths below ground level or isotherms are also available from the GEOMOL platform and the associated «Temperature Model - Data» map on map.geo.admin.ch. The horizon surfaces are taken from the GeoMol15 geological 3D model and the temperatures from the GeoMol15 temperature model. This temperature block model is derived from a FE-method temperature model (Geowatt AG, 2015), which is based primarily on 31 vertical temperature profiles and the horizon surfaces from the Seismic Atlas of the Swiss Molasse Basin (2012). The FE temperature modelling method assumes conductive heat flow only and does not consider convective heat flow.

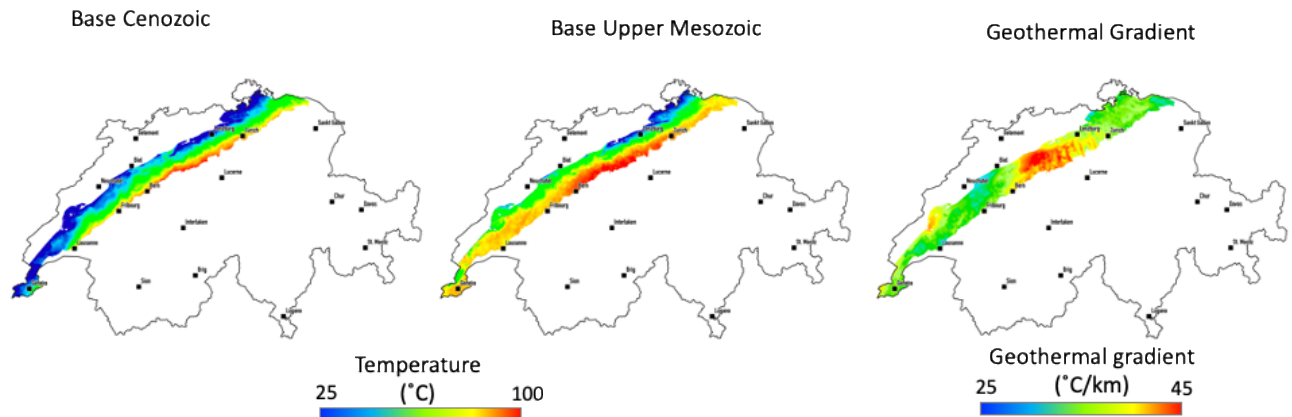


Figure 3-11. Example of temperature distribution map across the Swiss Molasse Plateau (source: map.geo.admin.ch).

3.5.3 Petrophysical data

A compilation of porosity and permeability literature data is shown in Table 3-5.

Table 3-5. Porosity and permeability data (modified from Guglielmetti & Moscariello, 2021).

Geologic Unit	Data Type	Data Source	Density (kg/m ³)			Porosity (%)			Permeability (mD)		
			min	Max	Avg	min	Max	Avg	min	Max	Avg
Cenozoic	Literature	Abdelfettah et al., 2014; Adamer & Montadon, 2000; Altwegg, 2015; Altwegg, et al., 2013; Mauri et al., 2017; Rusillon, 2018; Wagner et al., 1999, GeoMol, 2015, Kälin et al, 1992	2000	2600	2400	4.3	9.6	6.84	0.1	50.75	13.1
	Outcrop, Well Log*	Rusillon, 2018	2200	2500	2400						
	Well cores (bulk)	Rusillon, 2018	2680	2730	2700	3.2	18.6	11.2			
Lower Cretaceous	Literature	Abdelfettah et al., 2014; Adamer & Montadon, 2000; Altwegg, 2015; Altwegg, et al., 2013; Mauri et al., 2017; Rusillon, 2018; Wagner et al., 1999, GeoMol, 2015	2500	2700	2600	0.6	1.8	1.15	0.02	1.8	0.9
	Well Log*	Rusillon, 2018	2500	2750	2650						
	Well cores (bulk)	Humilly-2 well cores (bulk)	2700	2700	2700	6.2	13.8	11.1			
Upper Jurassic	Literature (Tithonian)	GeoMol, 2015				0.5	18	3.15	0.07	0.07	0.07
	Literature (Kimmeridgian)	GeoMol, 2015				0.6	10.8	5.38	<0.01	1.83	0.46
	Literature (Oxfordian)	GeoMol, 2015				0.7	8.33	2.09	0.01	1.4	0.15
	Well Log*	Rusillon, 2018	2600	2700	2700	0.1	9.98	0.4			
	Outcrop, Well Log*	Rusillon, 2018				0.1	10.4	2.4			
	Well cores (bulk)	Rusillon, 2018, Hefny et al. 2020	2700	3500	2700	0.6	13.3	2			

3.5.4 Borehole and Seismic data

Figure 3-12 shows the location of the exploration wells and the 2D-3D seismic data over the study area.

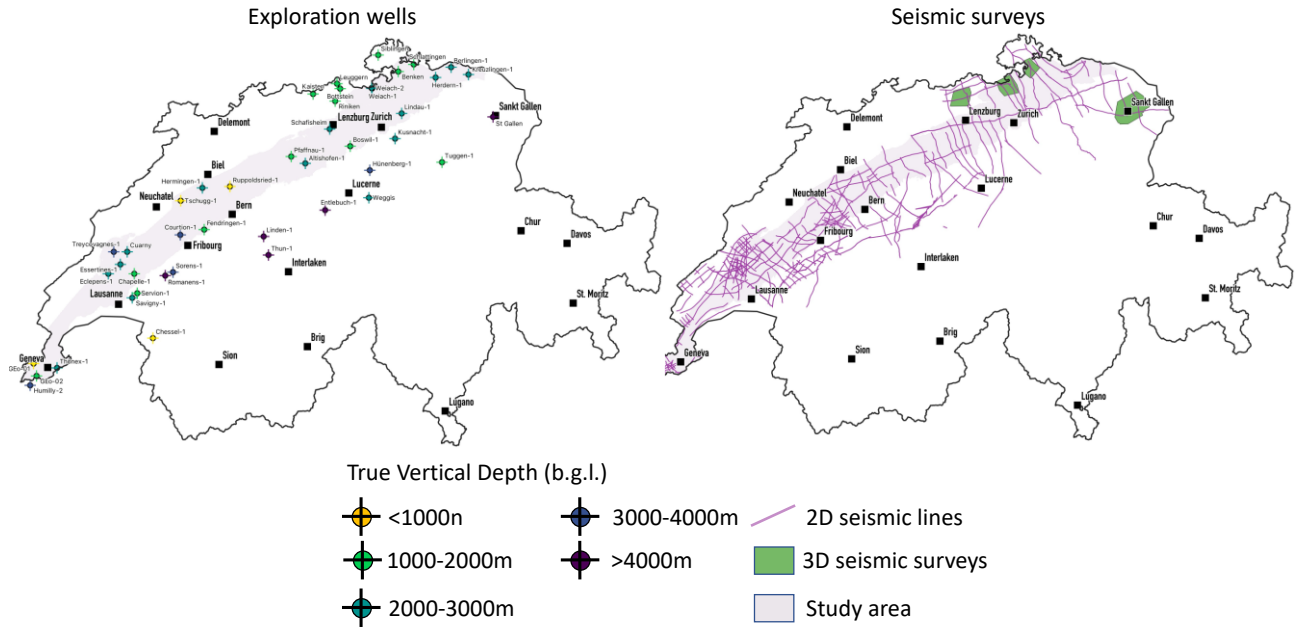
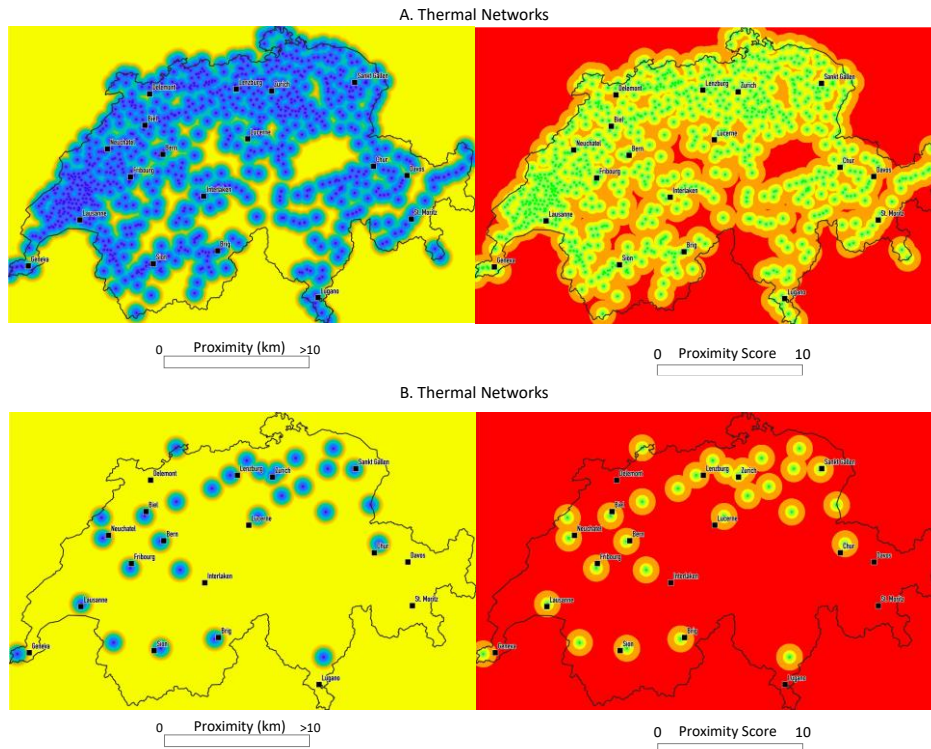


Figure 3-12. Borehole and seismic data (source: map.geo.admin.ch).

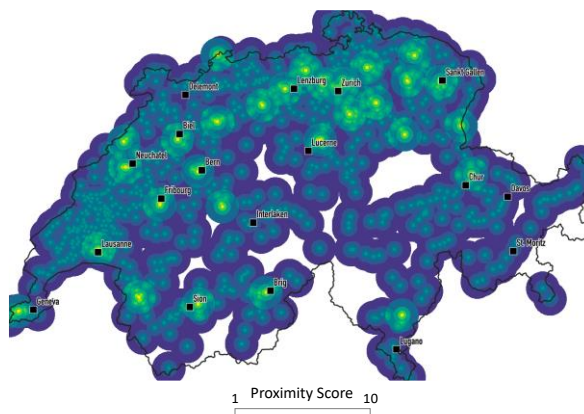
3.6 Results

3.6.1 Proximity analysis of surface components

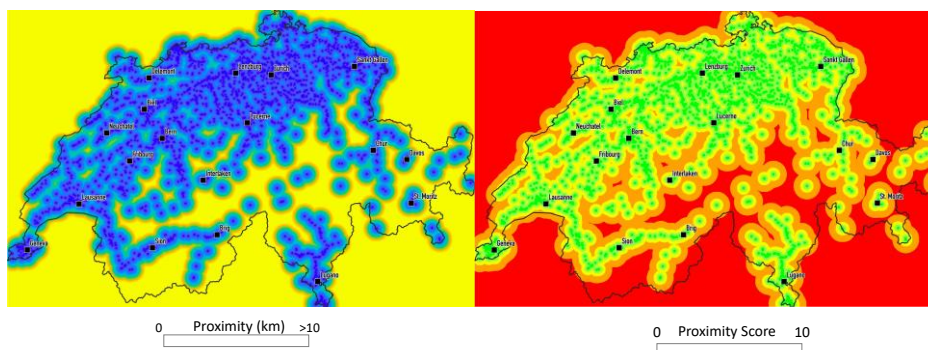
The results of the combination of the proximity analysis for the thermal networks and waste incineration plants indicates that in general thermal networks are rather homogeneously distributed across the SMP where the highest concentration of waste incineration plants can be observed, in particular in the North-Eastern part of the Plateau resulting in a highest favorability in that region compared to the Western part (Figure 3-13 A-C).



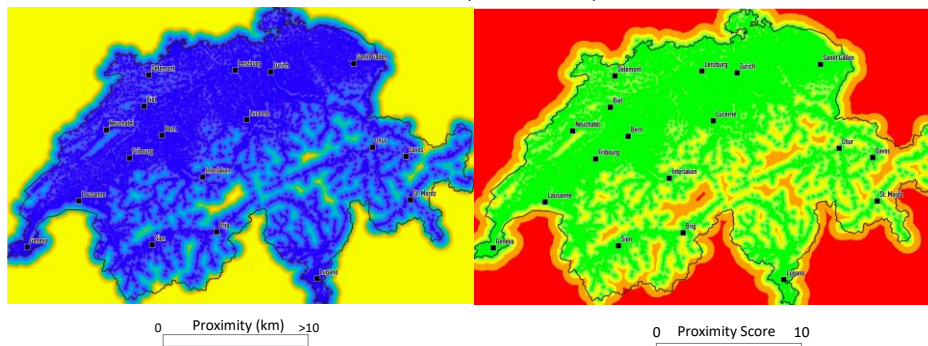
C. Proximity Score



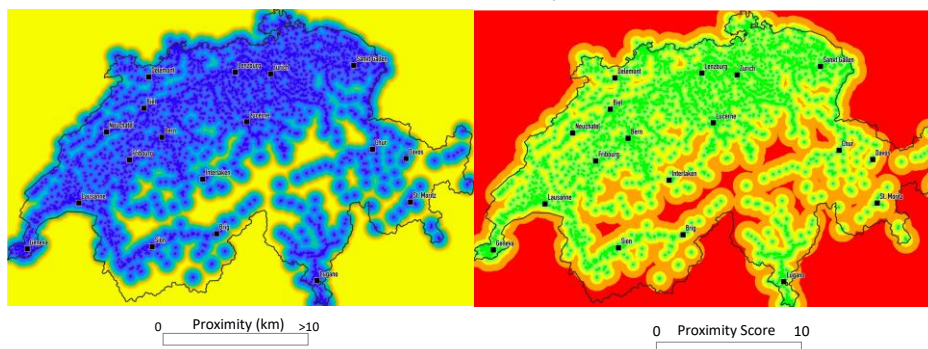
D. Excess Heat



E. Heat Demand (Home & Services)



F. Heat Demand (Industry)



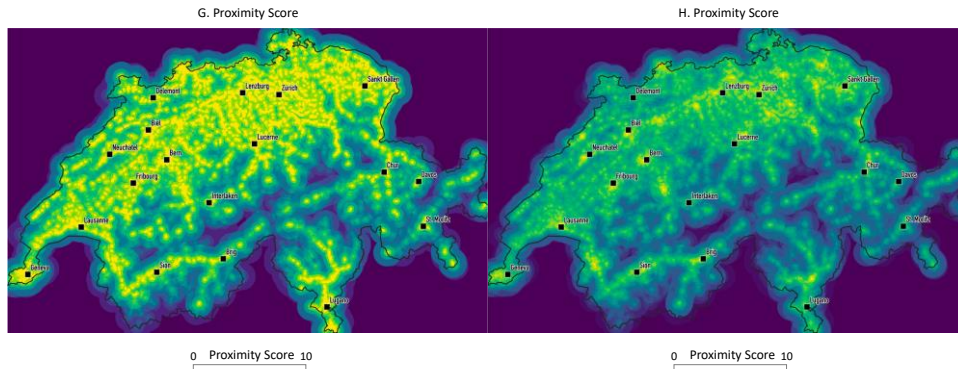
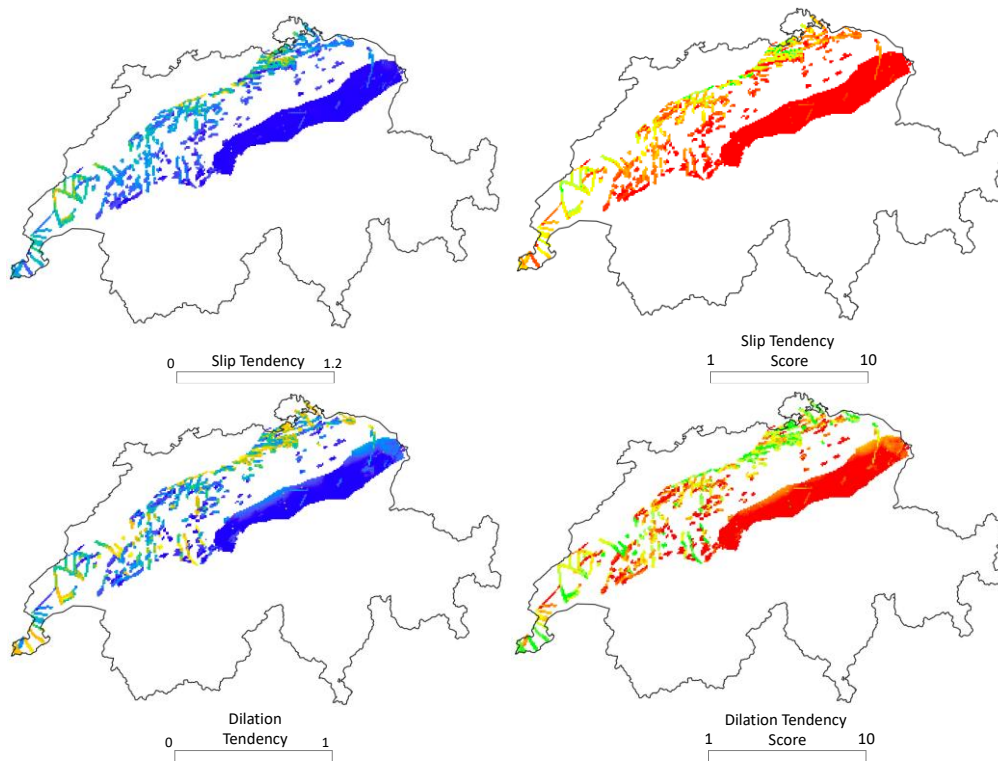


Figure 3-13. Surface elements proximity analysis (source: map.geo.admin.ch).

The distribution of the excess heat and the heat demand is mostly concentrated across the SMP (Figure 3-13 D-G) and eventually the consolidation of the proximity results is shown in Figure 3-13H which clearly reveals as the most favourable, sites are located in the proximities of the main urban centres.

3.6.2 Fault Favourability

In this study we assumed that the fault corridors represent the main geologic feature controlling the potential of storage in the Mesozoic carbonates. In this study we considered that the presence of faults having high slip and dilation tendencies, coupled to high Von Mises stress represent the most favourable targets. The overall fault favourability in the study area is shown in Figure 3-14.



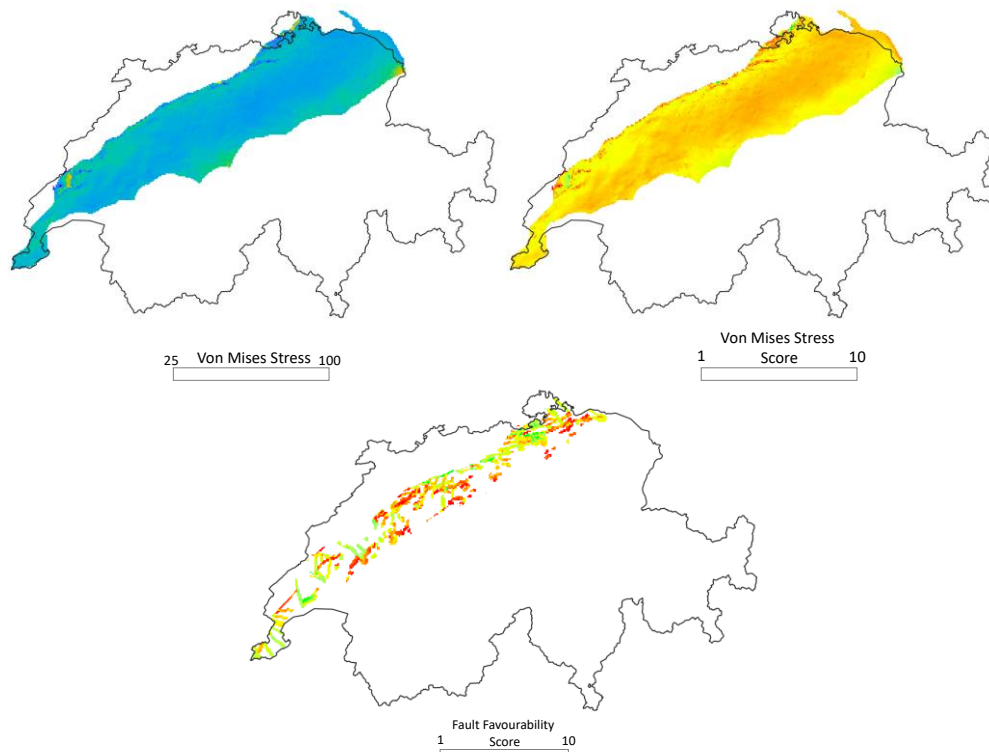


Figure 3-14. Slip tendency, dilation tendency and Von Mises stress analysis (modified from Valley and Miller, 2020) and final fault favourability.

3.6.3 Transmissivity threshold

Transmissivity is the hydraulic property of a reservoir to transmit a fluid throughout its entire saturated thickness. It is given by the reservoir permeability multiplied by its thickness. In our study we used the transmissivity value of $5 \cdot 10^{-13} \text{ m}^3$ (Birdsell et al. 2021) as a techno-economic threshold to run out those scenarios which would make an HT-ATES system economically unattractive. The results are shown in Figure 3-15 which reveals how the Cenozoic and the Mesozoic are overall favourable, excluding the scenarios which results from the minimum permeability values of 0.1 and 0.01 mD respectively.

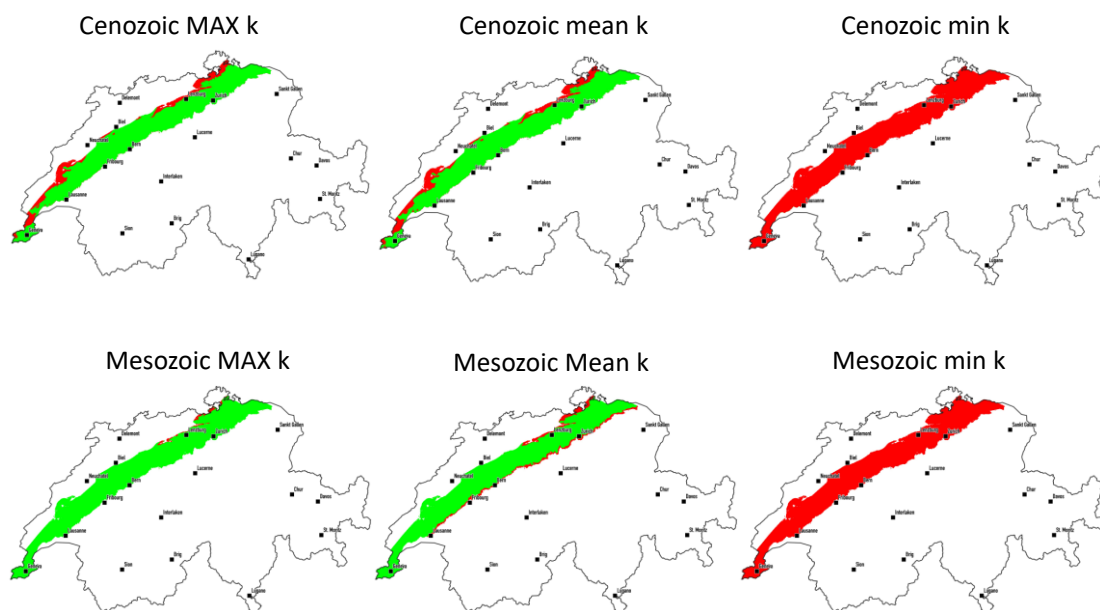
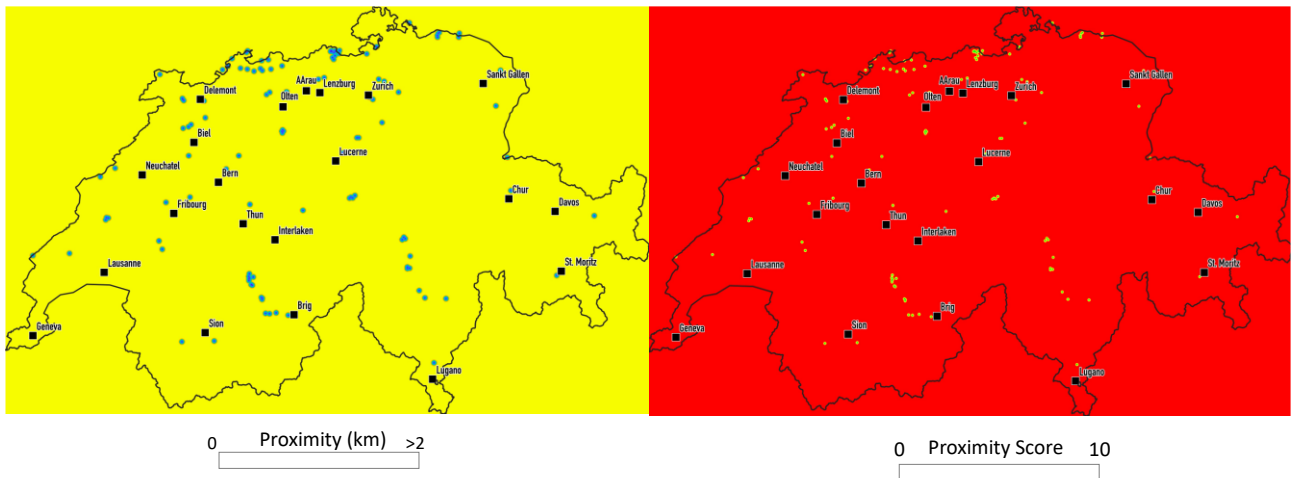


Figure 3-15. Transmissivity threshold analysis. Green: transmissivity $> 5 \cdot 10^{-13} \text{ m}^3$. Red: transmissivity $< 5 \cdot 10^{-13} \text{ m}^3$.

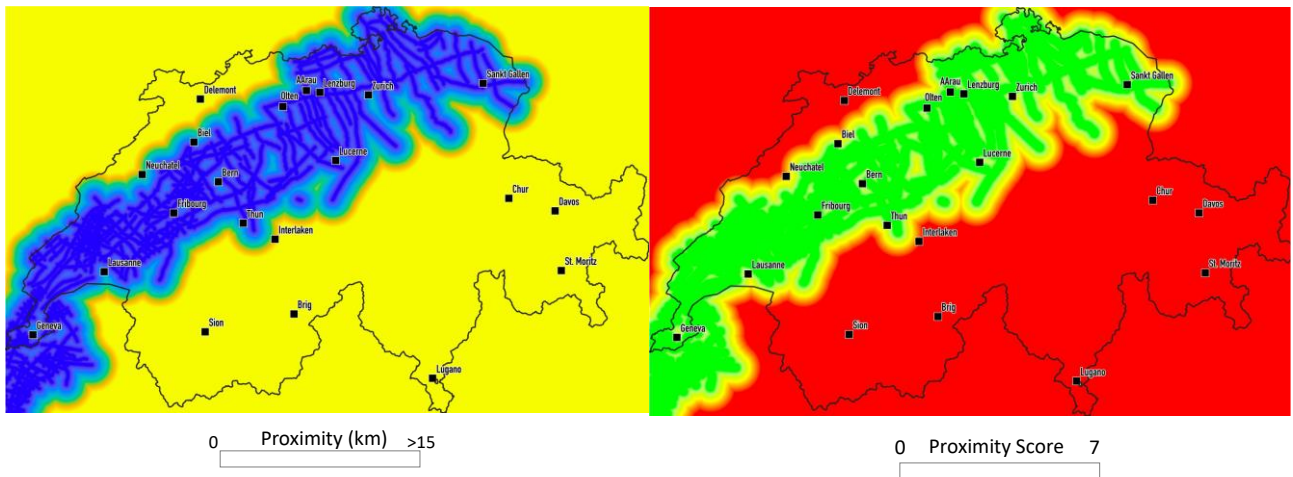
3.6.4 Proximity analysis of exploration boreholes and seismic data

The results of the proximity analysis on the main source of data that allowed the reconstruction of the subsurface information (e.g. 3D geologic grid, temperature distribution, petrophysics) reveal that the SMP has always been the focus of subsurface exploration in Switzerland, initially for hydrocarbon resources, followed by nuclear waste disposal repository identification and only in part for geothermal resources. 2D seismic data cover homogeneously the SMP setting the base for an overall understanding of the subsurface structures. In this study we don't differentiate between different seismic surveys (i.e. possibly different resolutions and target of investigation) and type of borehole data (i.e. logs, hydraulic tests, fluid chemistry, depth). Locally, exploration borehole can for sure provide the most precious set of information. Eventually, 3D seismic surveys which have been carried out by NAGRA for the identification of potential sites for nuclear waste deposit and near the city St. Gallen for geothermal exploration can provide very important information at high resolution and at the reservoir scale.

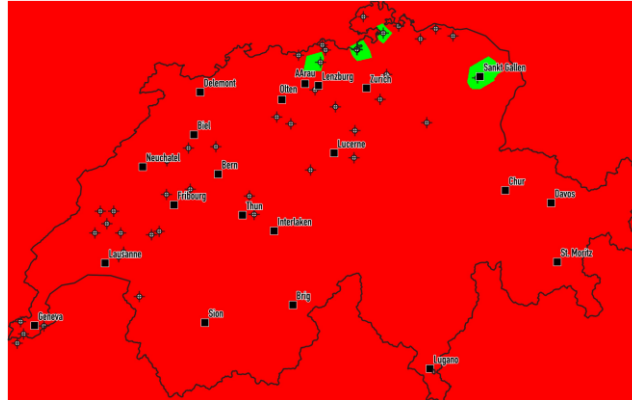
A. Exploration Wells



B. 2D seismic lines



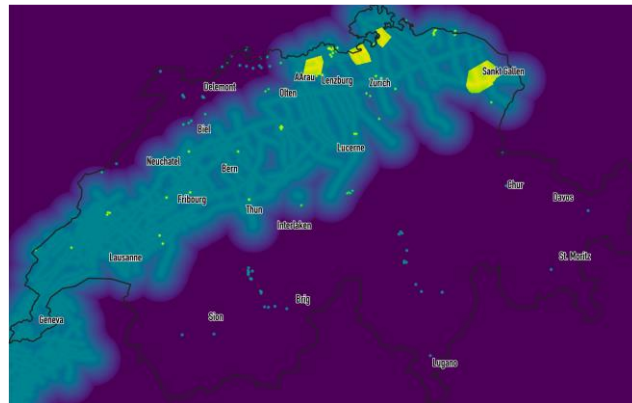
C. 3D seismic surveys



0 Proximity Score 9



D. Proximity Score



0 Proximity Score 10



Figure 3-16. Subsurface data sources proximity analysis (source: map.geo.admin.ch).

3.6.5 Storage capacity assessment

For the Cenozoic units we observe a very clear increase of the HT-ATES charging capacity with increasing thickness, with a minor further increase for locations with deeper and thicker reservoir (Figure 3-17a). The minimum scenario results in capacities below 1MW, while the mean and max scenarios result in capacities up to 62MW and 305MW respectively (Figure 3-17a).

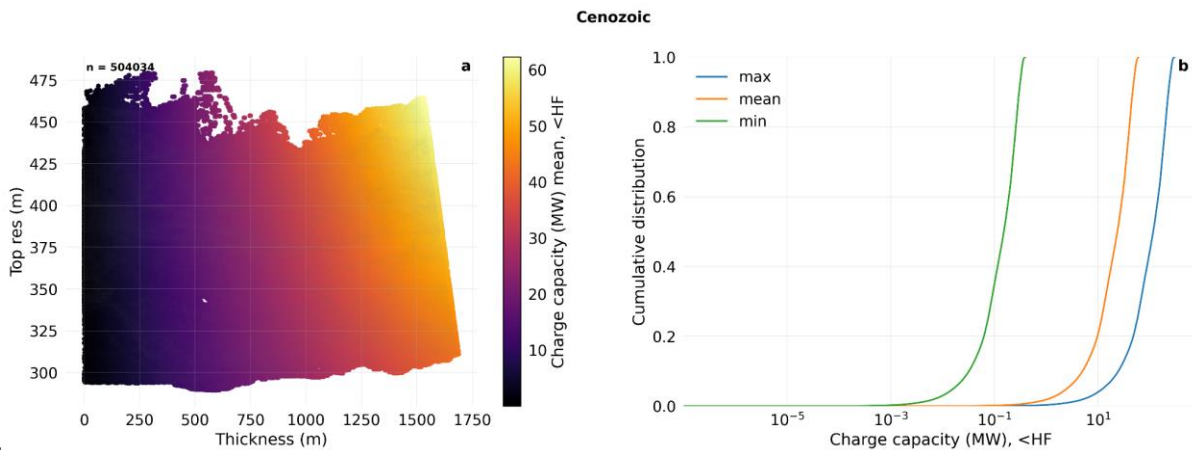


Figure 3-17. Datapoints of mean HT-ATES charge capacity of the Cenozoic units as a function of top reservoir depth and reservoir thickness (a) and cumulative distribution of the charge capacity for the min, mean and max scenarios (b).

For the Mesozoic we observe a similar increase of charge capacity mostly with increasing thickness with an optimal point appearing for a top reservoir depth of circa 800m and a thickness of circa 1200 m (Figure 3-18a). The clear diagonal shape of the datapoint indicates the lower boundary of our model at a depth of 2000 m for the combined values of top reservoir plus the reservoir thickness. The min, mean, max and faulted scenario result in HT-ATES storage capacities of below 0.07MW and up to 25MW, 2649 MW and 2138 MW respectively (Figure 3-18b).

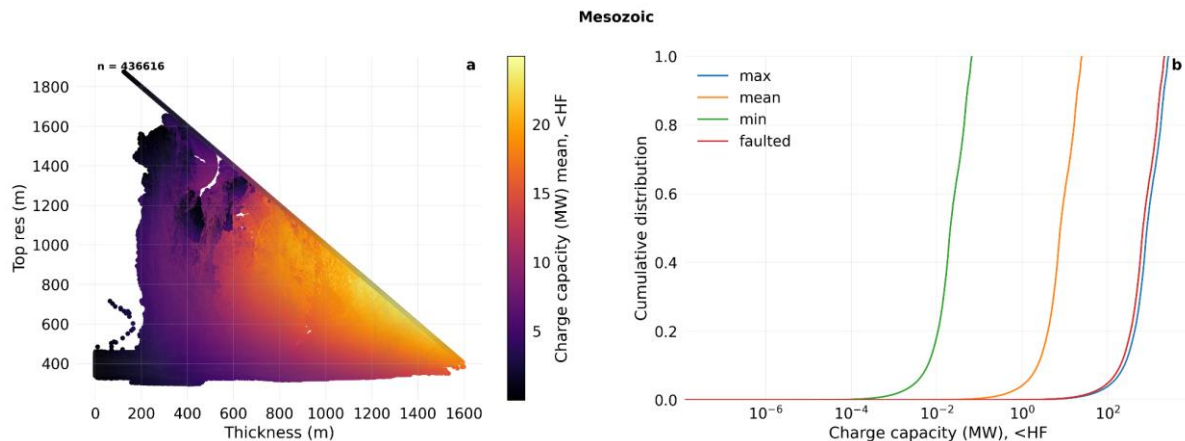
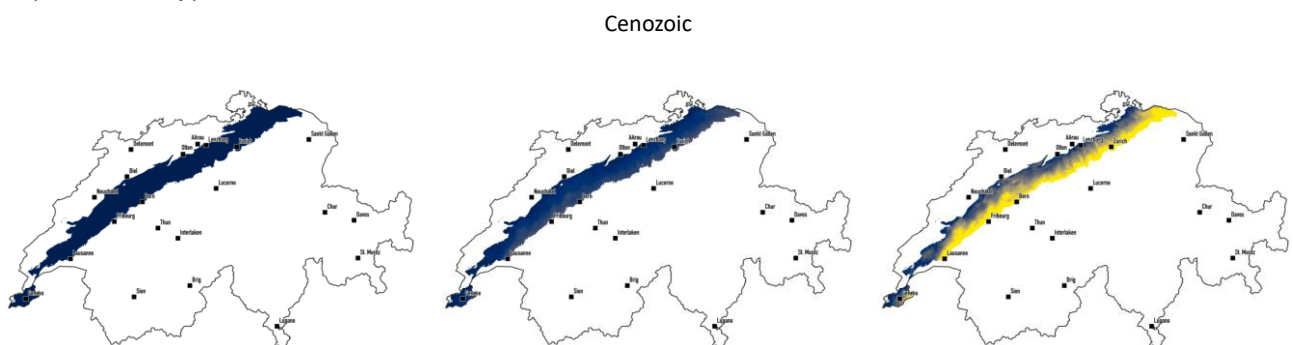


Figure 3-18. Datapoints of mean HT-ATES charge capacity of the Mesozoic units as a function of top reservoir depth and reservoir thickness (a) and cumulative distribution of the charge capacity for the min, mean and max scenarios (b).

The results of the scenario modelling show how the Cenozoic has some theoretical potential storage in the southern part the study area, where also some major cities are located (Zurich, Bern, Lausanne) for the scenario that account for the maximum value of permeability (300mD) also because of the large thickness of the Cenozoic sediments whereas in case of permeability values below. It must be pointed out that in this study we considered as potential reservoir the entire thickness of the Cenozoic sediments, however we know large vertical and lateral lithological heterogeneities locally characterize this Unit, and only part of the entire unit is suitable for storage. Therefore, a more detailed characterization of the *net-to-gross* assessment will need to be performed for an accurate assessment at a more site-specific scale. For the average permeability value of 3.5 some regions the same region also shows some storage potential. However, the low permeability scenario (0.1 mD) can be excluded, as also confirmed supported by the transmissivity analysis, not reaching the threshold of $5 \cdot 10^{-13} \text{m}^3$.

This same result applies to the faulted Mesozoic, where the worst-case scenario in terms of permeability values (0.01 mD) represents a tight reservoir not suitable for any fluid circulation. According to the results for the two other scenarios (permeabilities of 3.5 and 350 mD), faults can be promising targets as shown in Figure 3-19. According to the data available, fault structures can be suitable as targets in Aarau, Biel and Geneva. However, as demonstrated by the GCo-01 well in Geneva, high permeabilities characterizing fault corridors lead to high wellhead pressure and natural artesian flow being, therefore, a limiting factor for storage. A more detailed characterization of the hydraulic properties of the fault structures will be necessary in the future to improve such type of assessment.



Faulted Mesozoic

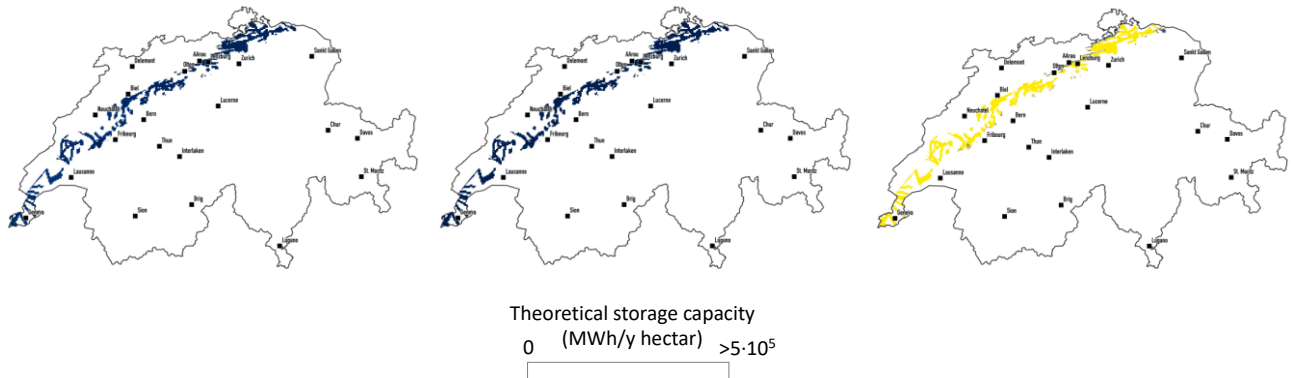


Figure 3-19. Theoretical storage capacity assessment.

3.6.6 Favourability assessment

The results of the favorability assessment are presented in Figure 3-20

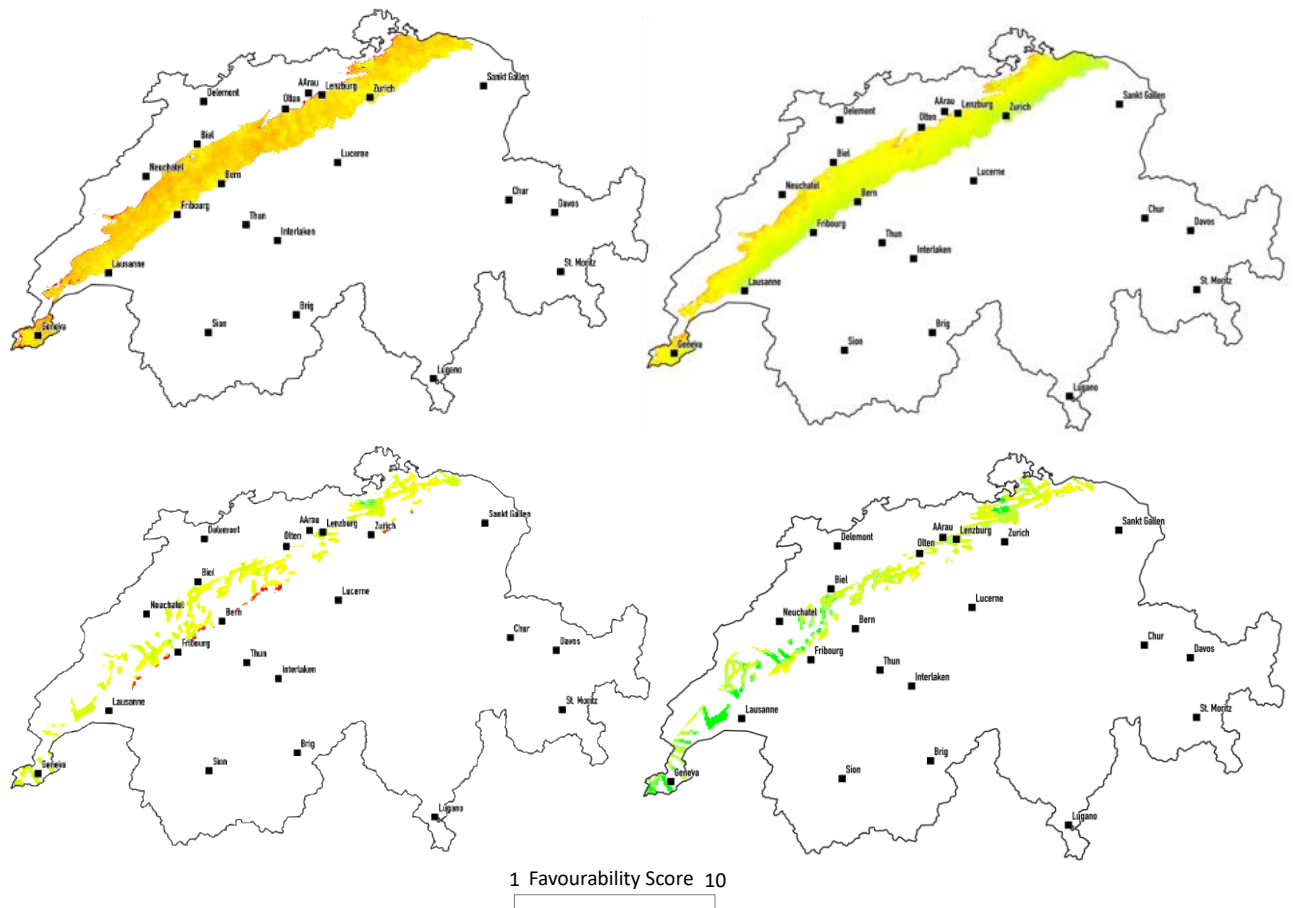


Figure 3-20. Favourability assessment for the Cenozoic and faulted Mesozoic reservoirs.

3.7 References

- ADEME, 2017. La chaleur fatale.
- Birdsell, D.T., Adams, B.M., Saar, M.O., 2021. Minimum transmissivity and optimal well spacing and flow rate for high-temperature aquifer thermal energy storage. *Appl. Energy* 289, 116658. <https://doi.org/10.1016/j.apenergy.2021.116658>
- Daniilidis, A., Mindel, J.E., De Oliveira Filho, F., Guglielmetti, L., 2021. Techno-Economic assessment and operational CO2 emissions of High-Temperature Aquifer Thermal Energy Storage (HT-ATES) using demand-driven and subsurface-constrained dimensioning. Under Rev.
- Guglielmetti, L., Moscariello, A., 2021. On the use of gravity data in delineating geologic features of interest for geothermal exploration in the Geneva Basin (Switzerland): prospects and limitations. *Swiss J. Geosci.* 114, 15. <https://doi.org/10.1186/s00015-021-00392-8>
- Mindel, J., Guglielmetti, L., De Oliveira Filho, F., Fleury; Driesner, T., 2021. Site-specific preliminary performance assessment and predictive analytics of high temperature aquifer thermal energy storage systems based on thermo-hydraulic simulations. Press.
- Suisse Energie, 2018. Guide Chauffage à distance / froid à distance - Rapport final Août 2018.
- Valley, B., Miller, S.A., 2020. Play-Fairway Analysis for Deep Geothermal Resources in Switzerland 1–12.
- Zuberi, M.J.S., Bless, F., Chambers, J., Arpagaus, C., Bertsch, S.S., Patel, M.K., 2018. Excess heat recovery: An invisible energy resource for the Swiss industry sector. *Appl. Energy* 228, 390–408. <https://doi.org/10.1016/j.apenergy.2018.06.070>

4 Screening of National Potential in Germany

Systems for seasonal heat storage have been developed in Germany since 1984. The following Figure 4-1 indicates all the realized pilot storage systems in Germany.

Location	Year	Type
<u>Friedrichshafen</u>	1996	TTES
<u>Hamburg I</u>	1996	TTES
<u>Hamburg II</u>	2010	TTES
<u>Hannover</u>	2000	TTES
<u>München</u>	2007	TTES
<u>Augsburg</u>	1998	PTES
<u>Chemnitz</u>	2000	PTES
<u>Eggenstein</u>	2008	PTES
<u>Steinfurt</u>	1998	PTES
<u>Stuttgart</u>	1985	PTES
<u>Attenkirchen</u>	2002	BTES
<u>Crailsheim</u>	2008	BTES
<u>Neckarsulm</u>	2001	BTES
<u>Berlin</u>	1999	ATES
<u>Neubrandenburg</u>	2004	ATES
<u>Rostock</u>	2000	ATES

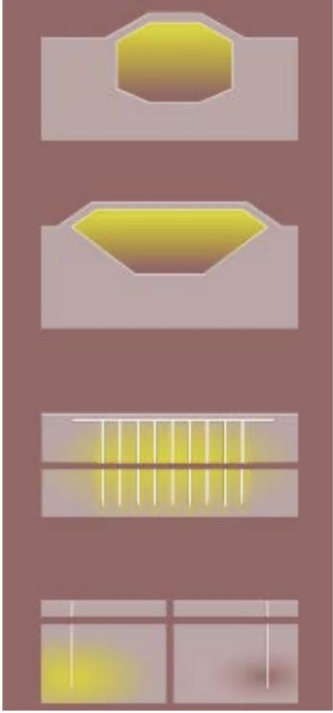


Figure 4-1. Summary of Thermal Energy Storage Systems in Germany²

In 2018 the State Agency for Nature, Environment and Consumer Protection NRW (LANUV) commissioned a potential study for the state NRW on the utilization of mine water, which was coordinated by the GZB (now Fraunhofer IEG). Figure 4-2 depicts different forms of mine water utilization.

The following screening of the national potential for the state NRW concerning MTES is divided into the categories

- Natural potential of available warm mine water (>20 °C) and
- Possible locations for MTES

² Source: <http://www.saisonalspeicher.de/Projekte/ProjekteinDeutschland/tabid/91/Default.aspx>

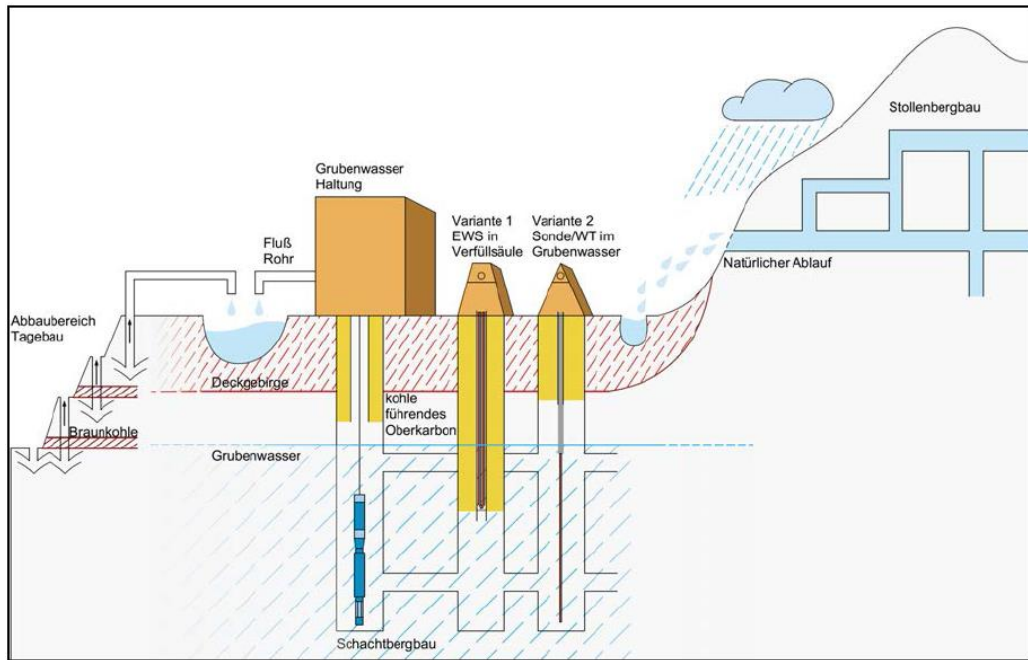


Figure 4-2. Forms to extract thermal heat from mine water (LANUV, 2018).

4.1 General overview of existing calculated potential (LANUV, 2018):

Recent potential study of the LANUV (2018) summarized for NRW:

- An estimated overall potential for Direct-Use of mine water from all former shafts of **11.8 MW**
- This could cover an annual heat demand of **82.5 GWh_{th}** without any form of MTES.

Also, a direct thermal potential of the future 7 central main Mine Water Drainage Sites of the Ruhr-Area has been evaluated. Those results are:

- A summarized potential for all central mine active drainages of **804 MW**
- This could yield/cover an annual heat demand of **1,440 GWh_{th}**

For 2035, a cover of **4,2 GWh_{th}** could be predicted, if the erection of modern low-ex urban heat grids has been accelerated in the upcoming years.

Current existing local and urban heat grids need a T_{\min} of **50 °C**. As a first conclusion, mine water as natural source for direct heat injection into existing heat grids is not feasible so that heat pumps are and will be necessary without any temperature increase by MTES.

4.2 State of the Art Mine Water Projects in NRW (Germany)

In the table below, the current projects in NRW including mine water as source for heating purposes in combination with heat pumps are summarized (Table 4-1):

Table 4-1. State of the Art Mine Water Projects in NRW (Western-Germany).

Region:	Former Mine (Heat Source)	Consumer (Heat Sink)	Source-Temperature	System:	Status:
Rheinisch-westfälisches Steinkohlerevier	Bochum – Robert Müser	Fire Station, Schools	~ 20 °C	Open-loop (heat pump)	In Operation since 2012
Rheinisch-westfälisches Steinkohlerevier	Essen – Auguste Victoria	Buildings of University	28-35 °C	Open-loop (without heat pump)	In Operation since 2006

Region:	Former Mine (Heat Source)	Consumer (Heat Sink)	Source-Temperature	System:	Status:
Rheinisch-westfälisches Steinkohlerevier	Marl – Auguste Victoria	4 Apartment buildings	~ 20 °C	Closed Loop (heat pump)	In Operation since 2010
Rheinisch-westfälisches Steinkohlerevier	Bottrop – Prosper Haniel	Residential and commercial area	Without MTES: ~50 °C; as HT-MTES: up to 90 °C (calculated)	Open-loop (without heat pump)	Realization pending
Rheinisch-westfälisches Steinkohlerevier	Bochum – Dannenbaum	Residential and commercial area)	~ 25 °C	Open-loop (heat pump)	Realization pending
Rheinisch-westfälisches Steinkohlerevier	Essen – Heinrich	Residential Care Home	~ 22 °C	Open-loop (heat pump)	Closed since 2004
Aachener und Erkelenzer Steinkohlerevier:	Alsdorf –Anna	Energy Museum „Energeticon“	~ 25 °C	Open-loop (heat pump)	Test Phase since 2019

The extraction of warm mine water from former collieries depends on the existing mine layout, so that

- Open loops or
- Closed loops

are both possible (see Table 4-1 and Figure 4-2) and have to be considered individually.

Preferring an open loop system, the mine water is actively pumped to the heat exchanger by submersible pumps installed in the mine layout (i.e. shafts) or dewatered by artificial former constructed galleries as well as by natural occurring springs (i.e. at geological interfaces) (see Figure 4-2). After the thermal exchange, the mine water is reinjected again into rivers and watersheds of rivers, respectively. Currently, these are basically the three main rivers *Ruhr*, *Emscher* and *Lippe* in the German Ruhr-Area (Figure 4-3).

On the other hand, heat can be extracted performing a closed loop system by two individual thermal circuits and installing shell and tube heat exchanger through parts of the mine layout with a closed circulating heat transfer medium inside. Within a second circuit of surface heat pumps, the energy is supplied to the heat sink. This is preferred if shafts have been fully or partly grouted (see also Figure 4-2).

In **1956**, the Ruhr-area encountered 152 operative mines with individual mine water drainage systems. Currently, 10 central mine water drainage sites are in operation:

After closure of the last two active mines Prosper Haniel and Ibbenbüren in 2018, a reduction to **7** central Mine Water Drainage Sites is foreseen. These are (briefly described above):

In the western Ruhr area, the Walsum site has already been developed into a well water maintenance site and pumping operations have already commenced with surface discharge into the Rhine. After overdamming of the existing mine workings in 2017, a mine water inflow from the former *West* colliery and the abandoned mines on the left bank of the Rhine is expected at the Walsum site. From this point on, it is planned to pump permanently from the current level of 750 m below sea level.

In the central Ruhr area, mine water is to be discharged to the Lohberg site after the closure of the last active Prosper-Haniel mine. Currently, discharges take place into the Emscher and Lippe rivers. For the future, mine water will be drained into the Rhine River. In order to create a pathway, a section has been excavated between Prosper-Haniel and Lohberg.

The dewatering system is scheduled to go into operation around 2035. With an estimated amount of 35 million m³/year, this is going to be the most important drainage site. Production temperatures of around 30 °C from a depth of 807 m bgl are expected. Temperature forecast models show that after the connection to Prosper Haniel, the temperature could rise from 30 °C to 35 °C within ten years (Figure 4-1).

The three more southerly dewatering facilities in the Ruhr-Area (i.e. Heinrich, Friedlicher Nachbar and Robert Müser) will continue to exist. The mine water here is comparatively low in mineral content. At the Heinrich site, a partial quantity will flow to Lohberg in the future. Due to a raising of the pump level, a decrease in temperature is to be expected for the former Heinrich colliery.

In the eastern Ruhr area, the *Haus Aden* site is responsible for central dewatering. Here, the mine water is to be permanently discharged into the Lippe River by submersible pumps at 640 m below ground level. In the long term, a decrease in temperature is to be expected here.

At the Ibbenbüren site, there are two dewatering subareas (Ostfeld and Westfeld). In the east field, active mining was still in progress until the end of 2018. In the Westfeld, after the closure in 1979, the mine water rose to 65 m below ground level, and has been drained by the Dickeberger adit.

The underground connections to the east field via the Buchholz and Glücksburg seams to the west of the Bockraden shaft were closed by pressure-resistant dams.

The plans for the east field envisage the installation of a well water drainage system with a low pumping height in the former Ostfeld-shaft. Corresponding temperatures as in the west field of approx. 13 °C are to be expected. The mine water from both fields is to be discharged via the Ibbenbürener Aa to the Ems. Those 7 central mine water drainage sites of the Ruhr-area are mapped in fig.4-3 (Drobniowski, 2016).

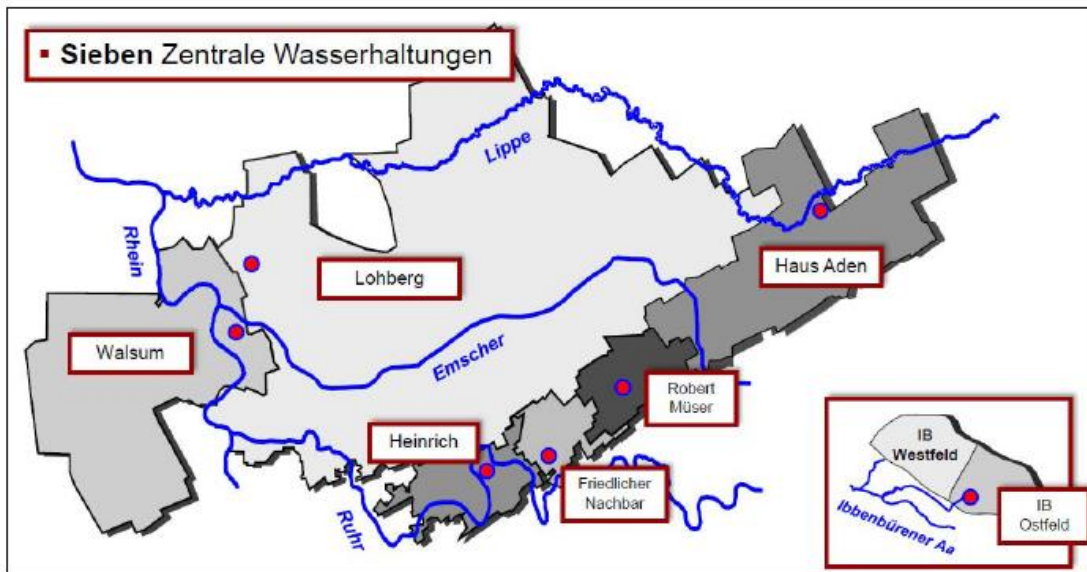


Figure 4-3. Central Mine Water Drainage Sites in the German Ruhr-Area (Drobniowski, 2016).

On the basis of the available data of the mine drainage sites, the production rates and the theoretically achievable thermal outputs and energy quantities from the mine water have been calculated for the reference years 2020-2050 and 2035-2050, respectively. It was assumed that the mine water will be cooled to a maximum of 6 °C. This could lead to usable temperature differences of max. 7 °C to 29 °C. These calculated results are summarized in Table 4-2.

Table 4-2. Thermal Mine Water Properties of the 7 central drainage sites (LANUV, 2018).

Former Mine	Reference Time	Max. ΔT [K]	Max. Mine Water Head [mbsl]	Output [L/s]	Mine Water Density [kg/m ³]	Specific Heat Capacity [kJ/kg*K]	Max. Thermal Power [MW]:	Theor. Supplied Thermal Energy [GWh/a]:
Heinrich	2020-50	12	434	634	999.2	4.1	31.4	274.6
Robert Müser	2020-50	14	196	336	1.000.2	4.2	19.6	171.7
Friedlicher Nachbar	2020-50	14	163	270	999.2	4.2	15.7	137.9
Haus Aden	2020 2035-2050	18 23	321	406 306	1,006.3 1,007.2	4.1 4.1	30.3 23.6	265.1 206.7
Walsum	2020-50	23	613	254	1,034.3	3.9	23.7	207.6
Lohberg	2035-50	29	472	1104	1,048.4	3.8	128.5	1,126.1
Ibbenbüren-Ostfeld	2023	7	n.n. ³	33	1,055.6	3.8	0.9	8.2
Ibbenbüren Westfeld	2020	7	n.n.	127	1,000	4.2	3.7	32.5

The planned mine water drainage of the central Ruhr-area for the biggest former collieries has been simulated by a “box-model” in order to calculate the maximum mine water heads. These play a vital role, if a thermal exploitation of mine water will be closer considered for one of the former biggest mines Figure 4-4.

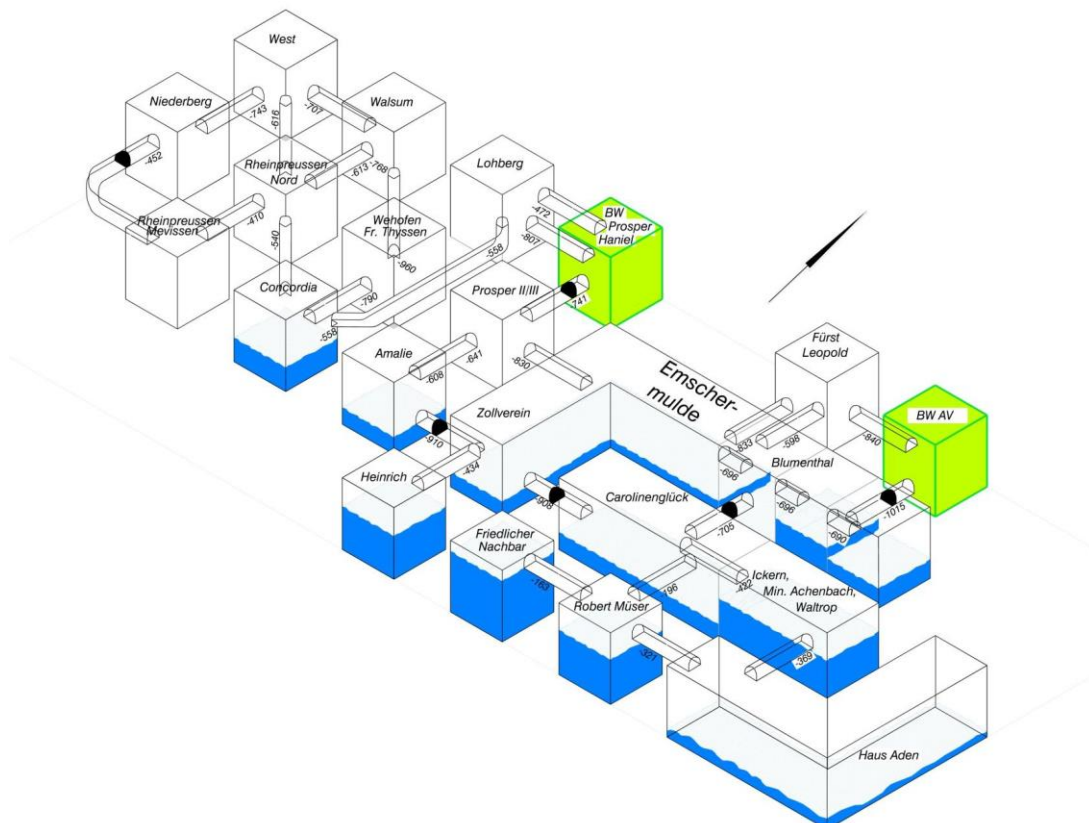


Figure 4-4. Planned mine water drainage system in the central Ruhr-area for the future (Drobniewski, 2016).

³ n.n.: no data available

4.3 Overview thermal utilization possibilities of existing shafts

More than 1,000 mines have been built in the German Ruhr-area in the past. In addition, there are a several former coalfields in the Aachen and Erkelenz-Area (south-western NRW), around 20 more in the Ibbenbüren (Northern Ruhr Area, see Figure 4-4) and some in the area of Minden (Northern NRW). Most of them have been backfilled after closure. For a certain number, access to the mine is still possible via degassing pipes located in the backfill column, which extend into the open shaft below the formwork floor (see Figure 4-2). Recent LANUV study analysed the potential of **135** shafts in the Ruhr-Area, where thermal energy could be exploited theoretically. All other shafts are either completely backfilled and thus no longer accessible or have other restrictions that make a thermal reutilization impossible. Table 4-3 summarizes the mean characteristics of the evaluated shafts in the Ruhr-Area.

Table 4-3. Properties of evaluated shafts for geothermal mine water purposes (LANUV, 2018).

Number of evaluated shafts for geothermal reutilization:		135
Geometry:		
Max Depth [m]		1.639
Mean Depth [m]		999
Grouting/Backfilling:		
Fully open/partly backfilled		28/107
Max Depth [m]		1,293
Mean Depth [m]		645
Shafts with degassing pipes located in the backfill column:		
>200 mm		73
Mean Diameter [mm]		372
Water Column:		
>200 m	2020	42
	2035	81
Mean Water Column [m]	2020	139
	2035	286

4.4 Possible Locations for MTES in the Ruhr-area (NRW)

In total approx. 1.93 Million m³ of Mine Water could be available after evaluating suitable shafts for thermal storage purposes. The total void volume (i.e. the whole storage capacity within the mine layout) is distinct bigger. Basically, former shafts for MTES reutilization have technical, operational and economic advantages in general than reutilizing former drifts as MTES.

Evaluation Factors for a MTES have been established by (Eikmeier, Mohr, & Unger, 1999). In particular, those are

1. Surface conditions:
 - Open space for new housing areas (with modern insulation of buildings and a district heat grids play the most vital role),
 - Small distance to miscellaneous areas (residential, industrial, commercial),
 - Availability of existing district heating grids (preferred are low-ex grids),
 - Other urban Infrastructure.
2. Subsurface conditions:
 - Mine layout and size,
 - Geological and hydrogeological boundary conditions (no active or passive mine water drainage, unaffected by infiltration and groundwater recharge),
 - Mine water quality (chemical composition, pH, conductivity, oxygen saturation ...),
 - Depth (characteristics of geological adjacent and overlying rock, from north to south in general decreasing),
 - Heat production (Open or closed loops).

With regard to a closer potential analysis for one of the favoured MTES site locations, all those aspects have to be implemented into pre-simulation numerical models. Those results - adapted to economic heat demands (and the heat grid infrastructure as well) - are rarely available yet, just for a few sites, i.e. Prosper-Haniel and Bochum–Dannenbaum, see Table 4-1).

Suitable shafts for a MTES are summarized in Table 4-4. The existing calculated potential is listed (in MW and GWh/a, respectively), which could be utilized by the available amount of mine water. The thermal output could be further increased by the storage of seasonal surplus heat in the future.

Table 4-4. Screening results of national potential for MTES locations in the Ruhr-area

Former Mine	Shaft	ID-Number	City	Mine Water Volume [m ³]	Assumed Thermal Power [kW]:	Thermal Output [kWh/a]:
Consolidation	Consol 9	26	Gelsenkirchen	11.914	205	1.413.173
Ewald	Ewald Fortsetzung 1	12	Oer-Erkenschwick	4.990	85	598.698
	Ewald Fortsetzung 3	16	Oer-Erkenschwick	7.680	120	838.383
	Ewald 3	27	Gelsenkirchen	3.932	150	1.049.760
	Ewald 5	29	Gelsenkirchen	7.486	79	553.964
General Blumenthal	General Blumenthal 11	8	Recklinghausen	10.692	78	542.163
	General Blumenthal 8	15	Recklinghausen	15.487	137	959.888
	General Blumenthal 6	25	Recklinghausen	8.006	176	1.226.989
Grimberg	Grimberg 3	31	Bergkamen	24.657	389	2.719.404
Hansa	Hansa 3	5	Dortmund	70.15	67	470.587
Haus Aden	Haus Aden 6	30	Werne	16.951	218	1.520.207
Hugo	Hugo 8	21	Gelsenkirchen	8.036	187	1.307.294
Ickern	Ickern 3	6	Waltrop	8.711	107	749.699
Königsborn	Königsborn 4	10	Altenböge	6.457	117	815.339
Kurl	Kurl 1	1	Dortmund	4.182	23	161.029
	Kurl 2	2	Dortmund	7.068	59	414.583
Lothringen	Lothringen 6	13	Bochum	6.184	-	-
Minister Achenbach	Minister Achenbach 7	11	Dortmund	9.902	133	930.629
	Minister Achenbach 1	14	Lünen	1.0183	135	943.548
Minister Stein	Minister Stein 5	7	Dortmund	11.022	71	498.170
	Minister Stein 4	19	Dortmund	26.681	197	1.373.842
Niederberg	Niederberg 1	18	Neukirchen-Vluyn	10.006	132	922.948
Schlägel & Eisen	Schlägel & Eisen 5	24	Herten	6.529	147	1.025.040
Waltrop	Waltrop 1	3	Waltrop	6.724	63	437.487
	Waltrop 2	4	Waltrop	6.552	62	431.412
	Waltrop 3	9	Waltrop	14.618	158	1.100.247
Westerholt	Wetterschacht Altendorf	20	Dorsten	5.070	111	771.975
	Westerholt 3	22	Herten	10.647	132	920.224
	Westerholt 1	23	Herten	6.814	166	1.156.321
Westfalen	Westfalen 2	17	Ahlen	21.523	188	1.313.509
	Westfalen 7	28	Hamm	13.763	141	984.468

Figure 4-5a shows a map of feasible MTES shaft locations listed in Table 4-4. Figure 4-5b illustrates the depths with focus on the amount of mine water.

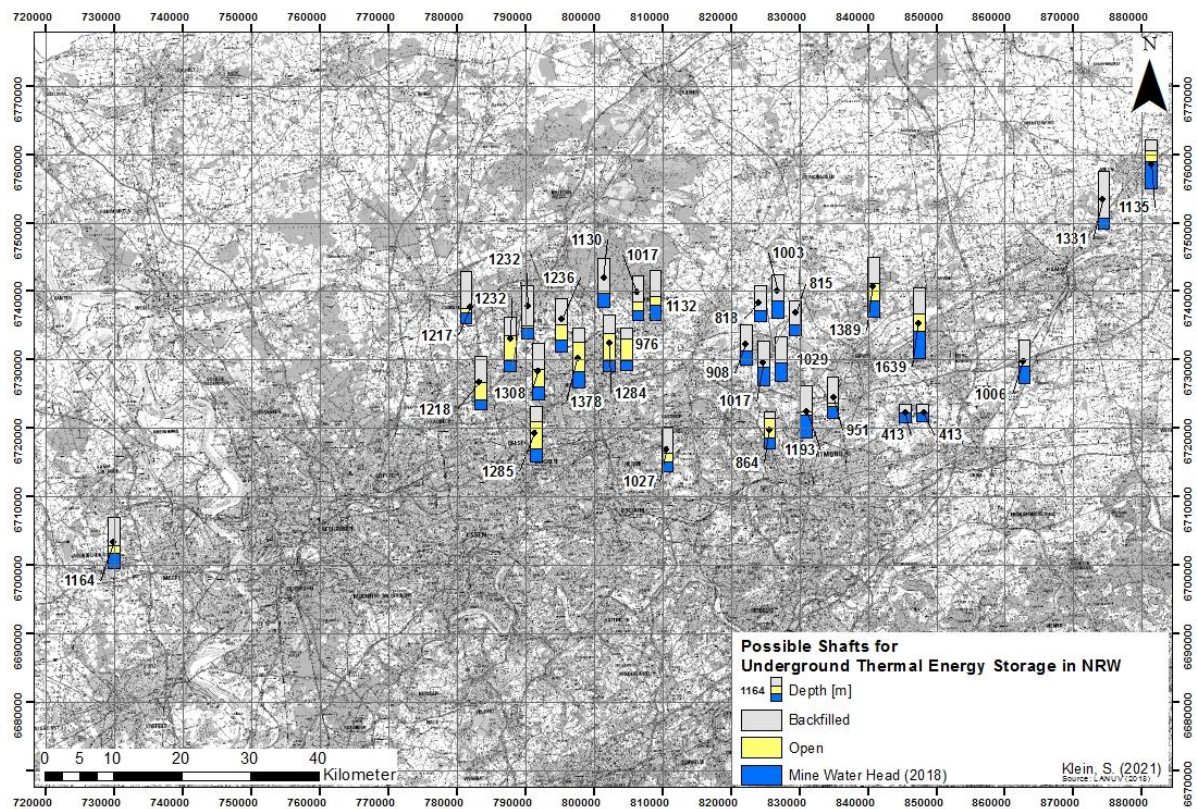
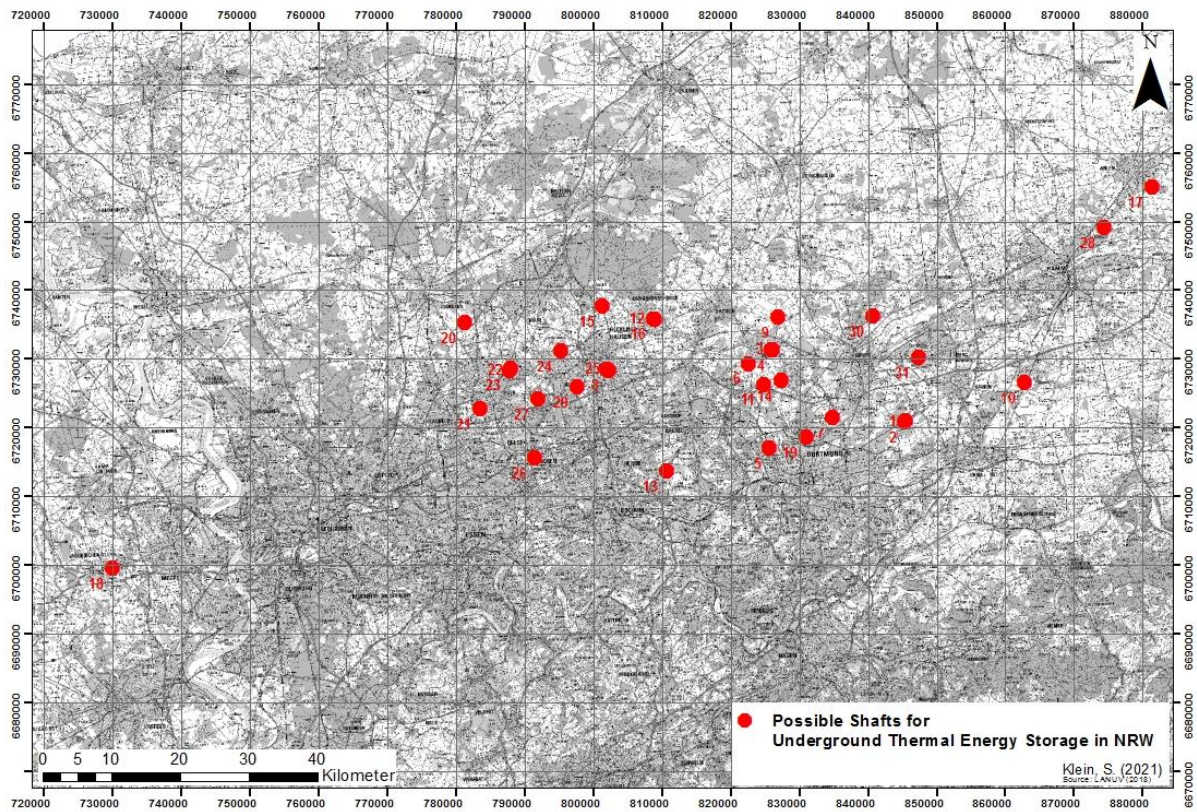


Figure 4-5. Map of the screening results for feasible MTES locations in NRW (Germany)

4.5 Status Quo

Due to the significant amounts of former collieries and the biggest population density in Germany, the Ruhr-area offers a big potential to include MTES within modern low-ex-heating grids. Although there is still only a small amount of realized mine water projects (see tab 4-1), those examples show that the utilization of mine thermal energy ranges from single buildings to urban residential, commercial and industrial areas, respectively. Since former mines reach depths of more than 1,000 mbsl, there is already an existing distinct potential of available warm mine water (>20 °C) (see tab. 4-2). For the future, MTES could be very lucrative for sites, where a high amount of waste thermal energy or surplus solar heat occurs and open space for new housing areas concerning the installation of low-ex-grids is available to remove the need for additional heat pumps.

4.6 References

- Drobniewski, M. (2016). *Die technische Ausgestaltung und der Stand des Grubenwasserkonzeptes*. Presentation.
- Eikmeier, B., Mohr, M., & Unger, H. (1999). *Saisonale Wärmespeicherung in Grubenräumen*. Abschlussbericht, Ruhr-Universität Bochum, Lehrstuhl für Nukleare und Neue Energiesysteme.
- LANUV-Fachbericht 90. (2018). *Potenzialstudie Warmes Grubenwasser*. Landesamt für Natur, Umwelt und Verbraucherschutz Nordrhein-Westfalen, Recklinghausen.

5 Screening of national potential in Denmark

5.1 Context

In the spring of 2020, the Danish parliament adopted a climate law committing to lower CO₂ emissions by 70% in 2030 (compared to year 1990 levels)⁴. To reach this goal a transition towards 100% renewables is important, and energy storage in the District Heating Networks (DHN) and heating/cooling sector in general is here a key element. The importance of energy storage, which includes UTES, is likewise emphasized at EU level to engage major reductions in CO₂ emissions and to use e.g. sources of surplus heat not present utilised in the heating sector (EASE, 2017).

In Denmark the first preliminary steps have been taken to establish knowledge and experiences on UTES technologies, and to share this knowledge with key stakeholders. The Danish participation in HEATSTORE supports an essential dissemination of lessons learned and best practices on UTES especially targeted district heating (DH) utilities, which supplies 64% of the households in Denmark. At present PTES is the best-known UTES technology in Denmark with five running systems, while there is only one BTES system and no HT-ATES systems established yet. The UTES screening process in Denmark focus primarily on the subsurface conditions regarding ATES and BTES, as PTES is less depending on geology and more related to large accessible areas at the surface.

The current approach for UTES screening in Denmark within HEATSTORE can be divided into three phases. The first phase is utilization, update and expansion of an already established web tool displaying relevant subsurface data such as information on lithology, groundwater, proposed yield of aquifers, GIS themes with areas of drinking water interests, polluted sites etc. (see section 5.2 and 5.7). Most of the data sources are hosted at GEUS due to the role as national datacentre for subsurface data.

The second phase in the Danish screening process was a survey of interests distributed to DH utilities in the Danish heating sector. The responses on this questionnaire have been evaluated and represent a decision base for a targeted effort and dialog in areas where e.g. free accessible surplus heat potentially could be utilized with the use of UTES (see section 5.5).

In the third screening phase within HEATSTORE a targeted geological characterization was carried out in five selected sites based on the results of the survey of interest and subsequently dialog with several interested utilities (section 5.6). An important criterion in this work has been to cover different geological settings in the Danish subsurface and thereby cover cases of regional relevance for others.

5.2 First edition web tool for national UTES screening

To aid the decision-making process regarding UTES in Denmark, a first edition web tool was developed with access to a variety of subsurface information relevant in the screening process (see Figure 5-1). The web platform was an outcome of the project "Evaluation of the potential for geological heat storage in Denmark, EUDP 1887-0017" (GEUS, 2019) that was finished in 2019 and comprised the following targets regarding 2D mapping of geological locations suited for heat storage:

1. Shallow deposits of clay, sand and gravel (10 to 300 m below the surface.)
2. Chalk and limestone (10 to 1000 m below the surface.)
3. Deeper sandstone reservoirs (500 m to 1500 m below the surface.)
4. Hard bedrock (Bornholm)

The shallow deposits in Denmark consist mainly of sand, gravel and clay of varied composition such as poorly sorted deposits of sand and gravel, very fine grained, impermeable clays, well sorted quartz sands, and unsorted deposits of glacial till. Since the shallow subsurface has been affected by glacial processes, the sediment distribution is very variable, and the extension of the individual formations is often limited and poorly determined. This combined with the fact that both groundwater conditions and thermal properties of the various deposits vary greatly, results in locally very varying possibilities for heat storage. However, the use of a relatively large amount of existing geological data, e.g. from a detailed, national groundwater mapping program, made it possible to screen the country for locations suitable for shallow geological heat storage.

⁴ <https://ens.dk/en/our-responsibilities/energy-climate-politics/danish-climate-policies>

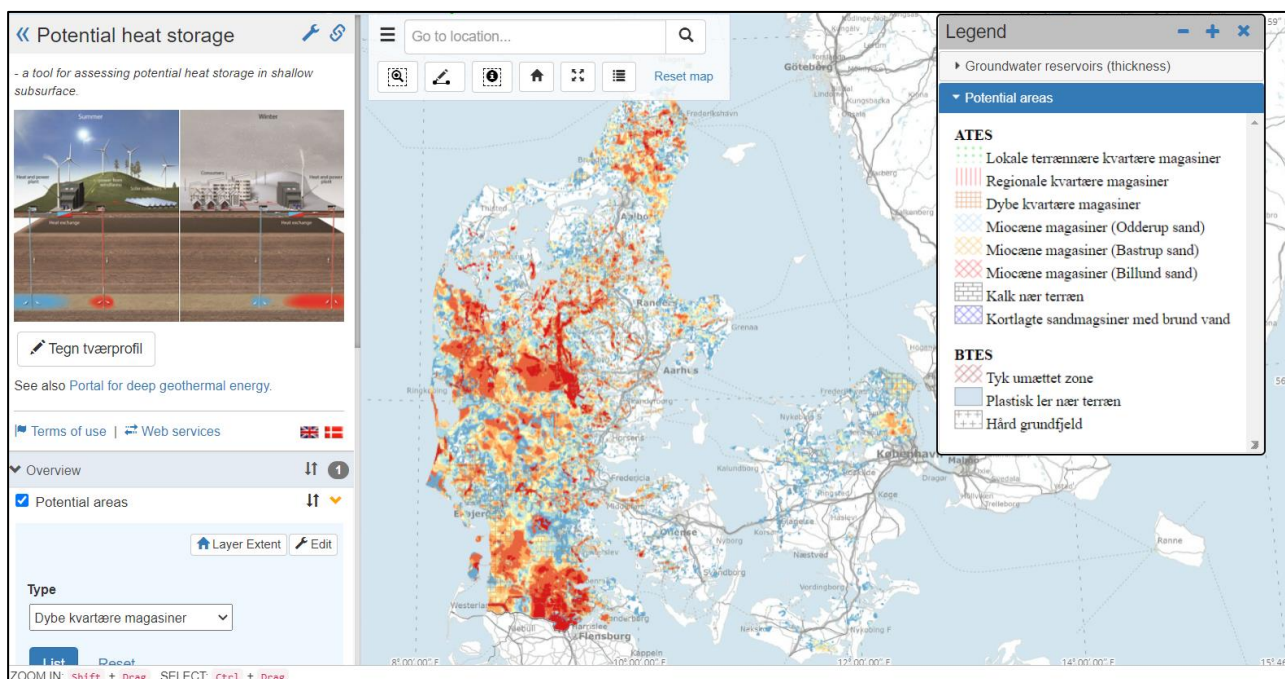


Figure 5-1. A screenshot from the web tool on potential geological heat storage in Denmark.

The chalk in Denmark is between 500 and 1500 m thick. It is a porous rock with low permeability. In parts of the country, up to 300 m of Danian limestone of varying composition is found on top of the chalk. Often the upper 10-20 m of the limestone / chalk formations is fractured and therefore often have a high secondary permeability. Below the chalk, older pre-Cretaceous deposits are found. They contain a number of sandstone intervals with reservoir properties potentially suited for heat storage or deep geothermal energy.

On the island of Bornholm extensive areas with sandstone, gneiss and granite bedrock potentially suited for heat storage are found from near the surface. Storage in bedrock with low permeability has for instance been tested in the other Scandinavian countries, such as Sweden.

5.3 Initial screening of shallow formations in first edition tool

The overall purpose of the initial screening was to map areas with shallow aquifers suitable for ATES and areas with limited groundwater flow suitable for BTES (GEUS, 2019).

5.3.1 Access to shallow subsurface information

The datasets included in the web tool (Figure 5-1) are primarily extracted from the Danish National Borehole Database (hosted by GEUS). The geological data include information on soil type and layer boundaries, whereas hydrogeological data provide information on aquifer transmissivity, groundwater chemistry and hydraulic head. In addition to this, environmental data and administrative data, locations on heat producing companies, appointed areas of drinking water interests, environmental protected areas, soil contamination and reports on the national groundwater mapping (The Danish Energy Agency and The Danish Environmental Protection Agency) are comprised in the tool. In the initial versions of the web tool, all the accessible data sources represent point information (boreholes) or 2D information in shape of GIS polygons, while the update and expansion carried out in the HEATSTORE project include 3D information and site-specific characterisations of the upper subsurface.

5.3.2 Main types of suitable aquifers

5.3.2.1 Shallow sandy aquifers

Large coherent areas with shallow deposits of sand and gravel were mapped based on GEUS Geological Soil Map (1: 200,000) supplemented with data from the Danish National Geophysical Database (hosted by GEUS). The shallow sandy areas were found all over the country but most widespread to the west.

5.3.2.2 Shallow limestone deposits

Areas where the top of the limestone is less than 25 m below the surface were mapped and primarily found in northern and eastern parts of Jutland, on the eastern part of Zealand, on Lolland and the easternmost part of Funen.

5.3.2.3 Deeper aquifers with a restricted water quality

In order to map areas that could potentially be suitable for heat storage at higher temperatures (> 20 °C) a number of deeper sand deposits outside designated water protection areas were mapped in the central part of Jutland. In addition, existing groundwater chemical analyses were used to find indications of poor natural water quality.

5.3.3 Areas with limited groundwater flow

5.3.3.1 Areas with a thick unsaturated zone

Areas with 20-30 m of unsaturated sediments above the water table were mapped using water level soundings and topographic models of the terrain. The areas were primarily found in Eastern Jutland. Monitoring results from a pilot BTES in Brædstrup in unsaturated sediments, have shown that the heat dissipation below the bottom of the storage is limited and it is assumed, that BTES can safely take place in the unsaturated zone also inside designated groundwater protection areas, provided local conditions are taken into account.

5.3.3.2 Shallow impermeable clay formations

Areas with impermeable clay deposits and no groundwater flow are potentially suited for BTES. Therefore areas with less than 25 m to the top of the clay formations were mapped and found in northern and eastern Jutland as well as on Funen and Zealand.

5.3.3.3 Areas with impermeable bedrock

On Bornholm, bedrock of granite, gneiss and sandstone are found near the surface of a large part of the island. Below the weathered subsoil and outside fault zones, these rocks are expected to be relatively impermeable and thus suitable for BTES. However, designated groundwater protection areas must be taken into account in feasibility studies for possible storage plants.

5.4 Local investigations of deeper formations

As part of other projects a few local investigations of the potential for heat storage in deeper formations have been conducted.

5.4.1 Access to deep geothermal information

The potential for heat storage in deep geothermal formations is not a part of the described web tool for national UTES screening, but information is available on a different platform ([deep geothermal webGIS DK](#)). This platform provides information on the distribution and geothermal potential of deep reservoirs in the Danish subsurface. Several geological map themes, relevant for geothermal energy is accessible, so stakeholders in the geothermal industry, as well as the authorities, can form an overview over the deep subsurface. Themes on geological uncertainty, data density and quality are likewise a part of the web portal. The target is primarily heat production potential of geothermal sandstone reservoirs located within the depth zone of 800-3000 m, and not specifically heat storage.

5.4.2 Evaluation of heat storage in deeper sandstone reservoirs in the Aalborg area

In the previous project "Evaluation of the potential for geological heat storage in Denmark, EUDP 1887-0017" (GEUS, 2019) a case study of the storage possibilities in specific sandstone intervals below the City of Aalborg (see Figure 5-5) has been conducted (Kristensen et al., 2016; Guldager et al., 2018).

When assessing the possibilities for geological heat storage in deep sandstone formations, estimates of the content of pure sandstone layers and their thickness, porosity and permeability is essential in order to assess the potential for storage in the individual formations. In the central Aalborg area the potential for heat storage in the Frederikshavn, Haldager Sand and Gassum Formations have been evaluated.

Within this area, the Frederikshavn and Haldager Sand Formations are generally found at depth of 700-1000 meters, whereas the Gassum Formation lies deeper (about 1.5 km). The analyses show that the Frederikshavn, Haldager Sand and Gassum Formations all have the potential to store hot water. Within each geological formation, the reservoir rock is made up of a series of sandstone layers characterized by high

porosity and permeability and intercalated with shale layers. It is assessed that the total thickness of potential reservoir sand within the individual formation is sufficiently large to provide the necessary volume for heat storage.

This assessment is supported by the calculated transmissivities and by the geological descriptions of the reservoir sandstone. However, a combined interpretation of borehole measurements and core analysis data shows that the sandstone layers in the Haldager Sand and Gassum Formations all have better reservoir properties than the sandstone layers in the Frederikshavn Formation. The transmissivity is the product of permeability and the thickness of potential reservoir sand. The transmissivity of the Frederikshavn Formation is in the order of 10-15 Darcy meters, whereas the transmissivity of both the Haldager Sand and the Gassum Formation is around 40-90 Darcy meters. Based on these calculations, the Haldager Sand and Gassum Formations are considered particularly suitable for heat storage. Conditions such as depth, temperature, mineralogy and internal layering may also influence the final choice of a reservoir.

In and around Aalborg, however, the quantity and quality of existing seismic data are poor, and the uncertainty of the screening carried out is relatively large. Prior to any drilling, it is therefore recommended that new seismic data is acquired in order to determine the depth and the thickness of the potential reservoirs more precisely and to identify existing faults. This will also give a better assessment of the continuity of the reservoirs. Even minor faults can break the continuity of a reservoir, but only larger fault systems can be recognized from the existing seismic data.

Based on the geological evaluation of the sandstone reservoirs in the area, numerical reservoir simulations have been carried out to evaluate the storage efficiency. The results indicate a recovery factor of c. 70% for the Frederikshavn and Haldager Sand Formations and c. 93% for the Gassum Formation in the first year in a relatively low-temperature storage scenario (65°C and cooling to 15°C before injection using a heat pump) and a recovery factor of c. 40% for the Frederikshavn and Haldager Sand Formations and c. 70% for the Gassum Formation in a relatively high-temperature storage scenario (80°C and cooling to 40°C before injection without a heat pump) due to a higher heat loss. After 7 years of operation the recovery factor is c. 85% for the Frederikshavn and Haldager Sand Formations and c. 98% for the Gassum Formation in the low-temperature storage scenario and c. 67% for the Frederikshavn and Haldager Sand Formations and c. 84% for the Gassum Formation in the high-temperature storage scenario. Furthermore, the simulations indicate, that it will take 3-4 well doublets to achieve a heat storage with an effect of 32 MW.

5.4.3 Evaluation of heat storage in deeper chalk formations in the Copenhagen area

In the previous project "High Temperature Energy Storage, HTES, EUDP 64016-0014" (Ross DK, 2018; Kristensen et al., 2017) the possibilities of establishing thermal storage in the chalk/limestone aquifer within the greater Copenhagen area (see Figure 5-5) in the depth range 400–800 has been examined.

The chalk in the storage zone is characterized by high porosity and low matrix permeability, but the presence of natural fractures means that the effective permeability can be higher than the matrix permeability. The evaluation of the storage potential is based on existing data and general knowledge of the subsurface, including data available from wells, core material, geophysical logs, seismic data and literature on geological aspects of the chalk.

The chalk section is subdivided into a number of flow units with different reservoir properties and each flow unit has been characterised with respect to the distribution of porosity, permeability, temperature and thermal properties. Based on this work a geological model was established and used for pointing out locations suitable for thermal storage in the chalk section and subsequent reservoir simulations.

The unit with the most favourable reservoir properties is the Lower Maastrichtian Hvidskud succession. The depth to the top of the unit varies across the study area due to basin character and post-depositional movements and erosion, but is generally around 600 m.

Reservoir simulations and groundwater modelling were conducted for estimating storage volumes, potential production and injection rates together with the expected pressure and temperature development as well as possible impact on/interaction with the groundwater zone. The model simulations indicate rather low flow rates in the reservoir, unless specific well configurations are used and/or well stimulation is applied. The simulations also indicate, that most likely, the chalk package between the groundwater and storage zones to some extent will act as a seal against upward fluid flow. The pressure disturbance in the storage zone will affect the formation pressure at the base of the groundwater zone to a limited extent, but most likely, the fluid flow in the storage zone does not interact with the groundwater zone.

Identical scenarios were simulated with both FeFlow from DHI-WASY GmbH and Eclipse from Schlumberger in order to compare and evaluate the performance of the two software packages. The results of the simulations point to comparable and rather similar results with respect to flow rates, heat transport, pressure development and temperature profile, meaning that both software packages can be used for analyzing and describing the reservoir performance in the depth range 0–800 m.

In the greater Copenhagen area, the Amager, Carlsberg, and Øresund fault systems are affecting the subsurface by intensive faulting, creating fractures in the chalk. Especially the Carlsberg fault zone is associated with a general increase in permeability and hydraulic conductivity. Such zones could potentially be relevant when considering thermal storage. However, there is a potential risk of 'loosing' the injected water, as the hot water may migrate into the fault zone.

Both the undisturbed and faulted parts of the chalk are considered a high-risk potential, as the matrix permeability is low and the effective permeability is not known. Further evaluation is therefore recommended prior to drilling a possible test well. However, the overall assessment of the study is that large-scale seasonal heat storage can be feasible in the evaluated chalk interval, but potential production and injection rates are difficult to assess based on the available data.

5.4.4 Feasibility study of high-temperature ATES in the Stenlille structure

In the previous project "HeHo -Heat Storage in Hot Aquifers, Danish Council for Strategic Research grant 10-093934" the Gassum Formation in the Stenlille structure (see Figure 5-5) that is presently used for gas storage was studied as an analogue for using hot geothermal reservoirs for heat storage (Pasquinelli et al., 2020).

Based on a 3D reservoir model, geological and technical characteristics of an aquifer relevant for heat storage in Denmark have been assessed. The model was established using analysis of geological core data, sedimentological descriptions, geophysical data including well logs and seismic lines. In the study finite difference modelling was applied to calculate the recovery efficiency, heat storage capacity and thermal breakthrough time in the reservoir.

Based on geostatistical methods, three different realisations of the reservoir model were established, and similar results were obtained for all three cases. The recovery factor of the thermal energy storage system was 70% after 4 years and 69% after 20 years. The storage capacity was 1.8×10^{18} J, and the thermal breakthrough time was 66–77 years. These results reflect the excellent reservoir properties of the Gassum Formation in Stenlille, characterised by a uniformly layered sand/shale sedimentology, a high average porosity of 25% and a high permeability of 1000 to 10.000 mD of sandstone intervals.

5.5 HEATSTORE survey of interests amongst District Heating utilities

In the context of HEATSTORE a survey of interests among approx. 400 District Heating (DH) utilities in Denmark was carried out in 2019. The DH utilities were asked ten questions on their specific interest, knowledge, and eventual considerations regarding UTES technologies.

In total 82 replies from DH utilities distributed throughout the country were received. In Figure 5-2 the responding utilities are distributed on municipality. Blue colours represent municipalities in which one or more utilities have completed the questionnaire.

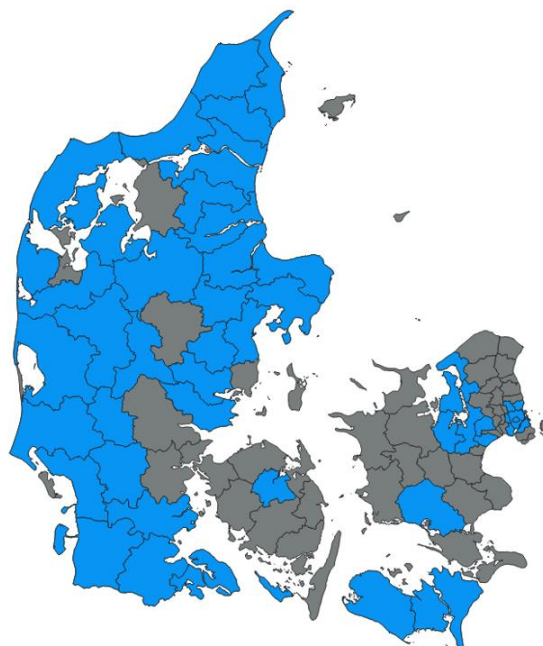


Figure 5-2. Visualisation of municipalities with DH utilities replying to the questionnaire (blue colour).

The survey outcome tells that most utilities (85%) do not have any actual plans on establishing a UTES system, whereas 40% find it possible or likely to implement UTES in the DHN in the future. Regarding PTES, that is the most established UTES technology in Denmark, 10% of the utilities are considering implementing PTES in the DHN in the future.

An output of the questionnaire was also an insight on the different types of surplus energy accessible or potentially accessible in the DH supply areas. The appointed sources of surplus heat are displayed at the graph in Figure 5-3. Wind energy, sun collectors and waste combustion are found to be the most likely sources of energy/heat input to a potential UTES system.

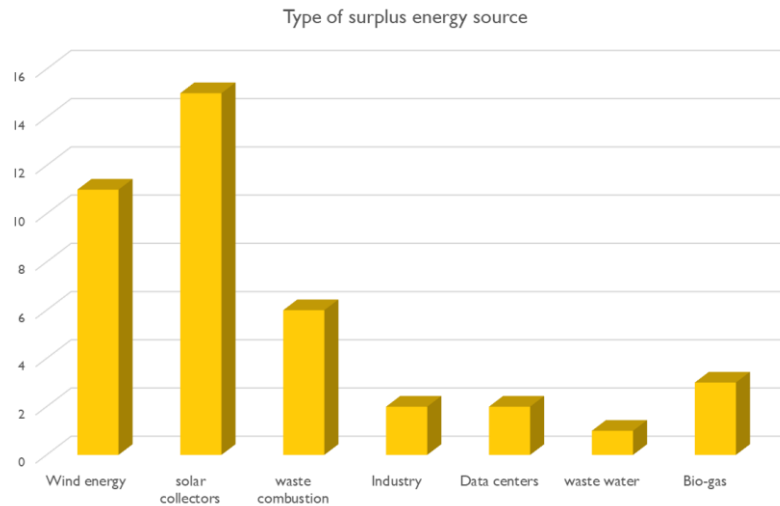


Figure 5-3. Appointed sources of surplus energy returned from the questionnaire. X-axis: type of energy sources. Y-axis: number of replies from questionnaire

Potential barriers have also been assigned by the DH utilities participating in the survey. Many possible barriers are indicated, see Figure 5-4, where the most obvious is the rather large initial investment.

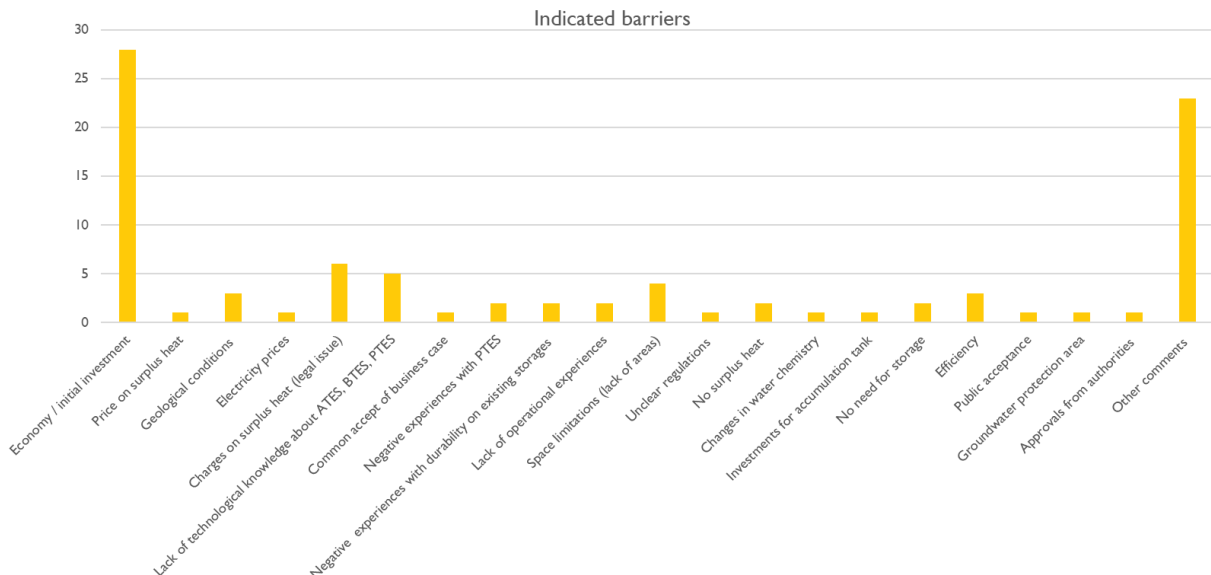


Figure 5-4. Indicated barriers highlighted by Danish DH utilities. Y-axis: number of replies from questionnaire.

Based on the survey results contact to and a dialog with interested DH utilities was established. This was done with the purpose and approach to line out the subsurface potential by a thorough geological characterization (approx. 0-300 m's of depth) based on exiting geological data.

5.6 Characterization of geology in specific areas

The aspect of characterizing the subsurface in selected geological and regional settings in Denmark is a step towards better understanding and knowledge towards the implementation of UTES. The areas of interest have been selected based on relevant criteria such as: a) local plans for heat storage from DH networks, b) accessible surplus heat source, c) local ambitions and plans to stop fossil fuel emissions, d) geological characteristics and geographical location. The outcome from the HEATSTORE investigations in each selected study area is a geological report with an initial evaluation of UTES potential based on existing data. If possible and relevant, existing 3D geological models of relevant structures have been updated.

The selected areas represent five different regions and geological settings in Denmark, see Figure 5-5. In area A) The storage potential is explored in Miocene sand deposits (sand lobes) in the central part of Jutland. In the area B) the potential beneath the city of Esbjerg (west coast of Denmark) is investigated. In area C) the potential in Quaternary deposits and limestone beneath Odense (third largest city in Denmark) is investigated. Area D) is aimed at characterizing the geology at the islands Lolland and Falster in the south-eastern part of Denmark dominated by chalk deposits with faults systems. Finally, in area E) the storage potential in the municipality of Aarhus on the East Coast of Jutland have been evaluated as part of the GeoERA project MUSE (Managing shallow geothermal Energy).

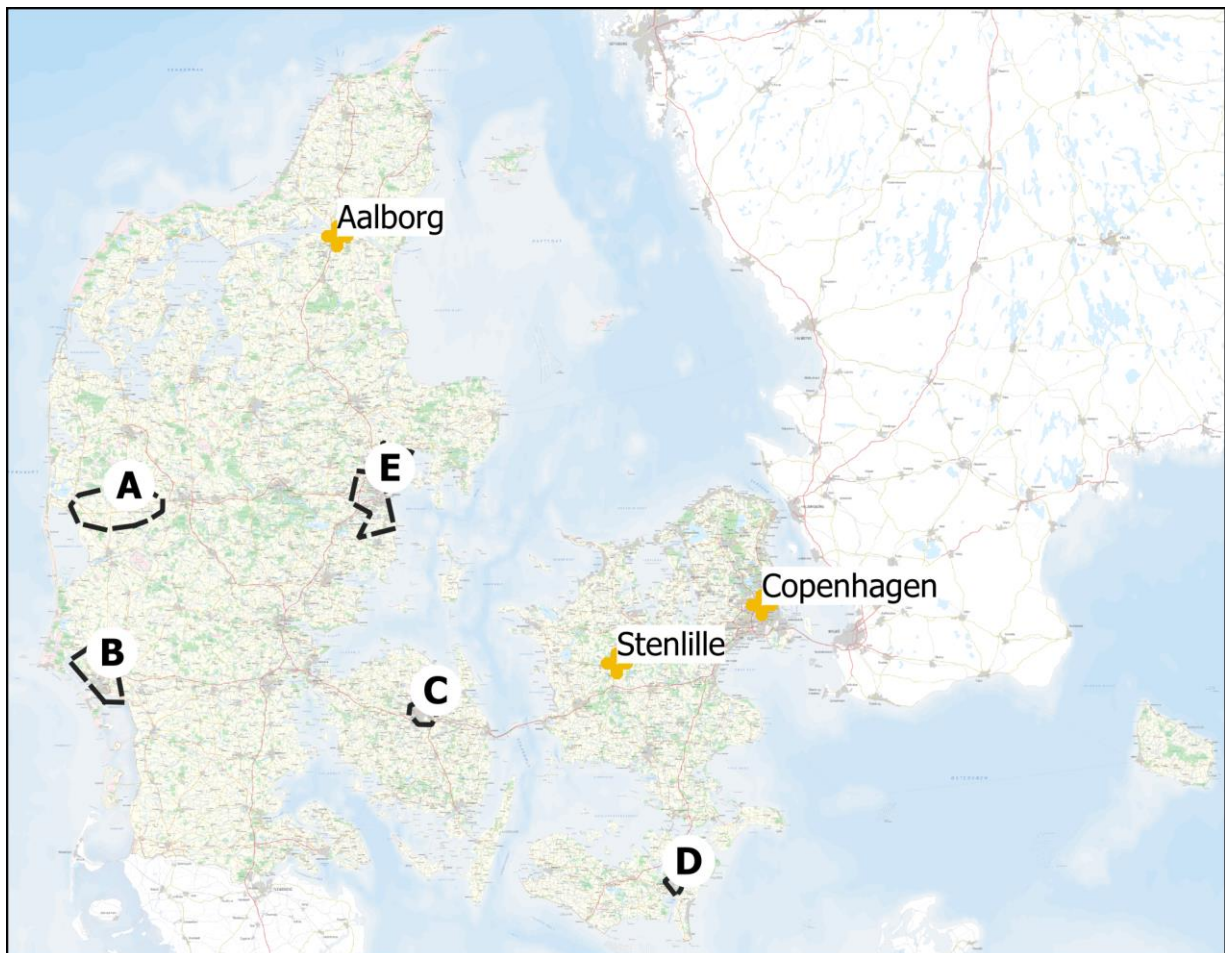


Figure 5-5. Overview of selected locations chosen for detailed geological characterisations. A) Miocene deposits in the central part of Denmark, B) Esbjerg area, C) Odense area, D) Guldborgsund, Southeast Denmark and E) Aarhus (part of GeoERA MUSE project). In Copenhagen, Aalborg and Stenlille the potential for UTES in deeper geological formations has been evaluated in previous projects.

In the following sections the results from the geological characterization in the selected areas are described in more detail.

5.6.1 Miocene deposits in the central part of Jutland

The focus area is located in the western and central part of Jutland. This area is characterized by having deep Miocene sequences, where the potential for UTES, in particular HT-ATES, is examined. Three stakeholders in the area have indicated interest in using the subsurface for storing excess heat, namely Ringkøbing District Heating utility, Videbæk energy utility and Arla Foods. Collaboration between some of the stakeholders on UTES storage has been discussed before this project.

The aim of this study is to evaluate the potential for high temperature ATES (HT-ATES) in Miocene aquifers at a depth of approximately 200-250 m below ground level. This interval is at present below target depth for drinking water interests. Available data from boreholes, geophysical data and seismic data as well as geological and hydrostratigraphical models has been utilized in the evaluation of the UTES potential. Several key boreholes are found in the area from which extensive data is thoroughly analysed. Data from the target depth close to the stakeholders are few and consists mainly of seismic data as well as a limited number of deep boreholes.

The Miocene sediments have been deposited in a deltaic environment with alternating transgressions and regressions, resulting in interchanging sandy and clayey formations, see Figure 5-6. The target formation, Billund Formation, is the deepest aquifer located in the area, below which highly plastic clays are deposited. The Billund Formation has been deposited as a series of deltaic lobes overlapping each other, where sandy aquifers may be separated by clayey intervals, see Figure 5-7.

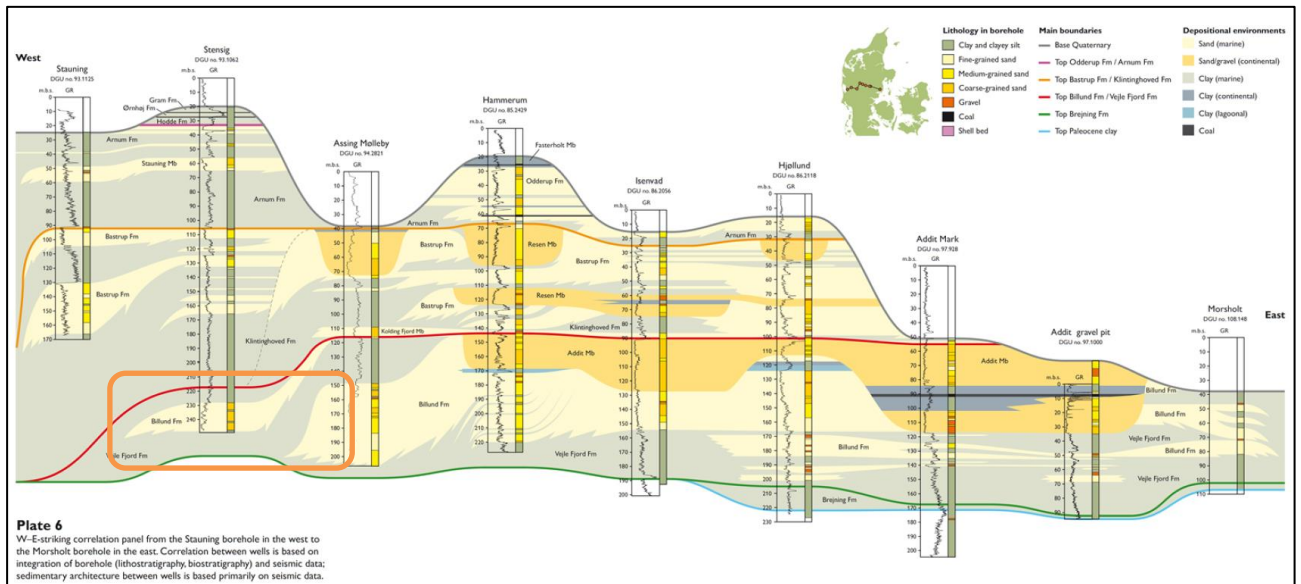


Figure 5-6. Correlation of the Miocene stratigraphy from West towards East. Yellow colours indicate sandy sediments, green colour indicate clayey sediments. Red line indicates max transgression of the Billund Formation. Area of interest corresponds to the western part of the panel. The orange box highlights the target aquifers in the study area.

The investigation shows that the Miocene sediments consists of sands and clays with a high content of organic matter as well as coarse quartz sands. The water quality in the deepest aquifers often indicates groundwater with a high content of organic matter, which is less suitable for drinking water. The hydrological properties of the deep aquifers are not well known due to very little data. The aquifer is highly inhomogeneous, and it contains clay layers in some areas. Data indicates that the aquifer disappears at the coast towards the South-West.

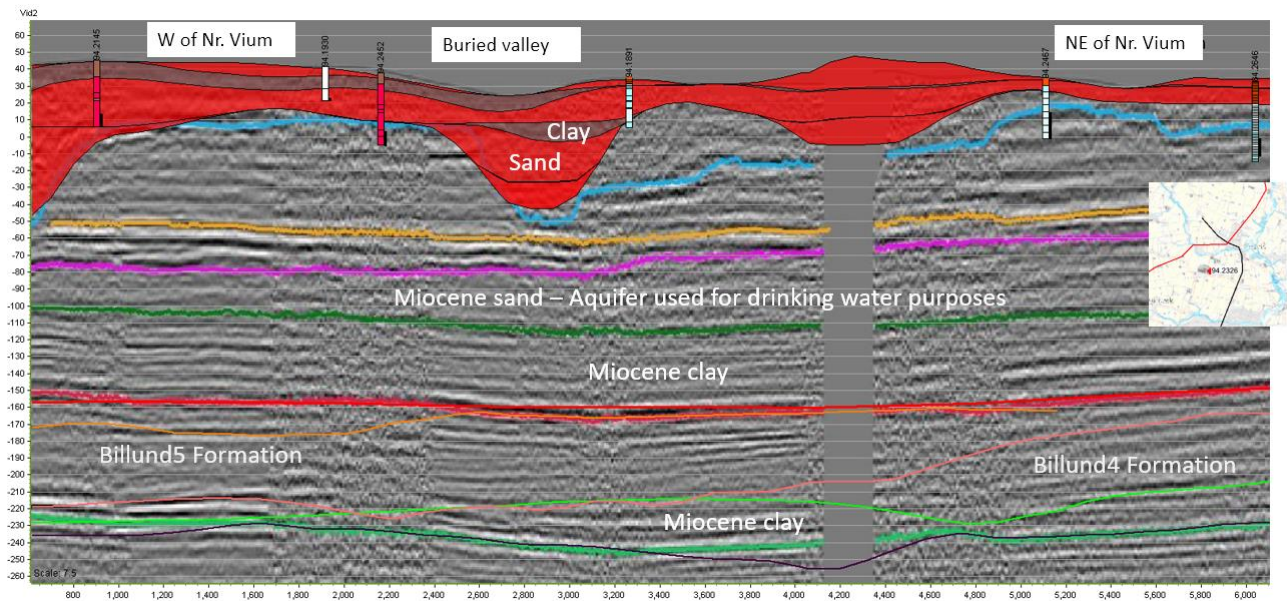


Figure 5-7. Seismic profile showing interpretation from the Miocene model as well as borehole data South of the city of Videbæk. The formation at approximately 200 meters below sea level has been interpreted as the Billund Formation. Note that the Billund Formation consists of two different lobes in this area, with Billund4 to the East and Billund5 to the West. The sedimentary composition of the formation is unknown as no borehole data from this depth exist in the area.

The Quaternary sediments in the area are highly variable in thickness due to the presence of buried valleys, especially in the western part of the area. A few of the buried valleys are estimated to reach depths of more than 200 meters, and it is therefore possible that Quaternary sediments locally are in contact with the deepest Miocene formations. The Quaternary sediments consist mainly of sandy meltwater sediment with layers of clayey tills.

The potential for HT-ATES has been evaluated in regard to the deepest Miocene aquifers in the area, see Figure 5-8. The aquifer has been identified in most of the available data in the area, though the seismic data indicates small or no presence in the vicinity of the city of Ringkøbing. The potential is very dependent on whether the aquifer is present at sufficient thickness and with suitable hydraulic properties. Data indicates that the aquifer is very inhomogeneous, both in thickness and in sedimentary composition. Therefore, it is necessary with detailed local investigations (test drilling) to clarify the expected potential (GEUS report 2021/14).

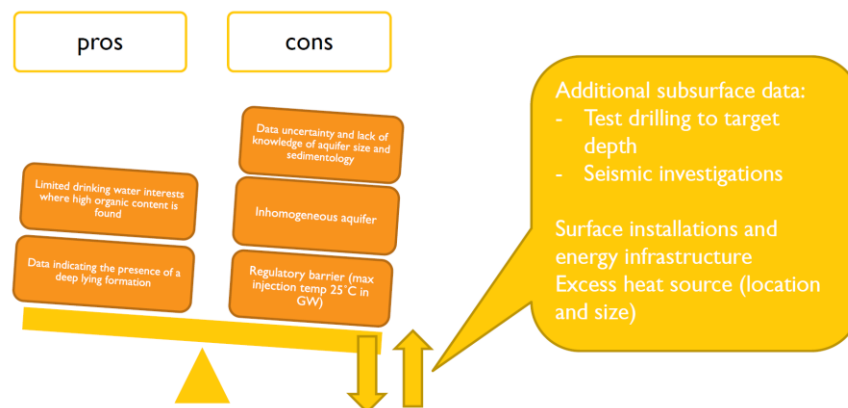


Figure 5-8. Sum up of screening process – pros and cons for UTES in the focus area. GW: groundwater.

5.6.2 Esbjerg area, Western Denmark

Esbjerg is located at the Danish west coast. The investigated sequence potentially suited for UTES consists of 5 m to more than 100 m of Quaternary sands and clays underlain by Miocene marine clays and silt with thin sandy layers (see Figure 5-9). The largest UTES stakeholder in the area is the DH utility “DIN Forsyning” with

more than 25.000 consumers. The utility is facing a need for heat storage in the nearest future and is currently considering several options for seasonal energy storage as an integrated part of the DH network. The aim of the investigations has been to evaluate the potential for BTES and High Temperature ATES (HT-ATES) in the upper c. 300 m of the sedimentary sequence. Below this depth, impermeable marine clays and limestone with no confirmed groundwater flow are found. All accessible existing subsurface data in the area (especially data from a major national groundwater mapping program from 1999-2015 and boreholes from the national borehole database JUPITER) has been used to evaluate the UTES potential.

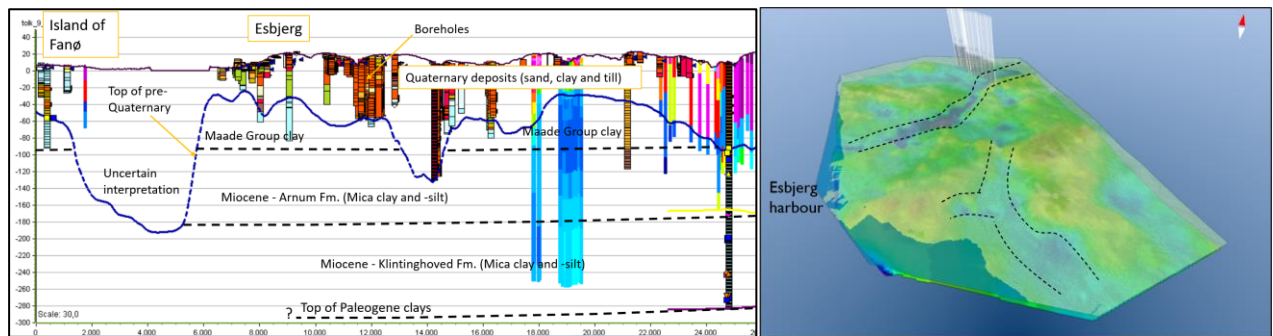


Figure 5-9. Left: West-northeast cross section through the Esbjerg area illustrating the interpreted geology. Many shallow boreholes are accessible in Esbjerg visualised by coloured poles on the profile. Right: 3D view of the focus area showing interpreted buried valleys.

The investigation shows a sequence of Quaternary deposits in the Esbjerg area that are mostly less than 25 m thick and dominated by meltwater sands in the areas beneath the city. North and east of Esbjerg, thicker sequences of Quaternary deposits in buried valley structures are found. Particular marine inter-glacial sediments are found deposited on top of the Miocene. The Miocene deposits are dominated by mica clay formations to a depth of approx. 300 m, see Figure 5-9. Only a few thin layers of fine sand given rise to low yields of groundwater are recognized in deeper boreholes and no regional Miocene sand units have been identified in the investigated area. The drinking water supply in Denmark is based on groundwater, and due to the fact, that the region generally is challenged by limited groundwater resources, the UTES potential in the area is generally overlapping with drinking water interest. Especially sand deposits in Quaternary buried valley systems in the northern part of the region are an important source for drinking water and may not be available for UTES.

The potential for HT-ATES in semi-deep aquifers without drinking water interests has been evaluated based on an interpretation of the Miocene deposits and is considered to be low in Esbjerg. Compilation of subsurface data indicate a buried valley system east of Esbjerg with poor groundwater quality, which could be of further interest in respect to HT-ATES, see Figure 5-9, right. The potential in the town of Varde towards the northeast, which is also is an important section of the DH grid, has not yet been assessed in detail.

The potential for BTES in and around Esbjerg is as opposed to ATES related to the very shallow layers. As described above, the shallow subsurface are dominated by thin deposits of meltwater sand. These are partly saturated and a general groundwater flow towards the west coast may potentially have a negative effect in terms of heat transport away from a shallow BTES. The underlying Miocene clays has no groundwater flow and could act as storage medium, but this may require insulation of the upper part of the bore-hole storage to avoid heat loss due to expected near surface groundwater levels. The findings in the geological characterization process are summarized in Figure 5-10 describing pros and cons. As illustrated further initiatives can change the balance regarding the feasibility of UTES in the Esbjerg area (GEUS report 2021/11).

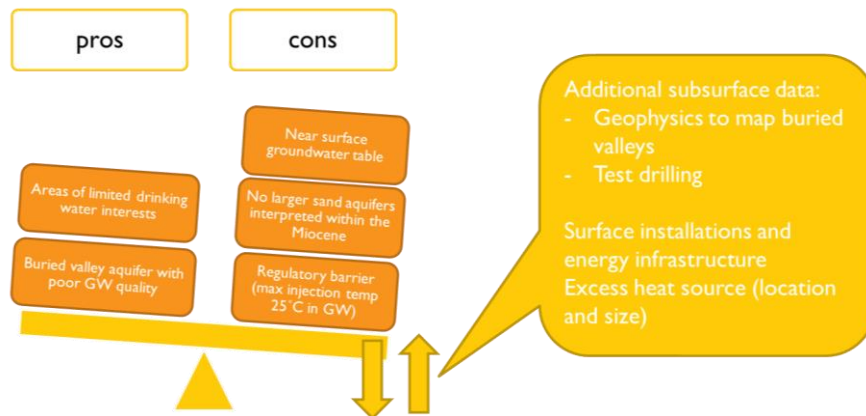


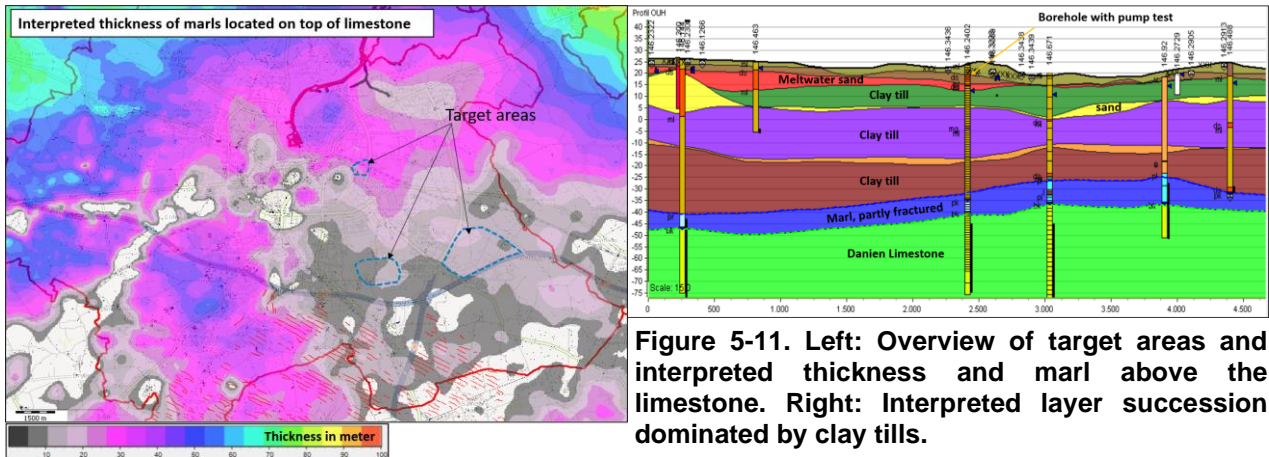
Figure 5-10. Sum up of screening process - pros and cons found for UTES in the Esbjerg area. GW: groundwater.

5.6.3 Odense area, Island of Funen

Odense is located at the island of Funen, defining the central part of Denmark. Odense has been selected as an area representing a geological setting consisting of both quaternary sediments and older marl and limestone deposits partly fractured by glacial processes throughout the ice ages, see Figure 5-11. The largest stakeholder in the area is the DH utility for Odense and suburbs, "Fjernvarme Fyn", with more than 100.000 consumers. The utility is facing a need for heat storage in the nearest future and is currently considering several options for seasonal energy storage as an integrated part of the DH network. Different surplus heat sources are accessible in the area, and a targeted view on the subsurface in these specific areas of interest has been carried out to push barriers of limited knowledge about the geology from an energy perspective.

The target has been to evaluate the potential for BTES and HT-ATES in the upper c. 150 m of the subsurface in the Odense area. Based on input from the DH utility regarding existing DH transmission lines and location of surplus heat sources, the study is focusing on the south-eastern part of Odense. Below approx. 75-100 m the geological layers consists of Danien limestone with almost no available data and presumably no or very limited groundwater flow. All accessible existing subsurface data in the area (especially data from a major national groundwater mapping program from 1999-2015 and boreholes from the national borehole database JUPITER) has been used to evaluate the UTES potential.

The geological interpretation of the available data in south-eastern Odense generally reveals a 40 to 60 m thick sequence of Quaternary deposits dominated by clay tills and only local meltwater sands units. Below the Quaternary sequence, Kerteminde marl varying in thickness from <10 m to 25 m is found, see Figure 5-11. The marl shows internal variations in the degree of fractures and thereby also permeability. Danien limestone is underlying the marls and the degree of fractures in the limestone is expected to be closely connected to the thickness of the overlying marl because of glacial deformation and erosion. The drinking water supply in Denmark is based on groundwater and the evaluation of the UTES potential must take drinking water interests into consideration. In the south-eastern part of Odense there are few or no drinking water interests due to a limited presence of aquifers and a high content of chloride in the marl and limestone. The latter indicate residual saline water in the old sediments and a limited hydraulic conductivity preventing freshwater (infiltration) flow from above, see Figure 5-11.



The potential of HT-ATES in the Kerteminde marl and limestone is very dependent of a sufficient permeability in the marl and limestone and based on available pumping information from (especially old) boreholes, the expected permeability is likely to be too low for ATES. A new exploration drilling would be able to clarify if there are more fractured deposits suitable for hot water injection and extraction.

The potential for BTES depend on the degree of groundwater flow and the clay tills and underlying marl/limestone could represent favourable areas with limited groundwater flow like the existing BTES in Brødstrup, Denmark (PlanEnergi, 2013). A challenge regarding BTES in this context could be to find a suitable surface to establish a borehole storage of sufficient size. Generally, experiences show that a BTES facility should have minimum storage volume of 20.000 m³ soil/rock to be profitable (Sibbitt & McClenahan, 2015). Based on the present datasets, the thermal conductivity is not known for the local sediment sequence (clay till and marl/limestone), but this could be acquired through a Thermal Response Test (TRT). A test drilling can also clarify the existence of internal sand/gravel layers with the clay till sequence, which compromise the storage efficiency. The findings in the geological characterization process are summarized in Figure 5-12 describing pros and cons. As visualized, further initiatives can change the balance regarding the feasibility of UTES (GEUS report 2021/12).

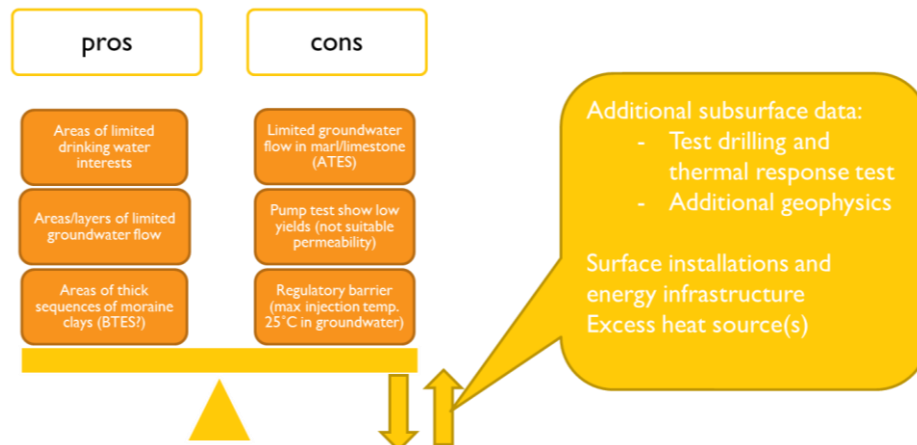


Figure 5-12. Sum up of screening process - pros and cons found for UTES in the Odense area.

5.6.4 Guldborgsund, Southeast Denmark

Within HEATSTORE the subsurface in Guldborgsund, situated in the south-eastern part of Denmark, has been characterized and evaluated for UTES potential in the Municipality. The local DH utility has initially recognized a considerable amount of surplus heat from a waste combustion and biomass facility, that potentially could be stored during the summer period, and thereby be implemented as an integrated part of the DH supply in the future. In the area a thick sequence of limestones and chalk is found near the surface only overlain by a thin cover of glacial deposits. The chalk and limestones are expected to be fractured partly by glacial processes partly by deeper fault that have been identified by geophysics. Similar geological settings are found in many

parts of Denmark and therefore some general conclusions of this study are expected to be valid elsewhere in similar geological settings.

The aim of looking at this area was to evaluate the potential for both High Temperature ATES (HT-ATES) and BTES in the upper subsurface (c. 0-300 m) in the Guldborgsund area. The study is focusing on an area, east of the town Nykøbing F, which is close to the DH facilities. A vast amount of existing geological and geophysical data especially from a major national groundwater mapping program from 1999-2015 and as well as the national borehole database (JUPITER) has been used in the evaluation.

In and around the study area a 10-20 m thick sequence of Quaternary deposits is found. The sediments are dominated by clay tills with local deposits of meltwater sands towards east. Below glacial deposits we find chalk formations down to around 400 m's of depth. The chalk is soft to very soft containing varying content of flint nodules. Boreholes and geophysics indicate local variations in the density of fractures and thereby also permeability. In general deformation and erosion by glaciers through-out the ice ages have probably caused fracturing of both glacial deposits and the upper part of the chalk. In areas of mapped faults lines, fresh water seems to have washed out old saline water to depth below 100 m, see Figure 5-13. Areas without visible faults appears to be more homogeneous containing salty pore water without freshwater.

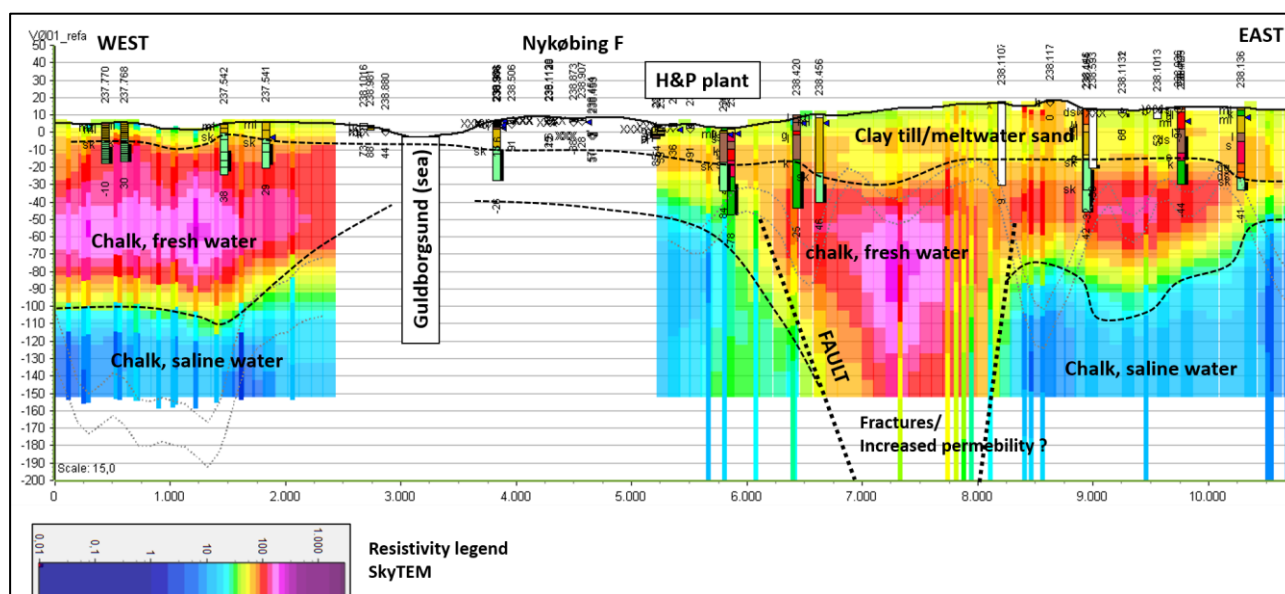


Figure 5-13. West-east cross section through the study area. As background is shown a 3D resistivity grid based on SkyTEM (AEM) data. Red colours are high resistivities representing chalk with fresh water in pore spaces or sands. Blue colours show low resistivities representing chalk containing saline water. Surplus heat source (H&P plant) is shown at 6000 m, and an interpreted fault is sketched at 6500-7000 m.

Because the supply of drinking water in Denmark generally and on Falster particularly is based on groundwater protection of aquifers for drinking water must be given high priority in the evaluation of the UTES potential.

The eastern part of the study area is designated as an area of drinking water interests, while the town area within Nykøbing F. is not, which is probably due to an increased content of chloride near the coastline.

Because (HT)-ATES in the chalk depends on a sufficient secondary permeability within the sediment, the fractured zone found in relation to fault lines are believed to hold a certain potential and could be a suitable target for further investigations. Furthermore, they are located rather close the heat and power plant producing surplus heat (waste combustion). More data is needed to identify the actual potential.

The potential for BTES depend on the degree of groundwater flow, near surface groundwater levels, and suitable areas for a storage facility. Areas of compact chalk are found in some areas of Guldborgsund area with a thin cover of Quaternary deposits. A limiting factor based on the existing data are found to be a near surface groundwater table and expected flow. Also, areas of compact chalk and clay do not seem to be present in close distance to the primary source of surplus heat in the area. Figure 5-14 sums up the result from the geological characterization in Guldborgsund divided into pros and cons (GEUS report 2021/13).

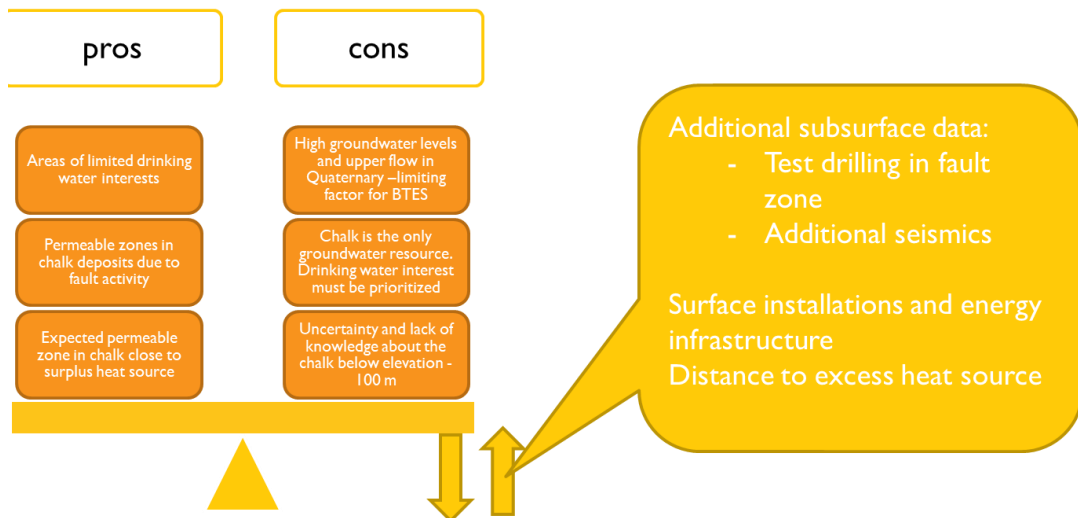


Figure 5-14. Sum up of screening process - pros and cons found for ATEs and BTES in the Guldborgsund area.

5.6.5 Aarhus (synergy with the MUSE, GeoERA, project)

This area comprises the municipal area of Aarhus, and the aim of the desktop case study is to investigate the possibilities of integrating SGE and UTES in a mature central heating system. Potential geothermal resources and UTES reservoirs have been mapped using a wide arrange of existing geological and geophysical data. Further on, the work will focus on mapping potential conflicts; prioritising possible sites in relation to expected yield and proximity to the existing grid; and the integration of the results into the local energy plans. The regional geological and hydrogeological characteristics of the Aarhus area are summarized in Figure 5-15, below (GEUS report 2021/26).

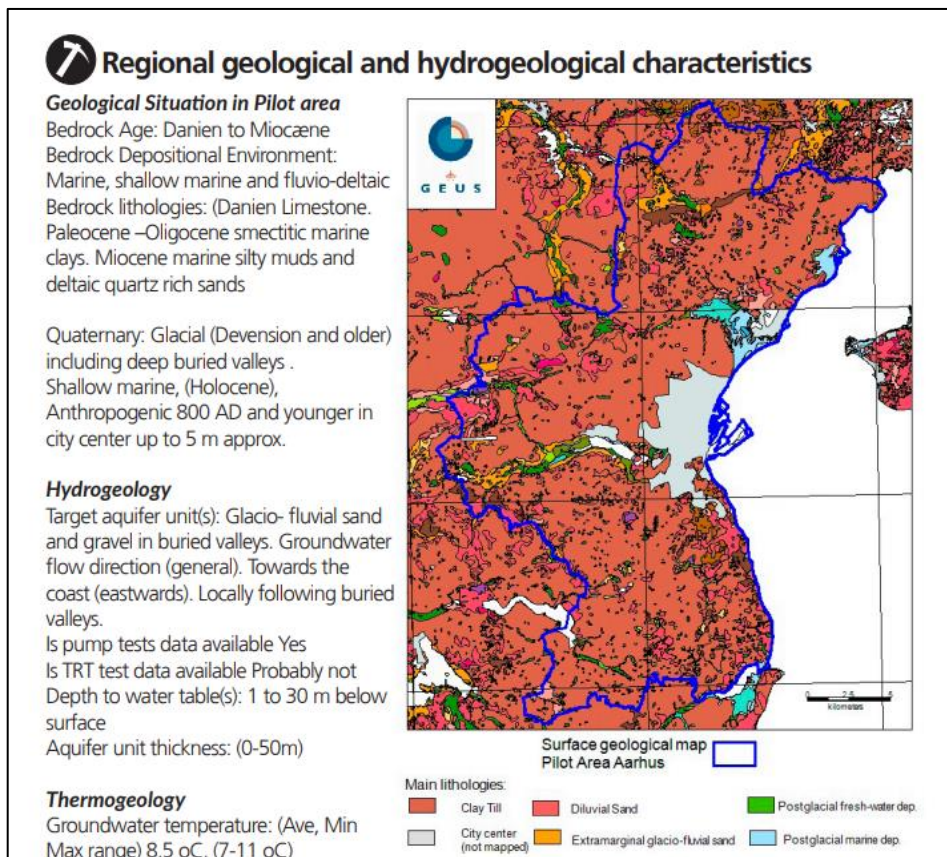


Figure 5-15. Geological data sheet for Aarhus.

In order to evaluate the potential for ATEs and HT-ATES the extension of groundwater bodies in the area have been mapped.

The groundwater bodies have been designated based on model layers of Quaternary sand more than 10 m thick in the national 3D groundwater resource model. The outline of the areas received from the model grid have been smoothed manually based on borehole information, see Figure 5-16.

Since both public and private extraction of drinking water is widespread, heat storage at higher temperatures is found not to be realistic in the greater part of the municipality. Only in the coastal section of two buried valleys this could potentially be an option following an Environmental Impact Assessment (EIA) and as well as an assessment of potential heat loss.

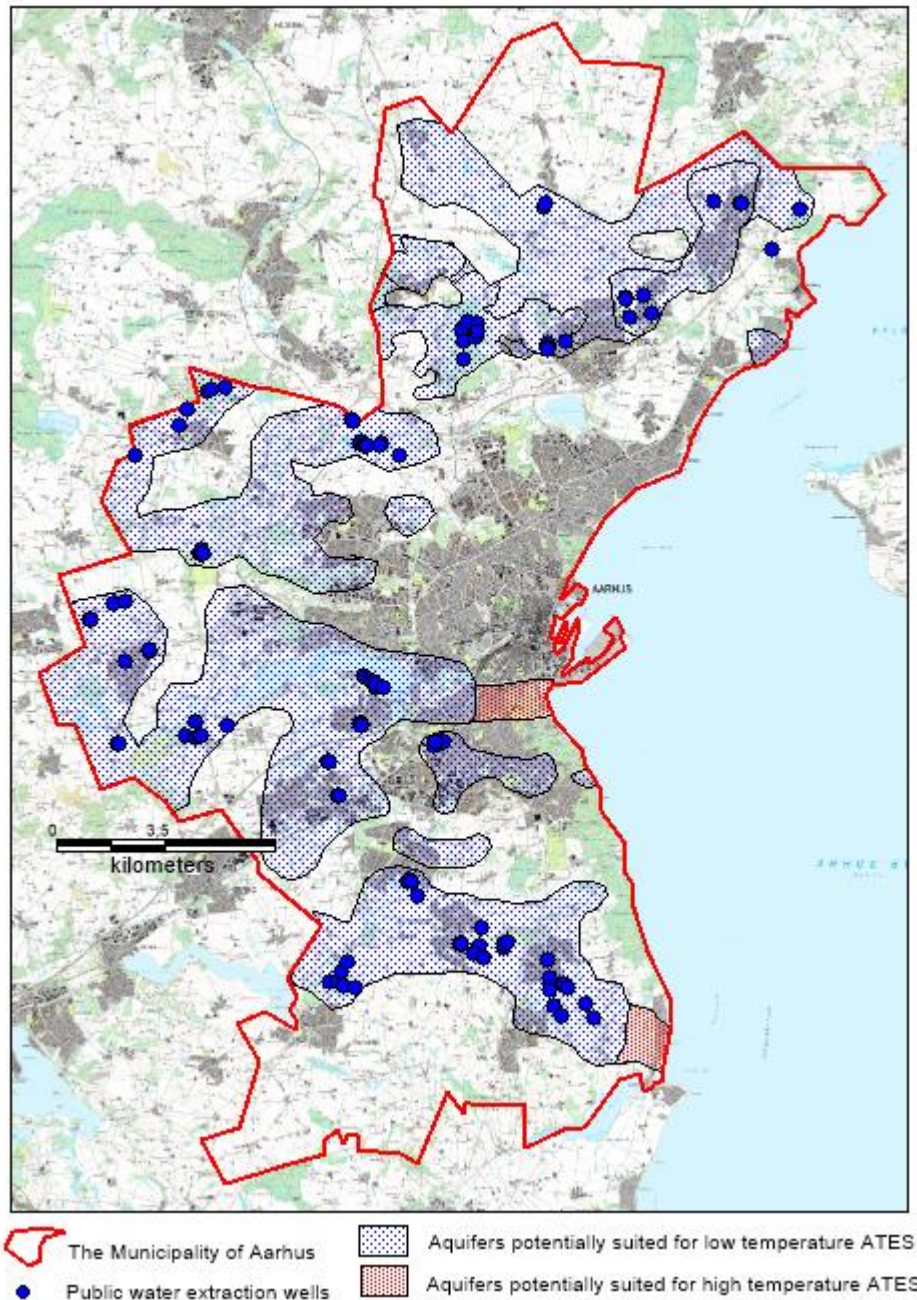


Figure 5-16. Areas potentially suited for ATEs.

In areas suited for BTES it is required that that the groundwater flow is minimal. In Aarhus two types of such areas have been recognized:

a) Areas with a thick unsaturated zone

Areas with >20 m of unsaturated sediments above the water table have been mapped using water level soundings for the national borehole database and topographic models of the terrain, see Figure 5-17. Monitoring results from a pilot borehole storage above the groundwater table in Brædstrup, Denmark, have shown that the heat dissipation below the bottom of the storage is limited. Therefore, it is estimated, that BTES can safely take place in the unsaturated zone also inside designated groundwater protection areas (provided local conditions are taken into account).

b) Shallow impermeable clay formations

In areas with impermeable clay deposits, no groundwater flow is expected. Therefore, such formations are potentially suited for BTES and areas with less than 25 m to the top of the clay formations have been mapped using maps of the pre-Quaternary surface (elevation and rock types), see Figure 5-17. Borehole data has been used to support the mapping.

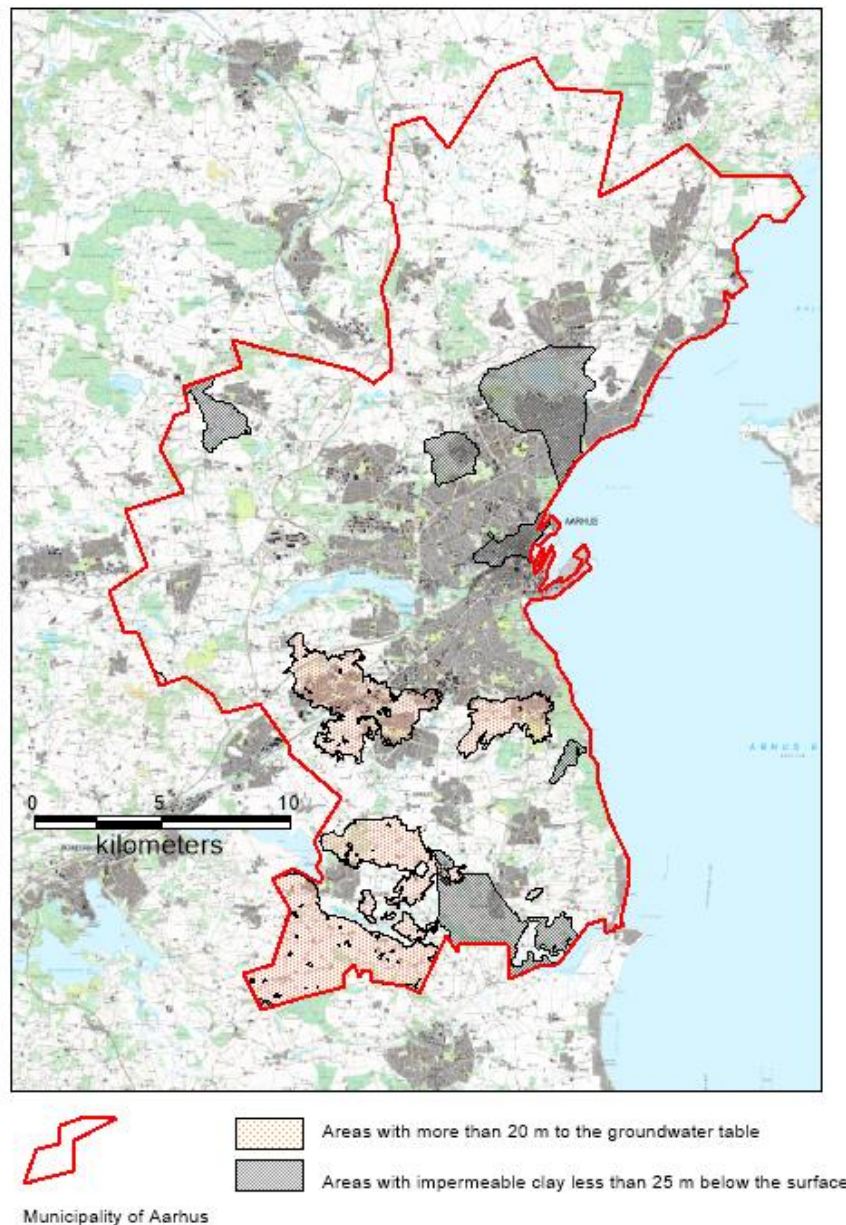


Figure 5-17. Areas potentially suited for BTES.

5.7 Expansion of web screening tool – new data and added value

To improve and ease the UTES screening process further for the Danish stakeholders, the initial web tool for screening of heat storage potential has been updated and expanded with new data in the HEATSTORE project. Information on aquifers and aquitards from the national Danish groundwater mapping program in terms of the 3D hydrostratigraphical FOHM model provided by Miljøstyrelsen (The Danish Environmental Protection Agency) has been compiled and incorporated in the web tool and also the described characterization of local geological conditions, see section 5.6, is included in order to represent examples and inspiration for all stakeholder with interests in thermal energy storage.

The additional data input will strengthen the applicability for the end-users and give a better overview and more and more detailed information in the process of appointing areas potentially suitable for especially ATES/HT-ATES and BTES, but also for PTES.

The Danish UTES screening platform will be available through the HEATSTORE UTES screening site containing subsurface and energy themes important in the screening process for UTES potential.

5.7.1 Purpose and functionality

The purpose of the web tool is to facilitate a screening of the potential for heat storage in the upper 2-300 m of the subsurface focusing on ATES, BTES and PTES.

The web tool application makes it possible to combine several different geological, hydrological, environmental and administrative map-themes in the screening process. It is possible to setup filters for displaying subsets of data and to select and show profiles across the selected map layers and link to the original borehole data.

5.7.2 Data overview

The web tool provide access to map layers showing areas with a potential for UTES divided into aquifers for ATES (local near surface Quaternary aquifers, regional Quaternary aquifers, deep Quaternary aquifers and Miocene aquifers in the western part of Denmark), aquitards or other units without groundwater flow for BTES and layers showing top soil information and depth to the uppermost groundwater table for evaluation of the possibility of PTES.

The map data is partly from the earlier first edition of the web tool and partly from a major national groundwater mapping program in Denmark. Furthermore, information can be found on existing boreholes used for shallow geothermal purposes in terms of Borehole Heat Exchangers and low-temperature ATES systems, available scientific/technical reports as well as a theme showing the location of heat producers in Denmark in 2018 provided by Energistyrelsen (The Danish Energy Agency).

The web tool includes the following geological data:

- 3D geology information from the national hydrostratigraphic model (modelled Quaternary units, Miocene units, Paleogene clays, limestone and chalk)
- Borehole data shown as cyclograms for quick overview
- Boreholes deeper than 10 m and with geological description
- Thickness of sand and gravel in boreholes in selected depth intervals
- Boreholes with paleogene plastic clay
- Overview of identified paleochannels (incised buried valleys)
- Overview of areas with silt, gyttja and peat

And the following groundwater data:

- Groundwater table in boreholes deeper than 10 m
- Yield in volume/hour/meter drawdown
- Abstraction wells
- Water type in terms of groundwater chemistry
- Regional maps of hydraulic head
- Classification of drinking water interests

Other data:

- Environmental protection areas
- Soil contamination areas
- Links to relevant accessible public reports describing geo-energy projects, e.g. local screening reports carried out partly within the frame of HEATSTORE

5.7.3 Perspectives for further activities

There is an increasing interest in the application of seasonal heat storage in the district heating sector in Denmark and the element of coupling surface and subsurface potential has been improved significantly in the HEATSTORE project with the expansion of the web tool for screening of heat storage potential. But the importance of coupling subsurface conditions and surface facilities must still be emphasized. Therefore, improving the availability of combined knowledge about the local geological conditions and relevant surface installations such as district heating networks and sources of surplus heat will be a prioritized goal beyond the project in order to equip decision makers and technical experts in the energy sector with the necessary tools in the initial energy planning phase.

5.8 References

- GEUS report 2021/11: Evaluation of potential geological heat storage – Esbjerg (heatstore.eu/downloads)
- GEUS report 2021/12: Evaluation of potential geological heat storage – Odense (heatstore.eu/downloads)
- GEUS report 2021/13: Evaluation of potential geological heat storage – Guldborgsund (heatstore.eu/downloads)
- GEUS report 2021/14: Evaluation of potential geological heat storage – Ringkøbing-Videbæk (heatstore.eu/downloads)
- GEUS report 2021/26: Evaluation of potential geological heat storage – Aarhus Municipality (heatstore.eu/downloads)
- GEUS, 2019: Evaluation of the potential for geological heat storage in Denmark. EUDP 1887-0017, Final report.
- Guldager, C., Poulsen, S. E. & Balling, N. 2018: Numerisk modellering af varmelagring i dybe sedimentære reservoirer med særligt henblik på Aalborg-området. Forskningsrapport, EUDP projekt 1887-0017. Institut for Geoscience, Aarhus Universitet.
- Kallesøe, A.J. & Vangkilde-Pedersen, T. (eds). 2019. Underground Thermal Energy Storage (UTES) – state-of-the-art, example cases and lessons learned. HEATSTORE project report, GEOTHERMICA – ERA NET Cofund Geothermal. 130 pp + appendices.
- Kristensen, L., Mathiesen, A., Nielsen, L. H. & Johannessen, P. 2016: Undersøgelse af de geologiske muligheder for lagring af varmt vand i undergrunden ved Aalborg. GEUS Report 2016/40.
- Kristensen, L., Mathiesen, A., Nielsen, C. M., Bjergager, M., Ditlefsen, C., Møller, I. Rasmussen, P., Nielsen, L. H. & Sonnenborg, T. 2017: Examining the possibilities of establishing thermal storage in the chalk/limestone aquifer in the greater Copenhagen area. GEUS Report 2017/22.
- Pasquinelli, L., Felder, M., Gulbrandsen, M. L., Hansen, T. M., Jeon, J-S., Molenaar, N., Mosegaard, K., & Fabricius, I. L. 2020: The feasibility of high-temperature aquifer thermal energy storage in Denmark: the Gassum Formation in the Stenlille structure. Bulletin of the Geological Society of Denmark, 68, 133-154. <https://doi.org/10.37570/bgdsd-2020-68-06>
- Ross DK, 2018: Termisk lagring (HTES). EUDP 64019-0014, Final report.

6 Screening of Potential in France: Focus on Ile-de-France

6.1 Context

In August 2015 the “Energy Transition Law for a Green Growth” (ETLGG) has been passed by the French Parliament. The global targets of the law mandate a 40% reduction of greenhouse gas emissions between 1990 and 2030, a fivefold increase of the quantity of renewable and recovered energies delivered by heating and cooling networks (DHCN) by 2030 (i.e. around 39.5 TWh/year). The share of renewable energy must also reach between 55% and 60% in DHCN by 2023.

Introduced by the 2015 law, the national low carbon strategy (*Stratégie Nationale Bas Carbone* in French) is a roadmap which aims for carbon neutrality within 2050 over the French territory. The measures to achieve this objective are set out in the Multi-year Energy Programming (*Programmation Pluriannuel de l’Energie* in French or PPE). This program forecasts an increase in the share of renewable heat between a factor of 2.2 and 2.6 by 2028 compared to the year 2017. In 2019, around 2 TWh of geothermal energy were produced nationally, of which 1.6 TWh supplying district heating networks (Hamm and Maurel, 2019). The geothermal energy is mainly developed in the Paris Basin in Ile-de-France region and more precisely in the deep geothermal Dogger limestone aquifer (Jurassic). To reach the objectives set by the 2015 law and by the low carbon strategy to develop renewable energy share, the exploitation of new geothermal resources, the valorisation of waste energy and the storage of energy are essential.

The share of renewable energy in France has increased from 27% to 47% between 2007 and 2013, and this trend is currently decelerating. Meanwhile, the deposit of industrial waste heat produced at temperature above 100 °C has been estimated to reach 53 TWh/y (ADEME, 2017). 16 TWh/y of waste heat at temperature above 60 °C is dissipated close to existing DHN.

For BRGM, the objective of the present study is to assess how UTES could be suitable to increase the share of waste heat and renewable energy in existing DHN in the region Ile-de-France which is home to the city of Paris (Figure 6-1).

The French ATES potential will be evaluated according to available public data, by combining subsurface data (e.g. depth of the targeted geological formation, thickness, petrophysical parameters, temperature distribution at different depth, geochemistry of waters), surface data (e.g. location of district heating and cooling networks, land occupation) and energy data (e.g. heat demand, heat demand distribution in time, excess heat sources, excess heat supply in time, geographical distribution). The final objective is to identify the most promising areas for potential future implementations. At this stage economical, regulatory and socio-environmental constraints will not be taken into account. The methodology applied to screen the potential originates from the application of (Schout et al., 2014) analysis of recovery efficiency for high temperature ATES based on Rayleigh number over aquifers with high geothermal potential in the Ile-de-France (IDF) region, in the Paris sedimentary basin.



Figure 6-1. Location of the Ile-de-France (IDF) region, home to the city of Paris which will be under study for the case of France.

6.2 Available data

The available data used during the study are presented here below.

6.2.1 7.2.1 District heating network

The following information regarding the DHN were used:

- Yearly national survey about DHN (EARCF: *Enquête Annuelle sur les Réseaux de Chaleur et de Froid*) carried out by the *Syndicat National du Chauffage Urbain et de la Climatisation Urbaine (SNCU)* and the AMORCE association under the lead of the Ministry of Ecological Transition. 699 DH&CN operators answered the 2017 survey. In the report available online (<http://reseaux-chaaleur.cerema.fr/enquete-annuelle-du-chauffage-urbain-et-de-la-climatisation-urbaine>). BRGM has been accredited to assess the confidential results of this survey, which includes:
 - o Detailed energy mix (energy/year and power) including per sources (biomass, waste heat, etc.)
 - o Heat carrier fluid temperature
 - o DHN length & number of substations
 - o Heat use (residential, agriculture, etc.)
- ViaSeva association publishes every 2 years a DHN directory (<http://viaseva.org/annuaire-des-reseaux-de-chaaleur-et-de-froid/>), which is public but with a lower level of information. The information is available online for 535 DHN, including the maps of 350 DHN (<https://www.observatoire-des-reseaux.fr/cartographie-nationale/>)
- Display of the geo-spatialized data of DHCN, heat and cold consumption at different scale are provided by the Interministerial catalog of geographic data Geo-ide (http://carto.geo-ide.application.developpement-durable.gouv.fr/906/Carte_chaleur_nationale.map and <http://carto.geo-ide.application.developpement-durable.gouv.fr/73/energie.map#>);
- Besides, for Geothermal DHN, BRGM has estimated of delivered geothermal energy (for 50 operations in Paris Region)

Besides in France we can retrieve the CO₂ content of 675 DHCN (September 2021). The values are published in the *journal officiel*. Computations are compiled by ADEME (French Energy & Environment Agency) (<http://www.bilans-ges.ademe.fr/fr/basecarbone/donnees-consulter/choix-categorie/categorie/5>). This data was not used for this study.

In 2019, the IDF region has 113 district heating networks and a total of 1 854 km of network. 14 680 buildings are connected to a DHN and the amount of heat delivered is 11 335 GWh according to the national 2019 survey by (FEDENE, 2020)⁵. Figure 6-2 presents the location of the district heating and cooling networks in the region. The renewable energy share in the IDF networks is 53% and the CO₂ content is 0,136 kg/kWh. The three main renewable energy used to feed the heating network in this region are: waste heat (4 013 GWh and 14 sites recorded to DHN), geothermal (1 710 GWh with 38 network connected to deep geothermal operations and 7 to installation using heat pumps) and biomass (1 299 GWh).

⁵ <https://www.fedene.fr/wp-content/uploads/sites/2/2021/01/EARCF-Rapport-Global-%C3%A9dition-2020-Restitution-enquete-r%C3%A9seaux.pdf>

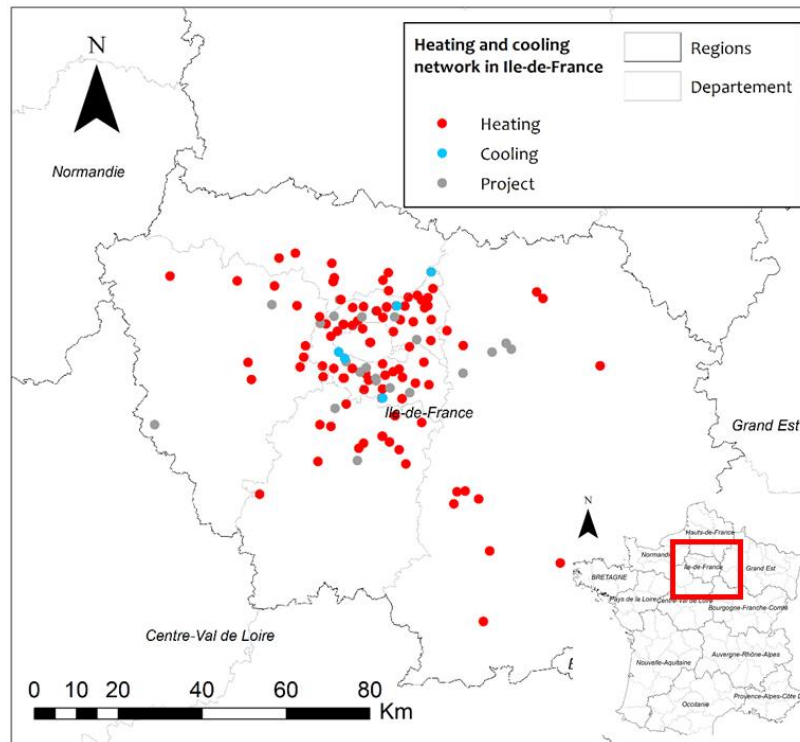


Figure 6-2. Location of DHCN in the Ile-de-France region (source SNCU⁶).

The outline of the district heating and cooling network is available over the Interministerial catalog of geographic data Geo-ide⁷ and for the Ile-de-France region is provided by DRIEAT (the directorate for environment, development and housing) and is presented in Figure 6-3.

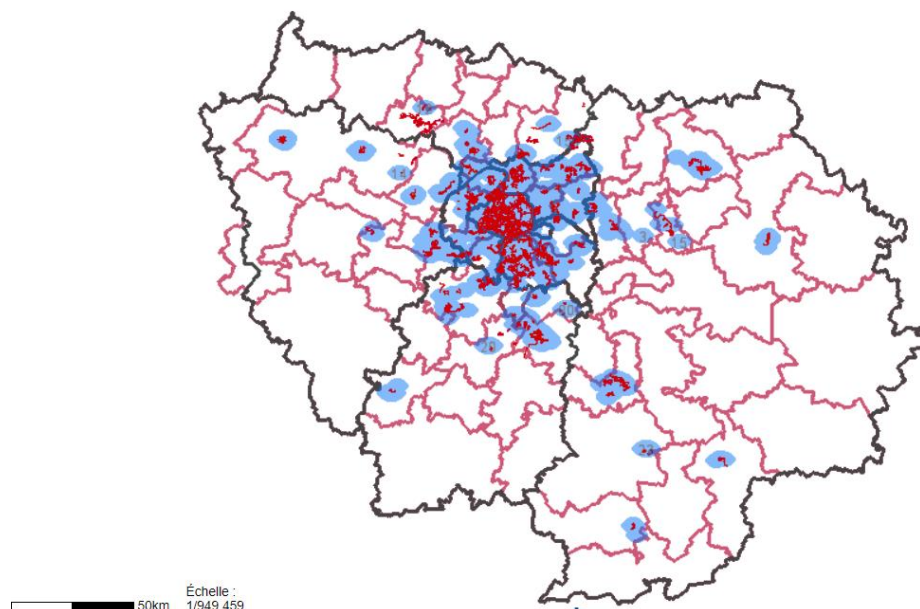


Figure 6-3. Outline of district heating and cooling networks in the Ile-de-France region (dark red) and delivery point (blue). Source: DRIEAT Île-de-France.

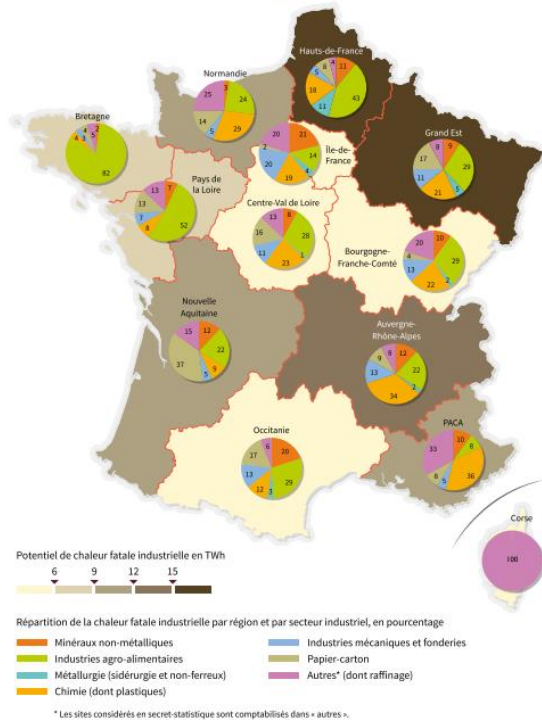
⁶ http://carto.geo-ide.application.developpement-durable.gouv.fr/906/Carte_chaleur_nationale.map#

⁷ <http://carto.geo-ide.application.developpement-durable.gouv.fr/73/energie.map#>

6.2.2 7.2.2 Waste heat

In 2017, the French Environment and Energy Management Agency (ADEME) carried out an analysis of the waste heat (ADEME, 2017). They concluded that 36% of the fuel used in industry (109.5 TWh/y) finishes as waste heat, including 52.9 TWh/y at $T > 100\text{ °C}$ (cf. Figure 6-4). Note that the waste heat from the incineration plants (4.4 TWh/y) is one order of magnitude below the amount of excess heat from the industrial sector. The available data is aggregated at regional level.

Répartition de la chaleur fatale industrielle par région et par secteur industriel



Répartition de la chaleur fatale industrielle ($> 100\text{ °C}$) par région et par secteur industriel

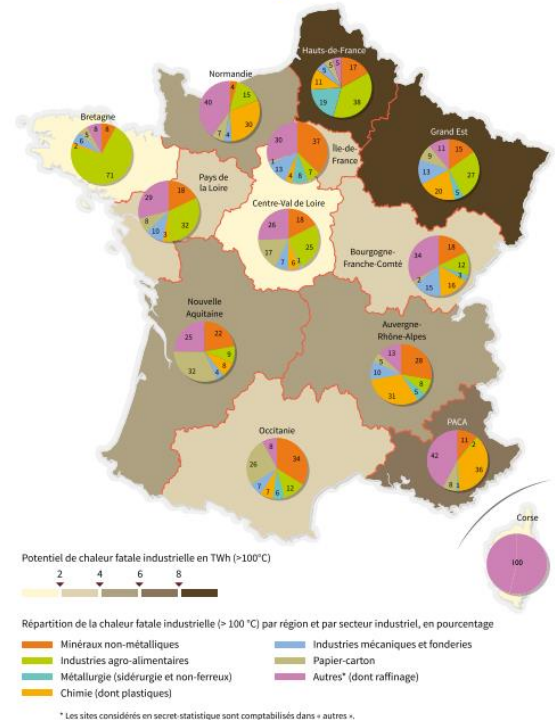


Figure 6-4. Spatial distribution of waste heat (left); focus for waste heat at $T > 100\text{ °C}$, per region and industrial sector (ADEME, 2017).

Since the details of the 2017 study could not be retrieved for the Heatstore project, the BRGM used the land occupation database (Corine Land Cover) to identify the location of industrial sites over the region Ile-de-France for the assessment study. Despite having no quantitative information on the amount of waste heat produced at local scale or the temperature of the waste heat produced, the land occupation database provides the contour of industrial areas and gives valuable insight of where the waste heat is produced in the Ile-de-France territory.

When industrial site are located within a range of 500 m from an existing district heating and cooling network (considering the outlines identified in section 6.2.1), part of the waste heat produced by industries could be directly injected in existing DHC networks. Indeed, we have seen according to the FEDENE survey that in average, the share of renewable energy and recovered waste heat within DHCN in this region Ile-de-France is 53% which means that room for improvement exists to meet the objectives fixed by the French government. The injection of waste heat could thus represent a good lever to reduce local carbon emissions. Fossil fuels including natural gas, heating oil and coal represent almost 40% of the energy mix within DHCN in 2019 in France (FEDENE, 2020).

Figure 6-5 presents an illustration of the above-mentioned elements, in a centred view over the Paris area (centre of the Ile-de-France region). In this figure, the outlines of DHCN and of the industrial and commercial areas as identified in the land occupation database are represented. Overall, the surface of industrial land within 500 m from existing DHCN represents 51% of the total industrial surface identified in the Ile-de-France region.

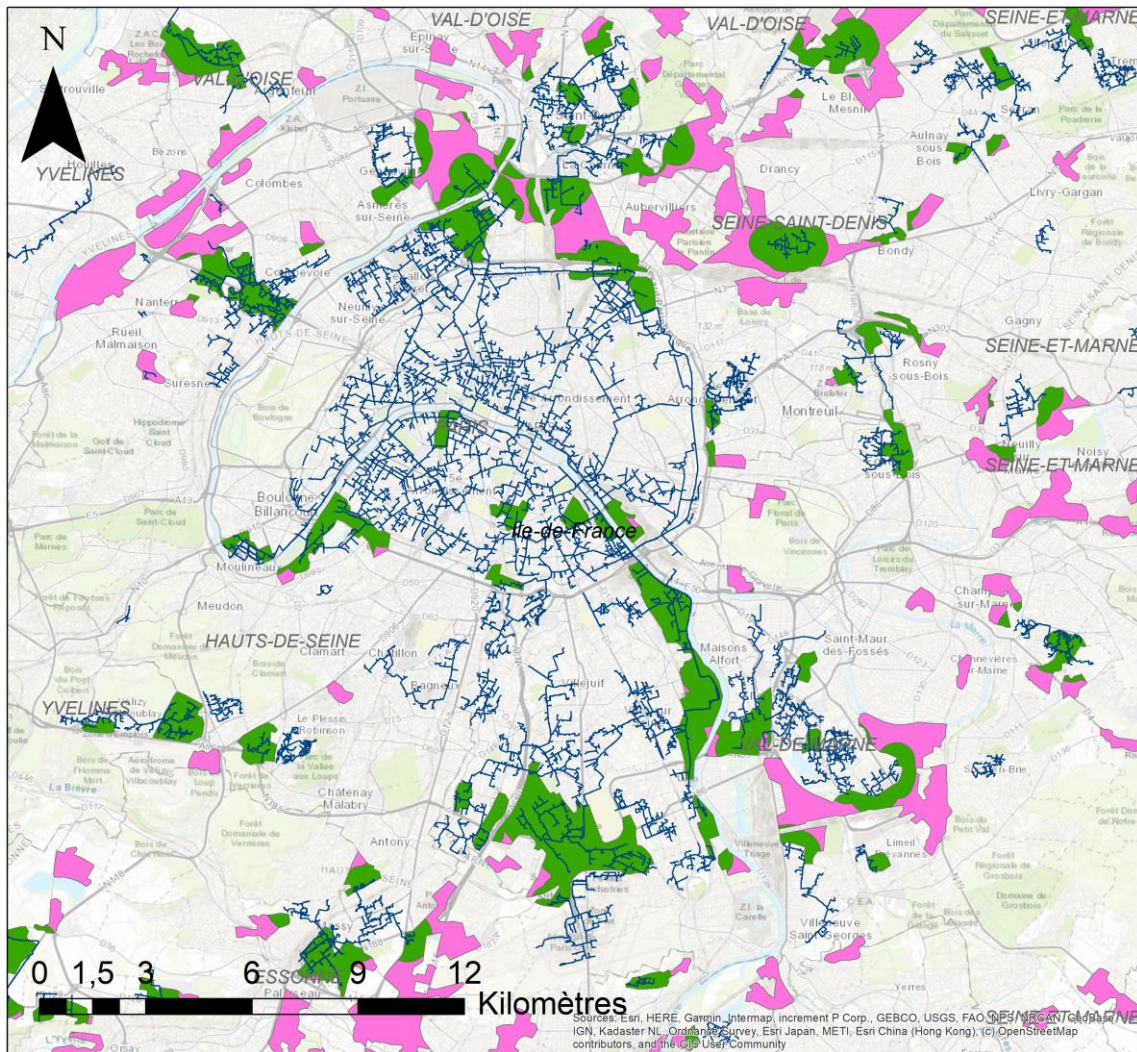


Figure 6-5. Location of Industrial and commercial areas (all in pink and within 500 m from existing DHCN in green) in the Paris area and its surroundings and outlines of existing DHC network in the Paris area.

The location of the 19 waste incineration units over the Ile-de-France region has been collected for the study and is presented in Figure 6-6. The data are provided by the SINOE website that lists information concerning waste treatment plants in France (name, location, date of opening, amount of energy (heat or power) produced, weight of incinerated waste)⁸. The amount of heat that could be valorised in DHN and the temperature of the heat source is however not specified.

⁸ data available at http://carto.geo-ide.application.developpement-durable.gouv.fr/906/Carte_chaleur_nationale.map#

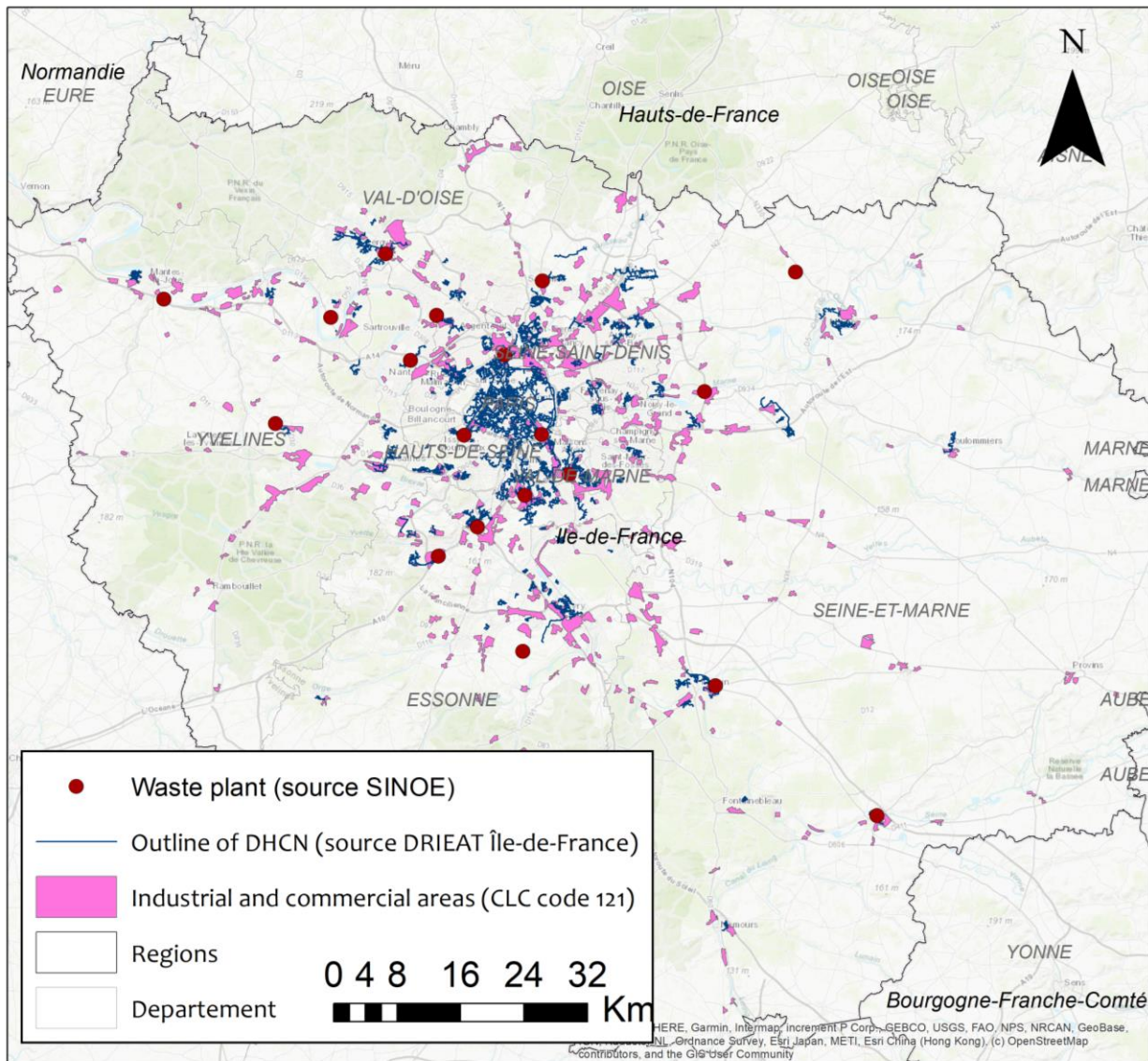


Figure 6-6. Location of waste treatment plants (red), industrial areas (pink) and DHCN (blue) in the Ile-de-France region (source: SINOE, Corine Land Cover, DRIEAT)

Most of the 19 waste incineration plants (9) are Combined Heat and Power Plants (CHP), while 5 are declared to produce only electricity, 2 only thermal energy. One plant has no valorisation declared, one plant has an empty field and one plant was excluded since the data turned out to be unreliable.

The SINOE data related to the waste incineration plants have been crossed to the confidential data related to the DHN (EARCF survey mentioned above). 19 DHN could be identified as connected to a waste plant, about half being explicitly mentioned in the SINOE data, while the remaining DHN had to be manually connected to a neighbouring plant. Indeed, the result of the crossing as a whole seems plausible, since the “purchase” of waste heat is 3896 GWh/y (from EARCF) and the “sale” 3684 GWh/y (from SINOE), a difference of about 6%. Note that the individual EARCF data cannot be disclosed for confidentiality results, only aggregated results can. One may estimate if some of the incineration energy produced by the plants identified is not used, neither for electricity nor for thermal energy production. In a first rough approach, we may consider that the incineration of one ton of waste produces 1.41 MWh⁹, that the efficiency of electricity production is $1/2.58 = 39\%$, and the

9

<https://www.google.com/url?sa=t&rct=j&q=&esrc=s&source=web&cd=&ved=2ahUKEwie38OXzdDyAhUHjhQKHVdZDiYQFnoECAIQAAQ&url=https%3A%2F%2Famorce.asso.fr%2Fpublications%2Fequilibre-economique-des-unites-de-valorisation-energetique-dt112%2Fdownload&usq=AOvVaw1OImA8aSvk8LpEPti842>

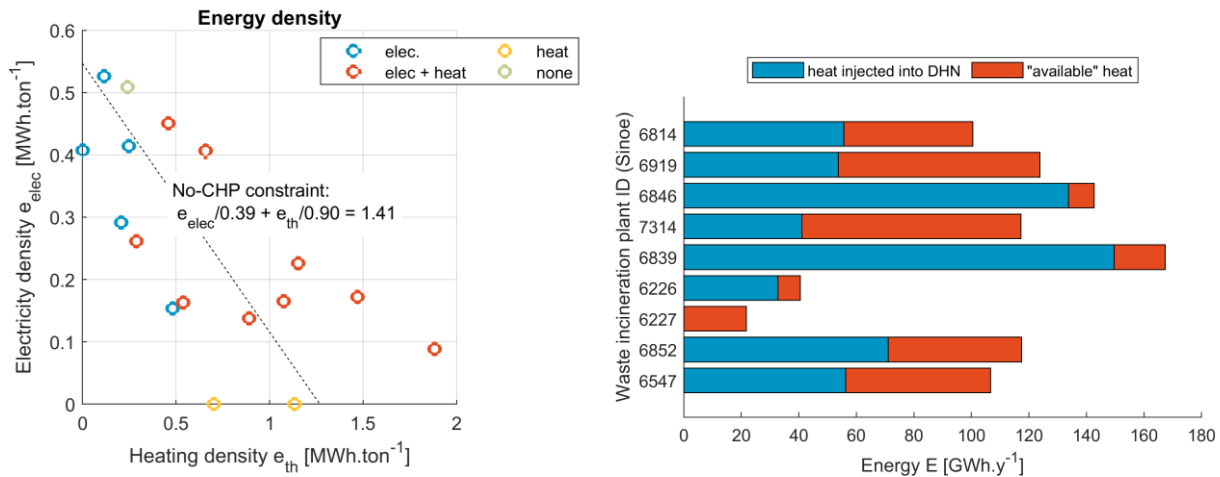
efficiency of thermal production is 90% due to miscellaneous losses between the boiler and the heat exchanger delivering energy to the network. This yields the following constraint as long as incineration energy is used either for electricity or heating production (but not for both as for a CHP):

$$(1) \quad \frac{e_{elec}}{0.39} + \frac{e_{th}}{0.90} = 1.41$$

where e_{elec} and e_{th} are respectively the ratio between the electricity (or heat) produced to the waste weight [MWh.ton⁻¹]. As presented over the left end side of Figure 6-7, 9 plants (not considering CHP) are far away on the left from this line, which suggests that the incineration energy is not fully valorised. One possibility to further valorise it would be to store the excess heat into the ground, under the condition that the neighbouring DHN need it. This available amount of energy can be estimated as:

$$(2) \quad E_{th} = W \left(\left(1.41 - \frac{e_{elec}}{0.39} \right) \times 0.90 - e_{th} \right)$$

With W the weight of incinerated waste [ton]. For this 9 plants, it accounts for 344 GWh.y⁻¹, to be compared with the 594 GWh.y⁻¹ of valorised heat injected into the DHN (Figure 6-7, right). Note that for CHP, the constraint can be exceeded since some of the heat is co-generated with electricity.



Besides, according to the excess heat study conducted by (ADEME, 2017), the waste heat produced in the Ile-de-France region is mainly below 100°C (2 180 GWh in 2017 i.e. 49% of total waste heat produced in the region) and between 100°C and 200°C (1 150 GWh i.e. 26% of total waste heat produced in the region). 21% of the excess heat originates from non-metallic minerals industries (e.g. stone, cement, concrete), 20% from foundry and mechanical industry, 19% from chemical and plastic industry, 14% from food industry, 4% from metallurgy (steel and non-ferrous), 2% from paper industry and 20% from other industries (among which part is covered by statistical-secrecy and includes as well refineries). However, this data could not be integrated in the study since it covers a much larger area than the Dogger area.

6.2.3 7.2.3 Underground data

6.2.3.1 Geological context of the Paris Basin

As pointed by (Bridger and Allen, 2005), the lithology, the depth, the areal extension, the thickness and permeability of a geological formation at local and regional scale are key elements considered to understand and characterize aquifers. Depending on the knowledge of the aquifer which is based notably on field observation, wells information, geophysical imaging, formation testing and modelling, one can estimate the suitability of an aquifer for underground thermal energy storage.

Geological and hydrogeological models of deep aquifer established by the BRGM over the French territory produced over the past years have been collected in order to assess different parameters of underground formations such as depth, thickness or temperature in different sedimentary basins and graben over France.

This overview was initially conducted to assess the geothermal potential in France for direct use of the resource and for co-generation purposes over the whole territory (Figure 6-8).

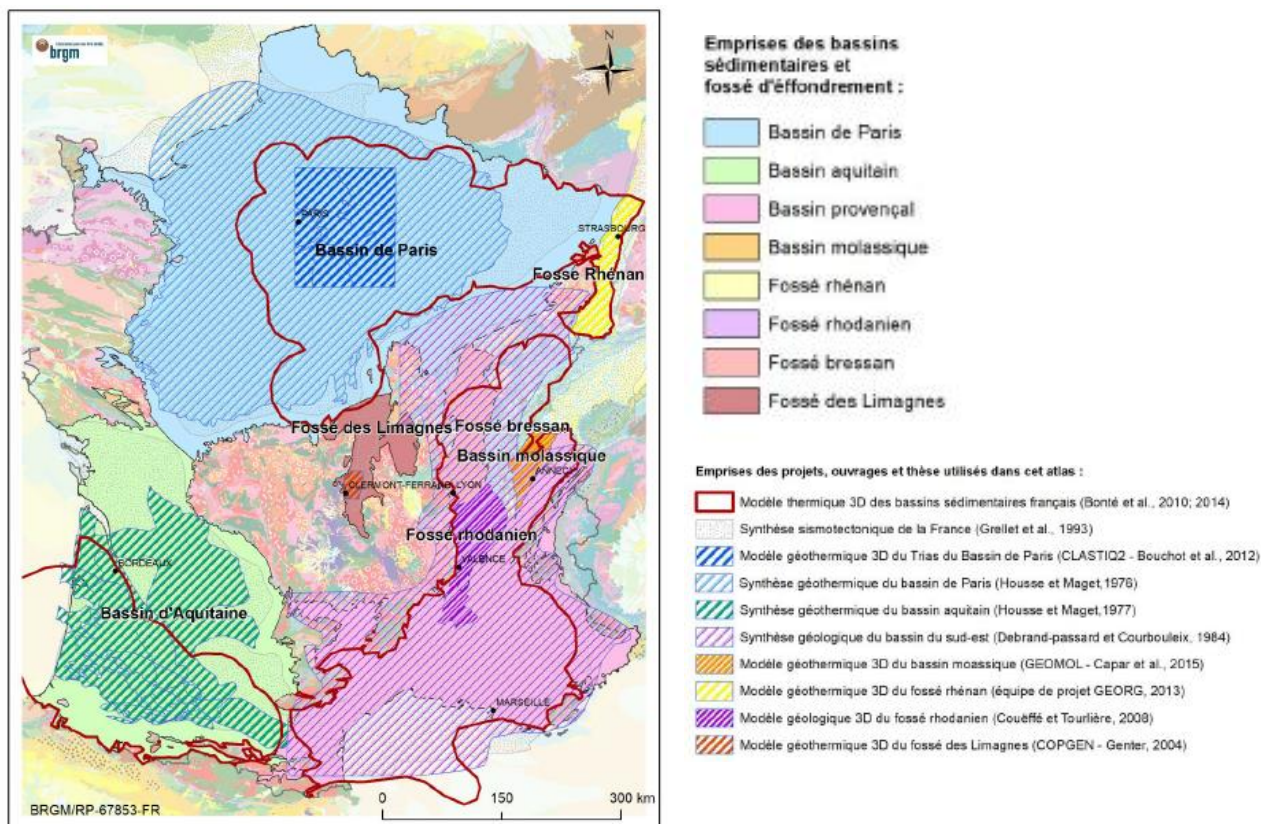


Figure 6-8. Extent of deep sedimentary basins and graben and location of geological and hydrogeological models and synthesis available in France by (Caritg et al., 2018)

The ATES potential will be estimated over the Île-de-France region which is located in the Paris sedimentary basin (cf. Figure 6-8). This basin is a large, nearly circular, intracratonic sedimentary basin which occupies a vast part of Northern France (110 000 km²) and extends northward below the English Channel. It is the largest onshore sedimentary basin in France, overlying deformed Carboniferous and Permian troughs in between four crystalline basement bodies (Massif Armoricain, Massif Central, Vosges, and Ardennes). It is connected with two other basins through two structural highs (the Aquitaine basin to the southwest with the “Poitou High”, and the South-East basin with the “Burgundy High”). Its origin is linked to a period of rifting in Permo-Triassic times. The central part of the basin, where the subsidence was the greatest, is filled with about 3 000m of sediments. From Triassic to late-Jurassic times, the Paris Basin was a broad subsiding area in an extensional framework, larger in extent than at present. Due to Tethys rifting and the opening of the Atlantic Ocean, the subsidence pattern dramatically changed during the Aalain (Lower Dogger) (Gaumet, 1997; Guillocheau et al., 2000). This tectonic history, along with carbonate production, controlled the deposition of sediments during Jurassic times by alternatively creating and removing space for the accumulation of carbonates and silico-clastic sediments. Further steps in the opening of the Ligurian Tethys and its evolution into an oceanic domain (Late Dogger) are also recorded in the tectono-sedimentary history (Guillocheau et al., 2000). However, the Paris Basin area has been essentially stable since the late-Jurassic. Four main lithostratigraphic units exhibiting aquifer properties are identified in the Paris Basin and are currently target by geothermal exploitation or by exploration projects: the lower Cretaceous sand formations (**Albian and Neocomian**) and the mid-Jurassic (**Dogger**) carbonate rocks and the Triassic sandstones formation. The Dogger, the Albian and the Neocomian aquifers are currently identified as the most promising targets below the urbanized Paris area for geothermal and also for storage purposes. The Triassic sandstones formation has had limited development in the Ile-de-France region for deep geothermal energy recovery but has proven to have important geothermal potential in the area. The knowledge of this reservoir remains limited at regional scale.

6.2.3.2 Reservoir unit description

The Albian strata are resulting from the erosion of the continent and are composed siliciclastic deposits. They are mainly made up of terrigenous detrital sands and clays. The total thickness of the apto-albian deposits varies from 0 m at the outcrop limits, to nearly 200 m below the Brie region. In the Albian, three major tectonic accidents influenced sedimentation: the Bray-Vittel fault, the Seine-Sennely fault and the Villers fault (Figure 6-9).

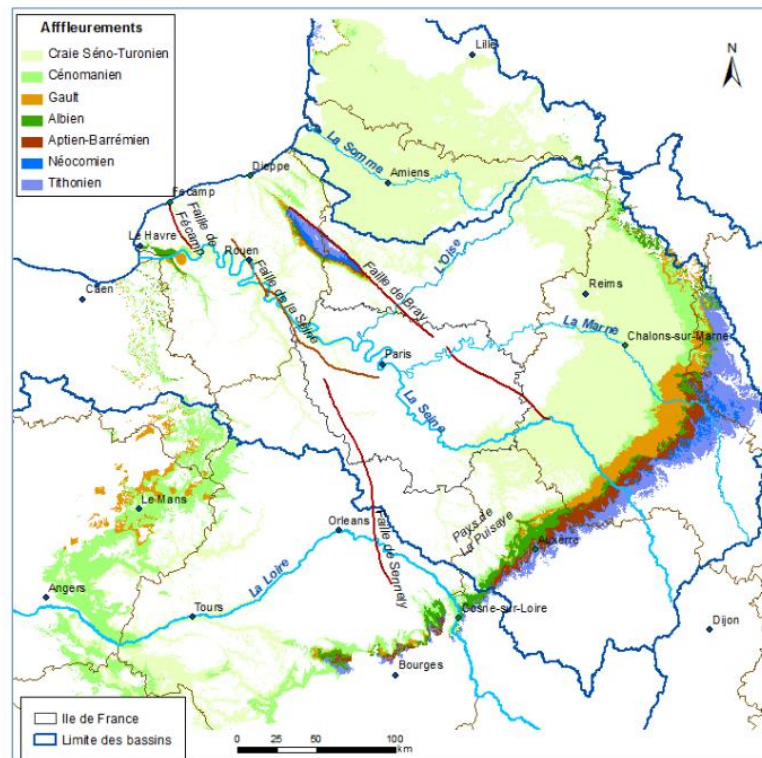


Figure 6-9. Location of Albian and Neocomian outcrop and main tectonic faults over the Paris Basin influencing the sedimentation over the formations (Seguin, 2015).

The deposits register the progressive flooding of the basin, and can be subdivided into 7 large units: the Brienne marls and the Gault clays (forming the upper-Albian unit), the Frecambault sands, the Tegulin clays and the Drillons sands (forming the mid-Albian unit) and the Armance clays, the Green sands (forming the low-Albian unit). There are lateral variations in facies, and significant variations in thickness resulting from the progression of subsidence as a function of tectonic events. The succession of different units is therefore not found throughout the basin, and the nature of the deposits is highly variable. Recent interpretations (Amédéo F. & Matrimon B., 2014, Guillocheau & al., 2000, Sévenier M. & Lasseur E., 2016) show that the most extensive sandy layer corresponds to Frecambault sands which present a remarkable continuity over the entire mid-Albian unit. The sands of Drillons (mid-Albian unit) correspond to deltaic deposit located in the southwest of the basin. The Green sands (low-Albian unit) include a fairly large clay fraction throughout the basin. At the end of the mid-Albian unit, and before the oceanization of the basin which corresponded to the deposit of the Gault clays in the upper-Albian unit, the proximal part of the basin was located in the south-east of the basin, between the threshold of Burgundy and Orléans. It is in this sector that the last sandy bodies of the Albian have been deposited.

Neocomian deposits can be subdivided according to (Mégnyen and Mégnyen, 1980) in different facies depending on the sectors. Thus, in the Paris Basin, the lower Cretaceous begins with continental facies known as the Wealdian facies, made up of alternating sands, sandstones and sandy clays with lignite layers, including a multilayer aquifer, of variable thickness between 20 and 90 m. The permeability of the facies is quite good in the sands, but the layers are relatively discontinuous. The formation continues with marine facies on the eastern rim (marl, marly limestone, shell limestone), with fairly low permeabilities and up to a hundred meters thickness. The carbonate series is located in the southeast part of the Paris Basin. In the center of the Paris Basin, the Neocomian is about 120 m thick. It composed of alternating fine sand and clay layers. Neocomian sand levels are generally more regular than those of the Albian. In the center of the basin, the sands of Châteaurenard and the sands of Château-Landon are contiguous, sometimes also with the sandstones of

Puiselet, and the sands of the Hauterivien. Below these sand formations, the Wealdian is composed of white sands, marls and ferruginous sandstones of the Valanginian and Griselles sands, which correspond to detrital deposits. These sands are homogeneous with a low percentage of clay.

The Dogger strata were deposited in a marine environment. The most productive layers are found in deposits of Bathonian age where two synchronous carbonate platforms grew and expanded in the Basin: the thin western Armorican platform and the thick central Burgundian platform. These platforms are separated by a narrow marly trough called the "Marly Belt". Bathonian deposits have been divided into three distinctive facies units that are diachronous, but can be differentiated on sedimentological diagenetic, and petrophysical grounds (Menjoz, 1990). These units are made of limestone commonly found on a depositional profile comprising an outer shelf, a barrier, and an inner shelf. These units are, in stratigraphic order, (1) the Cyclical unit, made up of open marine limestone and open marine marl progressively enriched in reef species and echinoderm bioclasts, (2) the Oolithe Blanche unit, mainly composed of oolitic limestone, high energy calcarenites that were deposited in an upper ramp environment which surrounded a lagoon and (3) the Comblanchian unit, composed of lagoon deposits made of wackestone and mudstone, that were deposited in the protected inner shelf of the central platform. Muddy limestone layers are interbedded with coarser layers. Chronologically, this unit corresponds to the full regressive trend of the Upper Bathonian, as well as the subsequent submersion by the Lower Callovian flooding (Lopez et al., 2010).

6.2.3.3 Available geological and hydrogeological information

The data related to the sandy formations of **the Albian and the Neocomian** come from geological and hydrogeological models (Seguin et al., 2015). This geological model was built from a model produced initially in 1997 and revised in 2015. It integrates additional geological logs, data from the BDLISA database (hydrogeological repository) and of the 2010 Paris Basin Tertiary geological model. In total, 1950 drill holes were used for the construction of the model in 2015, of which 1094 were already used for the 1997 model. This model represents the total extent of the Albian and the Neocomian formation, from the outcrops to the centre of the basin below the city of Paris. The information was integrated into the GDM® software and interpolated by kriging on a 2 km by 2 km grid to generate top and bottom depth maps of the Albian and Neocomian aquifers. The hydrogeological model was generated to simulate different scenarios of water withdrawal from the captive Albian aquifer and to simulate the operation of geothermal doublets in the Albian. The hydrogeological model was calibrated in transient regime (from the year 1841 to 2012) and integrates withdrawal over this same period (water supply mainly), piezometric chronicles over 24 wells (extracted from the national groundwater database ADES), two boreholes exploited for water supply in the Neocomian and four boreholes in the Albian with dynamic measurements. From this work, permeability distributions were obtained for the two aquifers after calibration of the dynamic data. The values vary for the two aquifers between of 10^{-5} m/s to 10^{-4} m/s at the centre of the basin, in the Ile-de-France region. The temperature field within the Albian aquifer was obtained in a steady state on a regional scale from temperature data available in the ADES database and gave an average gradient of 2.7 °C / 100 m for the Albian formation which was then considered uniform over the whole formation. The temperature model was calibrated at steady state in the Albian as a first step, before being used in transient regime to perform hydrothermal simulations of doublets. For the Albian and Neocomian aquifers, the following data were collected: (1) height of the top and bottom of the formations in m NGF (Seguin, 2015), (2) thickness of the formations in m (calculated by the difference between top and bottom height of the formations), (3) permeability in m/s (resulting from the calibration of the hydrodynamic model (Seguin, 2015)), (4) transmissivity in m^2/s (calculated from the thickness and permeability of the formations) and (5) temperature of formations in °C (calculated in steady state from a uniform gradient of 2.7 °C / km).

The data collected for the **Dogger** limestone formation have been produced by (Hamm et al., 2017) for the study of the geothermal potential of the aquifer. The main properties of the aquifer were obtained by kriging well data from 155 geothermal wells at a mesh size of 250 m by 250 m and in a sector limited to the Ile-de-France region, where the aquifer is targeted for the exploitation and exploration of this deep geothermal resource. The extension of the model thus encompasses the Ile-de-France region and all the geothermal boreholes exploiting the resource in this sector in 2017. For the Dogger aquifer, the following data were collected and used for ATEs potential assessment: (1) height of the top and bottom of the formation in m NGF, (2) producing thickness of the formation in m (calculated by geostatistical kriging of well data), (3) hydraulic transmissivity in m^2/s (calculated from the intrinsic transmissivity, density and viscosity of the fluid), (4) temperature of the reservoir in °C (calculated by geostatistical kriging with external drift method using geothermal gradient in the Paris basin according to (Bonté et al., 2010) and depth of the formation), (5) fluid density (in kg/m^3) and viscosity in Pa.s (calculated using established correlations with temperature, salinity of the fluid and pressure of the reservoir) and (6) exploitation flow rate in m^3/h (estimated from the relationship

between productivity index (IP in m³/ h/ bar) and hydraulic transmissivity (m²/s) for an admissible drawdown of 10 bars).

Table 6-1 here below summarises the data collected so far for those aquifer formations and the associated information available from geological and hydrogeological models notably.

Table 6-1. Summary of geological formation identified as having a good development potential for geothermal energy production in the Paris basin and available data associated.

<i>Sedimentary basin</i>	<i>Geological or hydrogeological formation modelled</i>		<i>Available data</i>	<i>Source of information</i>
<i>National level</i>	Iso depth (1000 m, 2000 m, 3000 m and 4000m)		Temperature	Bonifé et al (2010), Bonifé (2014)
<i>Paris basin</i>	Lower Cretaceous	Albien-Neocomien	Temperature, top and base	Caritz et al (2014)
	Upper Jurassic	Lusitanien	formation depth, thickness,	Seguin et al. (2015)
	Middle Jurassic	Dogger	hydraulic transmissivity	Hamm et al (2017)
	Lower Jurassic	Lias		
	Upper and Lower Triassic	Rhétien, Keuper - Chaunoy and Buntsandstein - Donnemarie	Isophypse maps and isotherms	Caritz et al. (2018), Bouchot et al (2012), Housse et Maget (1976)
	Basement			

In 2020, about 50 doublets or triplets are in operation in the Dogger limestone and 6 are operating in the Albien and Neocomian sand aquifer.

The details of the methodology implemented for the estimation of ATEs potential in the Ile-de-France region is presented in section 6.3.

6.3 Elements of methodology

The analysis will estimate how the share of waste heat from incineration plants can be increased with UTES, especially for ATEs due to their large storage capacity in the Ile-de-France region.

The methodology implemented to identify the recovery efficiency of high temperature thermal energy storage in the Paris Basin is based on the work of (Schout et al., 2014). Given the effects of density driven flow, the analysis investigated the parameters controlling the recovery efficient of energy storage systems through numerical simulations and sensitivity analysis. (Schout et al., 2014) found a correlation between a modified dimensionless Rayleigh number and the recovery factor of aquifer thermal energy storage. The analytical solutions found have been applied to the Paris Basin formations to estimate the recovery efficiency of thermal energy storage in aquifers presenting high geothermal energy potential. The aquifer tested are the Albien and Neocomian sand aquifers, the Dogger limestone aquifer.

The dimensionless Rayleigh number is given by the following equation:

$$(3) \quad Ra = \frac{\alpha \cdot \rho \cdot g \cdot H \cdot C_a \cdot k_a^v \cdot \Delta T}{\mu \cdot \lambda_a}$$

where α is the coefficient of thermal expansion of water (in 1/K), ρ the density (in kg/m³), C_a the volumetric heat capacities of the aquifer (in J/m³/K), H the height of the reservoir (in m), k_a^v the vertical aquifer permeability (in m²), ΔT the temperature difference between the injected and ambient groundwater (in K), μ is the dynamic viscosity of water (in kg/m/s) and λ_a is the horizontal aquifer thermal conductivity (in W/m²/K). This dimensionless number indicates the strength of free convection (i.e. buoyancy flow) over heat conduction.

To improve this relation, (Schout et al., 2014) included missing parameters in an adjusted version of the Rayleigh number after having analysed the most influential parameters in sensitivity analysis. The missing parameters identified were thus the horizontal aquifer permeability (k_a^h) and the injection volume (V_i). The importance of the horizontal aquifer permeability is apparent from the formula for the characteristic tilting time, which indicates the importance of heat losses as a consequence of density-driven flows. Indeed, the recovery efficiency is driven by numerous phenomenon: thermal conduction, dispersion, regional groundwater and density-driven flow. Density driven flow is caused by the difference that exists between the injected fluids and the in-situ fluids. Since the hot fluid injected is less dense than reservoir fluids, the stored fluid has a tendency to flow in the upward direction in the aquifer. The thermal front then tends to tilt. (Hellström and Tsang, 1988) proposed a formulation to estimate the tilting time as a function of reservoir height, vertical and horizontal permeability of the aquifer, volumetric heat capacity, density and viscosity of the aquifer and the water. Considering this, (Schout et al., 2014) replaced k_a^v in equation (3) by $\sqrt{k_a^v \cdot k_a^h}$. Since the injection volume for a given aquifer height is inversely proportional to the aspect ratio, i.e. proportional to R_{th}/H , equation (3) was divided by R_{th}/H and gave the following equation:

$$(4) \quad Ra^* = \frac{\alpha \cdot g \cdot C_a}{\lambda_a} \cdot \frac{\rho \cdot H^2 \cdot \sqrt{k_a^v \cdot k_a^h} \cdot \Delta T}{\mu \cdot R_{th}}$$

where k_a^h the horizontal aquifer permeability (in m^2). R_{th} was then replaced by the following equation $\sqrt{(V_i \cdot C_w / \pi H C_a)}$ (horizontal extend of cylindrical volume of fluid) and equation (4) becomes:

$$(5) \quad Ra^* = \frac{\alpha \cdot g \cdot C_a^{1.5} \sqrt{\pi}}{\lambda_a \sqrt{C_w}} \cdot \frac{\rho \cdot H^{2.5} \cdot \sqrt{k_a^v \cdot k_a^h} \cdot \Delta T}{\mu \cdot \sqrt{V_i}}$$

where V_i is the injected volume with a constant flow rate.

The correlation between this modified Rayleigh number Ra^* and the recovery efficiency is identified in the following equations:

$$(6) \text{ When } H \text{ (in m)} \in]10; 60 [\quad \varepsilon = \left(0.82 - \frac{1.7}{H^{1.2}} \right) \cdot e^{\left(\frac{-1.2}{H^{1.35}} + 2.2 \cdot 10^{-3} \right) \cdot Ra^*}$$

$$(7) \text{ When } H \text{ (in m)} \in]60; 200 [\quad \varepsilon = \left(0.82 - \frac{1.7}{H^{1.2}} \right) \cdot e^{\left(\frac{-2.7}{H^{1.7}} \right) \cdot Ra^*}$$

Following this analysis and once the recovery efficiency has been estimated for each aquifer, a GIS analysis is conducted to select zones with the most convenient distances between waste heat resources (i.e. industrial zones identified in the occupation database and the location of waste treatment plants) and existing DHN.

6.4 Recovery efficiency in the mid-Jurassic Dogger limestone aquifer

The maps used for the estimation of ATEs recovery efficiency in the Dogger limestone aquifer are the result of geological modelling at the mesh of 250 m by 250 m and geostatistical interpolations of well data over a similar mesh. Figure 6-10 presents the map of top formation depth (in mNGF) and the extension of the model used for the assessment over the Dogger limestone aquifer.

The interpolations are based on the calculation of variograms and a number of external constraints such as the depth of top formation of the Dogger limestone, the geothermal gradient, the position of a marly through on the western side of the basin (Hamm and Arnaud, 2017). The interpolated maps of fluid density (in kg/m^3) and viscosity (in Pa.s), transmissivity (in m^2/s), productive thickness (in m) and exploitation flow rates (in m^3/h) have been used to estimate the modified Rayleigh number in the Dogger aquifer and the recovery efficiency of ATEs in this aquifer.

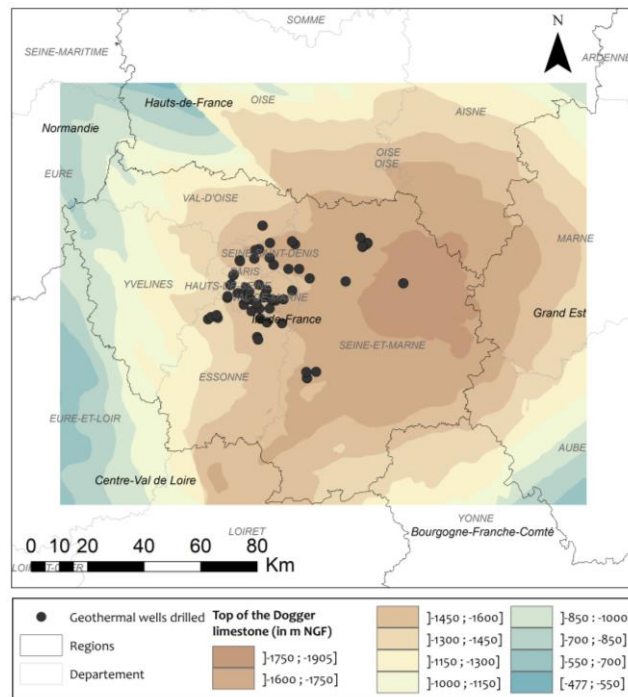


Figure 6-10. Depth map of the top formation of the Dogger limestone in the Paris Basin (in m NGF) and location of geothermal wells used as input data for the geostatistical interpolations of aquifer and fluid properties.

Few hypothesis have been considered for the analysis of recovery efficiency while applying (Schout, 2014) methodology. The duration of production/injection cycle is considered to last 6 months and the constant used in the equation (5) is taken as estimated in the paper. Indeed, the volumetric heat capacity of the aquifer and of the water, the thermal conductivity of the aquifer presented in the article are of the same order of magnitude than the one considered in the Dogger limestone aquifer. The thermal expansion of water being unknown in the Dogger formation, it was decided to use the value presented in the paper. The ratio between horizontal and vertical permeability is unknown and will be subject to sensibility analysis presented below. The variation of temperature between injected and produced fluid during the storage period is considered to be constant and will also be subject to sensibility. The cases of a delta of 30°C and of 60°C will be considered when estimating the recovery efficiency.

Figure 6-11 presents a result of the estimation of the modified Rayleigh number according to the formulation presented in equation (5) (Schout et al., 2014) in the limestone Dogger aquifer. As shown here, the modified Rayleigh number varies from $10^{-0.33}$ to $10^{2.15}$. The higher values identified describe the domination of conduction dominated heat transfer over free convective heat transfer.

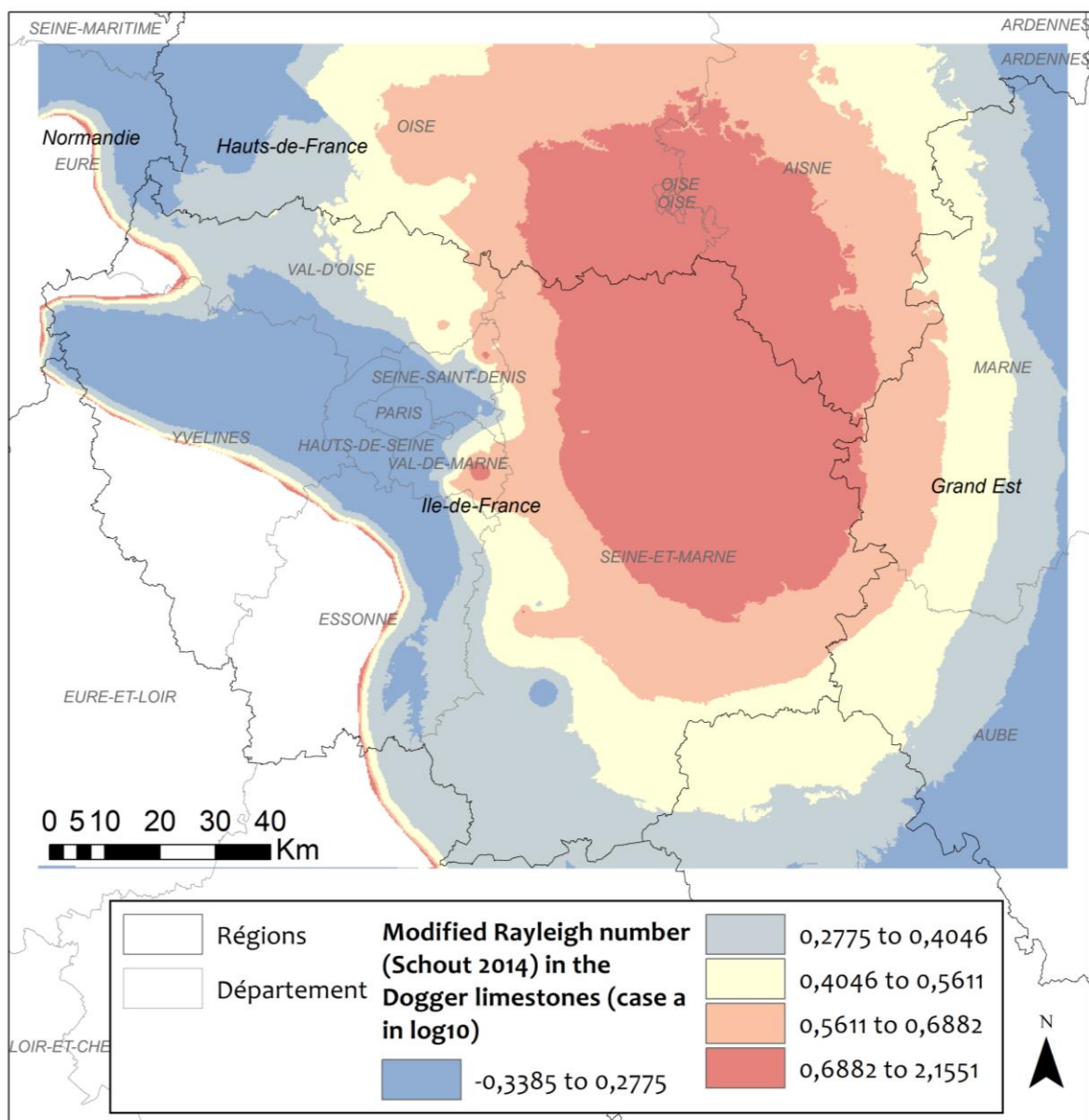


Figure 6-11. Modified Rayleigh number (base 10 logarithm) in the Dogger limestone according to (Schout, 2014) analytical solution: base case A (temperature difference between injected and produced fluid of 30°C, constant using in Ra* estimation from (Schout 2014)).

When temperature difference between injected and produced fluid increases (Figure 6-12), the impact over the modified Rayleigh number and the recovery efficiency estimation of the Dogger limestone aquifer has proven to be slightly reduced. The main differences in the recovery efficiency are located south-west of the Ile-de-France region, along the marly through. With higher temperature injected in the reservoir, the free convection term tends to be strengthened and the recovery efficiency is thus reduced.

Sensitivity calculation have been performed for different ratio between horizontal and vertical permeability. When vertical permeability is reduced in comparison to the horizontal permeability (i.e. for higher k_h/k_v ratios or anisotropic medium), the buoyancy force will reduce and the thermal front will be less tilted than in isotropic medium. Heat losses are then reduced and subsequently the storage efficiency is improved (Gutierrez-Neri et al., 2011). Figure 6-13 shows the results of the sensitivity conducted for the Dogger limestone aquifer. The maps show in fact that higher recovery efficiencies are favoured when introducing anisotropy in the aquifer. Thinner aquifers also tend to limit the buoyancy flow and will increase the storage efficiency. The Dogger limestone is composed of multiple productive layers intercalated by low permeability layers, with total productive thickness around 10 to 20 meters in average (Lopez et al., 2010). The layers contributing to the flow are only a few meters thick as observed in production logging measurements across the geothermal wells drilled in the Ile-de-France area.

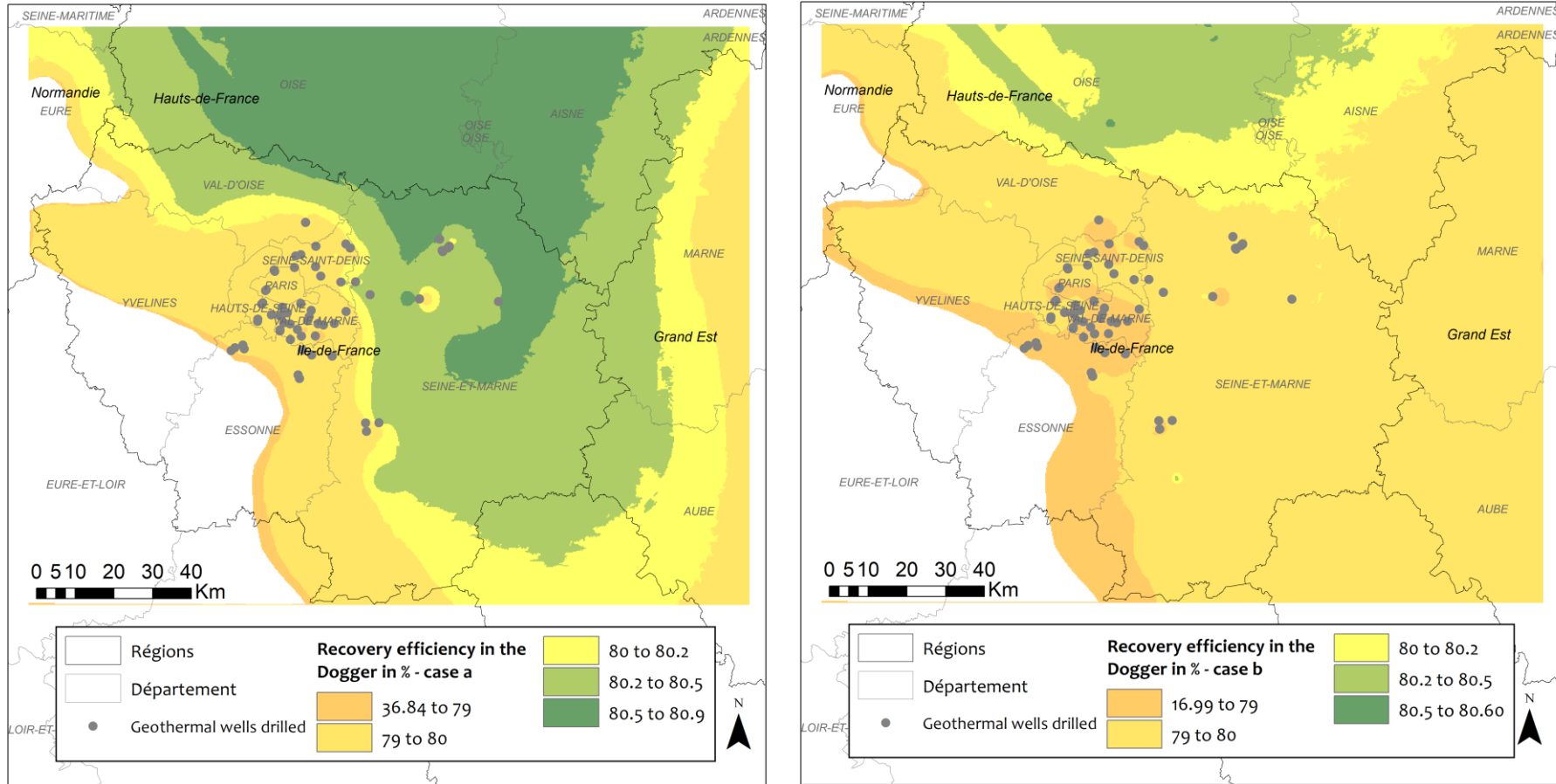


Figure 6-12. Recovery efficiency according to (Schout, 2014) analytical solution applied to the Dogger limestone aquifer for case A (left, with temperature difference between injected and produced fluid of 30°C) and case B (right, with temperature difference between injected and produced fluid of 60°C).

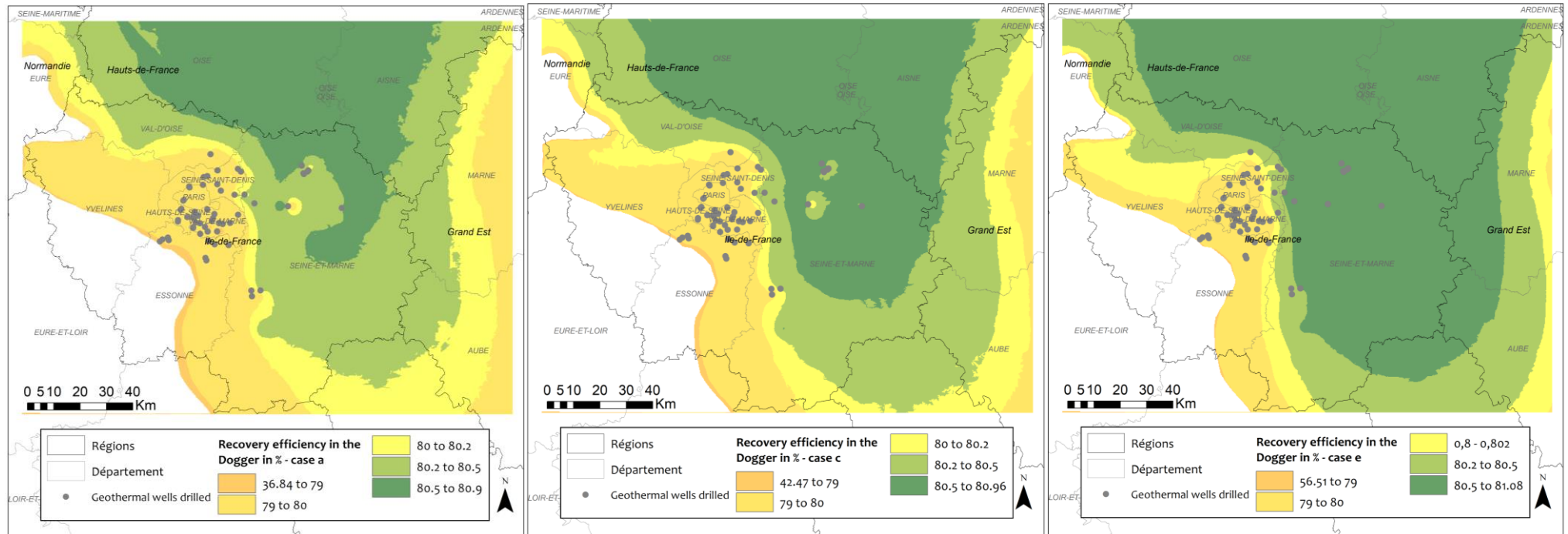


Figure 6-13. Recovery efficiency according to (Schout, 2014) analytical solution applied to the Dogger limestone aquifer with temperature difference between injected and produced fluid of 30°C and k_r/k_v ratio of 2 for case A (left), of 3 for case C (centre) and of 10 for case E (right).

Overall, the storage recovery efficiency factors calculated for the different cases in the Dogger limestone aquifer are in majority over 79%. The calculation presents some uncertainties related firstly to each parameters 2D map used (linked to geostatistical spatial interpolations notably) and also to the hypothesis considered for the calculation of the recovery efficiency. However, this methods allows to define a first estimation of recovery efficiency for ATEs systems in the area and provides positive indication on the, *a priori*, important storage potential of the Dogger limestone aquifer in Ile-de-France.

When looking at the location of industrial site, of waste plants and of existing district heating networks (Figures 6-14 and 6-15), it seems that ATEs potential is high below a majority of sites in the Paris, Hauts-de-Seine, Val-de-Marne, Seine-Saint-Denis, Seine-et-Marnes, Val-d'Oise departments. In the Yvelines and Essonne department, south-west of the Ile-de-France region, the potential is limited by the presence of a "marly belt" which separates the synchronous carbonate platforms of the western Armorican platform and the thick central Burgundian platform during Bathonien deposits. West of this area, the thickness of the aquifer and its permeability is limited and the geothermal and aquifer storage potential becomes limited.

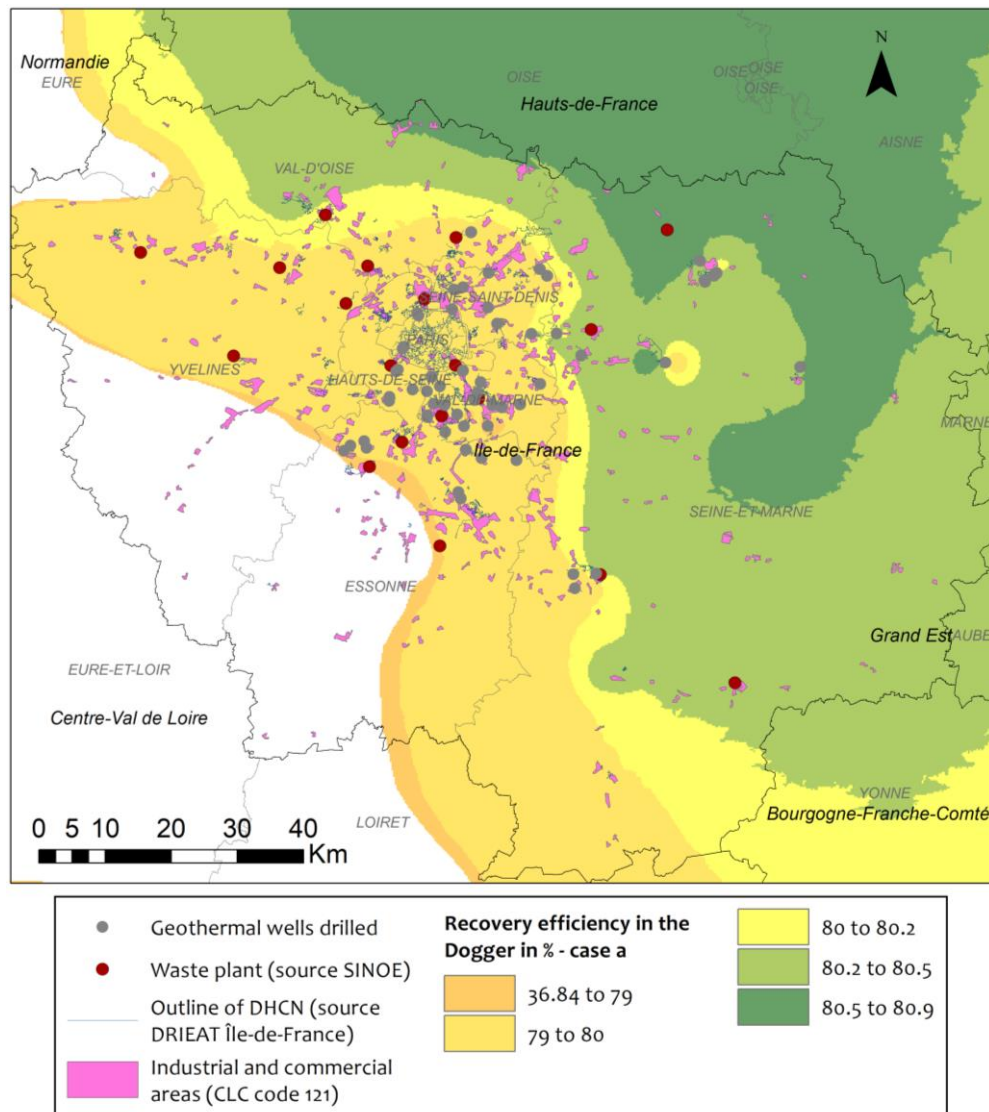


Figure 6-14. Recovery efficiency calculated in the Dogger limestone aquifer (case a) and location of heat source in the Ile-de-France region

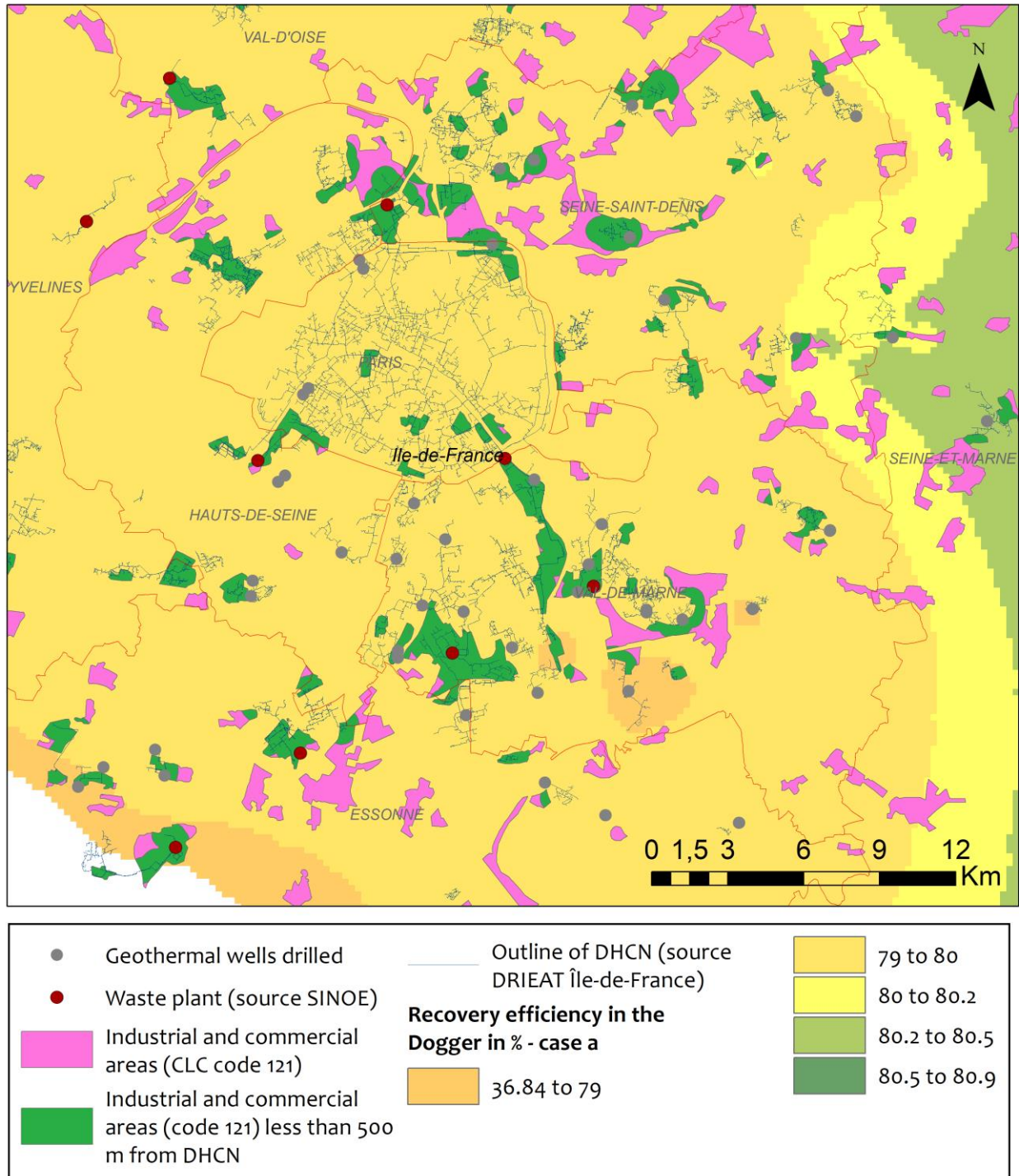


Figure 6-15. Recovery efficiency calculated in the Dogger limestone aquifer (case a) and location of heat source centered over the city of Paris at the heart of the Ile-de-France region.

6.5 Recovery efficiency in the Albian and in the Neocomien sand aquifers

For the Albian and the Neocomian aquifer formations, the available information for the underground is limited to the total height of the formation, transmissivity and permeability, temperature and top depth of the formation. Consequently, to estimate the recovery efficiency of the aquifers, few hypothesis were formulated.

First, the productive thickness is estimated to be a third of the total formation thickness. The reservoir pressure has been estimated from top depth map and by considering a linear evolution with depth (0.96 bars per 10

meters as observed from measurements in the Dogger aquifer, below the considered formations (Hamm and Arnaud, 2017)).

According to literature, the salinity of the fluids contained in the Albian and the Neocomian aquifers in the region of Paris is limited to 0.5 g/L (Hervé, 2007). The fluids can be assimilated to pure water and the density and viscosity can be estimated using tables from handbooks. Using the temperature map, the fluid density has been estimated between 993 kg/m³ to 1000 kg/m³ in the Albian aquifer (temperature ranges from 11°C to 38°C) and between 990 to 1000 kg/m³ in the Neocomian aquifer (temperature ranges from 11°C to 46°C). The fluid viscosity varies from 0.678.10⁻³ to 0.1271.10⁻² Pa.s in the Albian aquifer and down to 0.586.10⁻³ Pa.s in the Neocomian aquifer.

The result of the recovery efficiency estimation for the Albian and for the Neocomian aquifer is presented in Figure 6-16 and Figure 6-17. The calculation considers similar hypothesis than the case a of Dogger limestone estimation (see section 6.4). As for the Dogger aquifer, the recovery efficiency estimated in those two aquifer of the Cretaceous is higher than 79% in a vast majority of the Ile-de-France region.

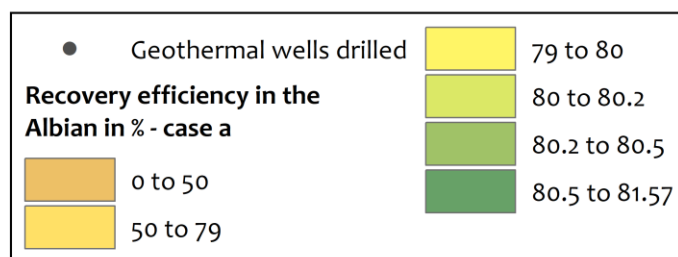
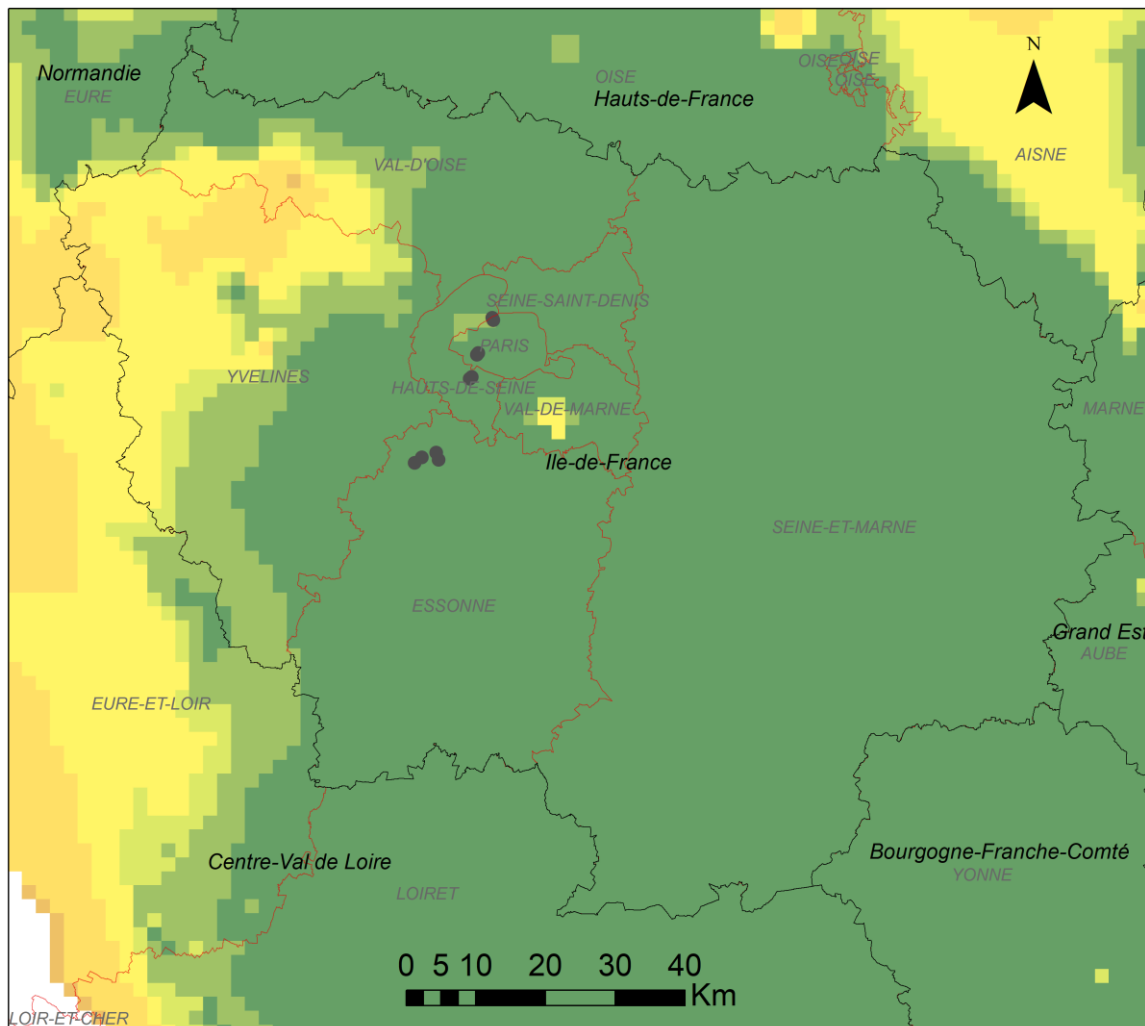


Figure 6-16. Recovery efficiency calculated in the Albian sand aquifer over the region Ile-de-France according to (Schout et al., 2014) and location of geothermal wells operating in this aquifer in 2019.

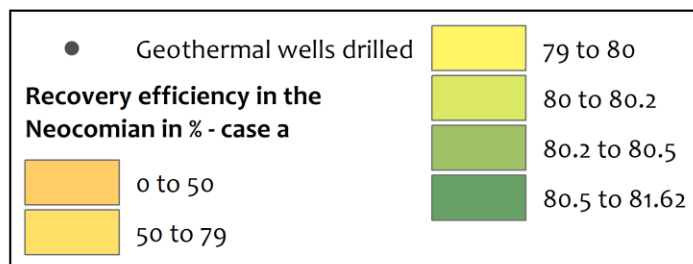
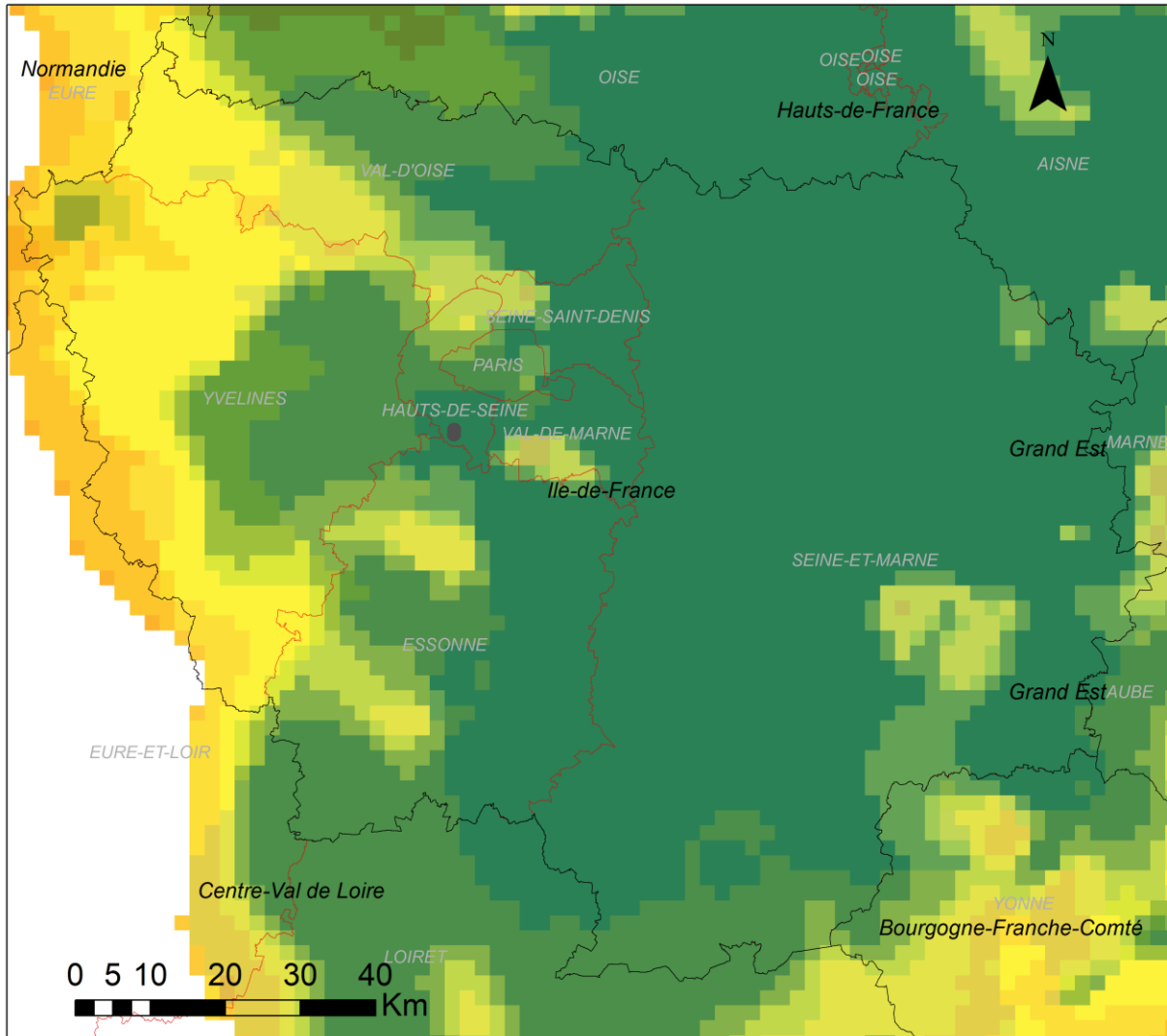


Figure 6-17. Recovery efficiency calculated in the Neocomian sand aquifer over the region Ile-de-France according to (Schout et al., 2014) and location of geothermal wells operating in this aquifer in 2019.

6.6 Conclusions

The Ile-de-France region has 119 district heating networks delivering about 11 300 GWh/y. 19 waste incineration plants feed some of the DHN, delivering about 3 800 GW/y (c.a. 34% of the consumption). A finer analysis could be carried out on 9 of these DHN since they are not equipped with Combined Heat and Power plant (CHP), which allows discriminating the thermal energy sent to DHN from the electricity produced by the waste heat (sent to the plant outside). The “available” waste heat has been estimated around 344 GWh.y⁻¹, to compare with the 594 GWh.y⁻¹ of valorised heat injected into the DHN. The potential is even higher if it includes the waste incineration plants equipped with CHP.

One key result is that all plants are above the Dogger aquifer and that for 17 plants the recovery ratio of a deep Dogger ATEs is expected to be c.a. 80%, 2 plants being at the margin of the aquifer whose characteristics are uncertain. ATEs could therefore play a key role in increasing the share of waste heat onto DHN. The secrecy of the data related to the DHN and the difficulty to link the DHN to the neighbouring waste incineration plants individually does not allow to display this energy potential per DHN.

Also, the waste energy produced by industrial sectors and by location could not be estimated. A qualitative approach from the analysis of land occupation database showed that most of industrial areas in the Ile-de-France region are located above the Dogger, the Neocomian and the Albian aquifers. For a vast majority of the industrial sites, the recovery efficiency of ATEs in the three aquifers was estimated to be above 80%.

6.7 References

- ADEME, 2017. La chaleur fatale.
- Bridger, D.W., Allen, D.M., 2005. Designing aquifer thermal energy storage systems. ASHRAE J. 47.
- Caritg, S., Tourlière, B., Bourguine, B., 2018. Cartographie des cibles géothermales de moyenne température pour la production d'électricité et de chaleur par cogénération en France métropolitaine, Rapport final BRGM/RP-67853-FR.
- FEDENE, 2020. Les réseaux de chaleur et de froid – résultats de l'enquête annuelle 2019 - édition 2020.
- Gaumet, F., 1997. Fondements géologiques pour la modélisation stratigraphique des systèmes carbonatés. Le Jurassique moyen de l'Angleterre à la Méditerranée. Ph.D thesis. Univ. Claude Bernard, Lyon I, Fr. 295.
- Guillocheau, F., Robin, C., Allemand, P., Bourquin, S., Braulta, N., Dromardt, G., Friedenberge, R., Garcia, J.-P., Gaulier, J.-M., Gaumet, F., Grosdoy, B., Hanot, F., Le Strat, P., Mettraux, M., Nalpas, T., Prijac, C., Rigollet, C., Serrano, O., Grandjean, G., 2000. Meso-Cenozoic geodynamic evolution of the Paris Basin: 3D stratigraphic constraints. *Geodin. Acta* 13 189–245.
- Gutierrez-Neri, M., Buik, N., Drijver, B., Godschalk, B., 2011. Analysis of recovery efficiency in a high-temperature energy storage system. 1e Natl. Congr. Bodemenergie 13–14.
- Hamm, V., Arnaud, L., 2017. Etude des opportunités de valorisation énergétique du potentiel géothermique en France métropolitaine – Cas de l'Albien et du Dogger. 78 p., 26 fig., 3 ann., Rapport final BRGM/RP-67262-FR.
- Hamm, V., Maurel, C., 2019. Projet Sybase : synthèse de bancarisation et suivi des opérations de géothermie de basse température en France métropolitaine. Rapp. Final BRGM/RP-68601-FR.
- Hellström, G., Tsang, C., 1988. Buoyancy flow at a two-fluid interface in a porous medium: analytical studies. *Water Resour Res* 24, 493–506.
- Hervé, J.-Y., 2007. Nappes de l'Albien et du Néocomien. Définition des conditions d'accès à la ressource géothermique en Ile-de-France. Rapp. Final BRGM/RP-55990-FR.
- Lopez, S., Hamm, V., Le Brun, M., Schaper, L., Boissier, F., Cotiche, C., Giuglaris, E., 2010. 40 years of Dogger aquifer management in Ile-de-France, Paris Basin, France. *Geothermics* 39, 339–356.
- Mégnyen, C., Mégnyen, F., 1980. Synthèse géologique du bassin de Paris. Mémoire du BRGM n°101.
- Menjoz, A., 1990. Lectures on the characterization and the exploitation of geothermal reservoirs in France. Rep. No. 2, United Natl. Geotherm. Train. Program, United Nations Univ. Reykjavík, Icel. 89.
- Schout, G., Drijver, B., Gutierrez-Neri, M., Schotting, R., 2014. Analysis of recovery efficiency in high-temperature aquifer thermal energy storage: A Rayleigh-based method. *Hydrogeol. J.* 22, 281–291. <https://doi.org/10.1007/s10040-013-1050-8>
- Seguin, J.-J., Castillo, C., Arnaud, L., 2015. Modélisation des nappes de l'Albien et du Néocomien du Bassin de Paris, Rapport final BRGM/ RP-64873-FR.